Nat.Lab. Unclassified Report NL-UR 2001/801

Date of issue: May 2001

Parameter Extraction for the Bipolar Transistor Model Mextram

Level 504

J.C.J. Paasschens, W.J. Kloosterman, and R.J. Havens

Unclassified Report

©Koninklijke Philips Electronics N.V. 2001

Authors' address data: J.C.J. Paasschens WAY41; Jeroen.Paasschens@philips.com
W.J. Kloosterman M0.576; Willy.Kloosterman@philips.com
R.J. Havens WAY41; Ramon.Havens@philips.com

©Koninklijke Philips Electronics N.V. 2001
All rights are reserved. Reproduction in whole or in part is
prohibited without the written consent of the copyright owner.

Unclassified Report: NL-UR 2001/801

Title: Parameter Extraction for the Bipolar Transistor Model Mextram Level 504

Author(s): J.C.J. Paasschens, W.J. Kloosterman, and R.J. Havens

Part of project: Compact modelling

Customer: Semiconductors

Keywords: Mextram, compact modelling, bipolar transistors, parameter extraction, circuit simulation, large-signal modelling, semiconductor technology, integrated circuits

Abstract: Parameter extraction is an important part in the whole process of using a compact model. We describe a general way of extracting parameters for Mextram. This includes a description of the measurements that have to be taken.

In general it is difficult to achieve a good set of high-current parameters for bipolar transistors. We therefore not only give a parameter extraction method for these parameters, but also show how they influence the characteristics. In this way the user has some information that can help in case the parameter extraction gives problems.

A separate chapter is devoted to the extraction of the parameters that belong to temperature scaling.

Although geometric scaling is not a part of Mextram we also present the basics for geometric scaling together with a way to extract the corresponding parameters. Statistical modelling is briefly discussed.

Finally we discuss how this parameter extraction strategy is implemented in the program IC-CAP of Agilent.

©Koninklijke Philips Electronics N.V. 2001

History of documentation

January 2000	: Release of parameter extraction documentation
April 2001	: Update related to update of model definition (see Nat.Lab. Unclassified Report NL-UR 2000/811) Update of chapter on geometric scaling
May 2001	: Initialisation regarding MULT-scaling updated

©Koninklijke Philips Electronics N.V. 2001

Contents

1 Introduction **1**

2 A single transistor at reference temperature **2**

2.1 Introduction 2
2.2 Measurements 2
2.2.1 What lay-out structure to be used 5
2.3 Initial parameter set 6
2.3.1 Parameters that can immediately be given an initial value 6
2.3.2 Parameters estimated from measurements 8
2.3.3 Parameters to be calculated 8
2.4 Parameter extraction strategy 12
2.5 Extraction of low current parameters 12
2.5.1 Base-emitter depletion capacitance 13
2.5.2 Base-collector depletion capacitance 15
2.5.3 Collector-substrate depletion capacitance 15
2.5.4 Avalanche 16
2.5.5 Reverse Early effect 18
2.5.6 Forward Early effect 21
2.5.7 Collector saturation current 22
2.5.8 Forward current gain 23
2.5.9 Emitter series resistances 24
2.5.10 Collector series resistances 28
2.5.11 Substrate saturation current 29
2.5.12 Reverse current gain 31
2.6 High current parameters 33
2.6.1 Self-heating 33
2.6.2 Output-characteristics and forward-Gummel 34
2.6.3 Cut-off frequency 36
2.6.4 Quasi-saturation 39
2.6.5 Extraction of high-current parameters 43
2.6.6 Avalanche at high currents 46
2.6.7 Reverse currents at high injection 46

©Koninklijke Philips Electronics N.V. 2001

2.6.8 Reverse transit time 49
2.7 Some alternative ways to extract parameters 49
2.7.1 No substrate present 49
2.7.2 Collector resistance when no substrate is present 50
2.7.3 Reverse Early voltage without reverse measurements 50
2.7.4 Grading coefficients from Early measurements 50
2.7.5 Base and emitter series resistances 51
2.8 SiGe parameter extraction 52
2.8.1 Gradient in the Ge-profile 52
2.8.2 Neutral base recombination 54
2.9 Some left over extraction issues 54
2.9.1 Thermal capacitance 54
2.9.2 Verification of Y-parameters 56

3 Temperature scaling **58**
3.1 The temperature parameters and their influence 58
3.2 Different extraction procedures for temperature parameters 60
3.3 Experimental examples 64

4 Geometric scaling **70**
4.1 General procedure 70
4.1.1 Mismatch between mask and electrical dimensions 71
4.1.2 Determination of the effective junction lengths 72
4.1.3 Choice of scaling parameters 73
4.2 Selection of transistors 73
4.3 Geometric scaling of Mextram parameters 74
4.3.1 Base-Emitter depletion capacitance 74
4.3.2 Base-Emitter overlap capacitance 75
4.3.3 Base-Collector depletion capacitance 76
4.3.4 Base-collector overlap capacitance 77
4.3.5 Substrate-collector depletion capacitance 77
4.3.6 Avalanche parameters 78
4.3.7 Reverse and forward Early effect 78
4.3.8 Collector currents 79

 ©Koninklijke Philips Electronics N.V. 2001

4.3.9 Base currents 80
4.3.10 Substrate current 81
4.3.11 Series resistances 81
4.3.12 High current parameters 84
4.3.13 Transit time parameters 84
4.3.14 Noise parameters 85
4.3.15 Scaling of thermal parameters 86
4.4 Making use of special structures 86
4.5 Statistical modelling 87

5 Implementation in IC-CAP 89
5.1 Usage of the built-in C-functions 89
5.1.1 `MXT_show_parms` 89
5.1.2 `MXT_cbe` 90
5.1.3 `MXT_cbc` 90
5.1.4 `MXT_csc` 90
5.1.5 `MXT_cj0` 90
5.1.6 `MXT_jun_cap` 90
5.1.7 `MXT_I0` 91
5.1.8 `MXT_VER` 91
5.1.9 `MXT_VEF` 91
5.1.10 `MXT_veaf_ib` 92
5.1.11 `MXT_veaf_ic` 92
5.1.12 `MXT_vear_ie` 93
5.1.13 `MXT_forward_ic` 93
5.1.14 `MXT_forward_hfe` 93
5.1.15 `MXT_forward_vbe` 93
5.1.16 `MXT_hard_sat_isub` 94
5.1.17 `MXT_reverse_isub` 94
5.1.18 `MXT_reverse_hfc_sub` 94
5.1.19 `MXT_reverse_hfc` 95
5.1.20 `MXT_reverse_currents` 95
5.1.21 `MXT_ic_vce` 96
5.1.22 `MXT_ft` 97

©Koninklijke Philips Electronics N.V. 2001

5.1.23 Changes w.r.t. Mextram 503 98
5.2 Parameters that influence C-functions 98
5.2.1 Autoranging 98
5.2.2 Smoothing 99
5.2.3 Noise filtering 99
5.2.4 Type of transistor 99
5.3 Optimisation using some simulator 100

References **101**

 ©Koninklijke Philips Electronics N.V. 2001

1 Introduction

The Philips state of the art Mextram bipolar transistor model has been put in the public domain in January 1994. Recently a new version of this model has been made [1, 2] with level number 504. Mextram is suitable for digital and analogue circuit design and has demonstrated accuracy in a wide variety of applications. The accuracy of these circuit simulations not only depends on a correct mathematical description of several physical phenomena like current gain, output conductance, base push-out, cut-off frequency, noise behaviour and temperature scaling, but also on a reliable, robust and unambiguous transistor parameter extraction method. The use of a very sophisticated model with poorly determined parameters will result in a bad prediction of circuit performance. The strategy for the extraction of the transistor parameters is an important task in the development of a transistor model. This report forms a kind of manual for extraction of Mextram parameters from measured transistor characteristics.

Most parameters of the Mextram model can be extracted directly from measured data [3]. Therefore we need depletion capacitance (CV), terminal currents versus biases (like DC Gummel plots) and S-parameter (f_T) measurements. To determine the parameters of the temperature scaling rules part of the measurements have to be repeated at at least one other temperature.

In this document the minimum data needed to extract Mextram transistor parameters is treated. Of course additional measurements (e.g. small signal Y-parameters) can be carried out and used in the parameter extraction method or for verification. We also do not discuss any methods that make use of special structures: we consider only those extraction methods that can be used with measurements on ordinary transistors.

To extract Mextram transistor parameters the extraction routines, that use simplified formulas, are implemented in the IC-CAP program of Agilent. The full Mextram model behaviour should be evaluated via an interface to a circuit simulator. Such circuit simulators can also be used to extract transistor parameters or to verify simulated and measured data not used during parameter extraction.

This report contains the following parts. In Chapter 2 we describe how one can extract the Mextram parameters for a single transistor at a single temperature. The extraction of the temperature parameters is described in Chapter 3. When geometric scaling has to be done for an integrated process one can refer to Chapter 4. Note that geometric scaling rules are not a part of Mextram itself. In Chapter 5 we give some information about the implementation of the parameter extraction in IC-CAP.

Note that to fully understand this report one also needs the formal model definition given in Ref. [1], where all parameters are defined and where all the model equations are given.

©Koninklijke Philips Electronics N.V. 2001

2 A single transistor at reference temperature

2.1 Introduction

The extraction of parameters of a single transistor at the reference temperature contains several steps. First the measurements are done, as described in the next section. When this is done one must calculate the initial values of (all of) the parameters. This is discussed in Section 2.3. One can then proceed to extract the parameters. We have split our discussion into several parts. The general extraction strategy is discussed in Section 2.4. In Section 2.5 we will discuss the extraction of the low-current parameters. This is rather straightforward. More difficult is the extraction of the high-current parameters since in that regime many physical effects play a role and interact. Section 2.6 is devoted to this. In some cases the parameter extraction as described does not work. We will discuss some alternative ways of extracting parameters in Section 2.7. This also includes the case when there is no substrate present.

Mextram can describe SiGe transistors. In many cases one does not need to change the way one extracts parameters. Mextram has however two extra formulations to describe physical phenomena not encountered in pure-Si transistors. The extraction of the corresponding parameters is discussed in Section 2.8. In Section 2.9 we finally discuss some left over issues in the parameter extraction.

2.2 Measurements

In this section we will shortly discuss the various measurements that are needed for parameter extraction. In Table 1 we have given an overview of the different measurement setups and bias ranges that can be used. We will discuss these below. The maximum collector, base and emitter voltages in the table are obtained from DC measurements. Therefore, and also to avoid charge storage during the capacitance measurements, it is recommended to start with the DC measurements.

To extract reliable parameters it is important that the measurements are done over a large range of collector, base and emitter biasing conditions. The number of data points in an interval is of minor importance. For some measurements, like the Early measurements and the output characteristic, we would like to have numerical derivatives. It is then important that the the noise is low, which means that the measurement time per bias point must be long enough.

Forward-Early measurement In the Forward-Early measurement the collector voltage is increased while keeping the base-emitter voltage constant (see Table 1). The maximum collector voltage $V_{CB,max}$ is obtained from this measurement as the voltage where the base current becomes negative. This collector voltage is about BV_{ceo} (Breakdown-Voltage from Collector to Emitter with Open base). The BV_{ceo} is strongly process dependent and varies from 3 V battery supply up to 50 V for automotive applications, or even higher.

 ©Koninklijke Philips Electronics N.V. 2001

Table 1: *The different measurement setups. The substrate voltage is normally set to* -1 V *with respect to the common in the different measurement setups (not of course in the substrate-collector depletion capacitance measurement).*

Measurement name	Bias setting	Meas. data
Forward-Early	$\mathcal{V}_{BE} = 0.65$ V, $\mathcal{V}_{CB} = 0 \ldots V_{CB,max}$	I_C, I_B
Reverse-Early	$\mathcal{V}_{BC} = 0.65$ V, $\mathcal{V}_{EB} = 0 \ldots V_{EB,max}$	I_E, I_B
Forward-Gummel	$\mathcal{V}_{BC} = 0$ V, $\mathcal{V}_{BE} = 0.4 \ldots 1.2$ V	I_C, I_B, I_{sub}
Reverse-Gummel	$\mathcal{V}_{BE} = 0$ V, $\mathcal{V}_{BC} = 0.4 \ldots 1.2$ V	I_E, I_B, I_{sub}
$\mathsf{R_E}$-flyback	$I_C \simeq 0$ A, $\mathcal{V}_{BE} = 1.0 \ldots 1.5$ V	I_E, $\mathcal{V}_{CE}$
$\mathsf{R_{Cc}}$-active	$\mathcal{V}_{BC} = 0.6$ V, $\mathcal{V}_{BE} = 0.7 \ldots 1.3$ V	I_C, I_B, I_{sub}
Output-characteristic	$I_B = \frac{1}{4} I_{Bset}$, $\frac{1}{2} I_{Bset}$, I_{Bset},	
	$\mathcal{V}_{CE} = 0.0 \ldots (V_{CB,max} + 1\,\mathrm{V})$	I_C, I_{sub}, $\mathcal{V}_{BE}$
Base-emitter depl. cap.	$\mathcal{V}_{BE} = -V_{EB,max} \ldots 0.4$ V	C_{BE}
Base-collector depl. cap.	$\mathcal{V}_{BC} = -V_{CB,max} \ldots 0.4$ V	C_{BC}
Substrate-coll. depl. cap.	$\mathcal{V}_{SC} = -V_{CB,max} \ldots 0.4$ V	C_{SC}
S-parameters	$\mathcal{V}_{CB} = V_{CB,1}$, $V_{CB,2}$, $V_{CB,3}$, ...	
	$\mathcal{V}_{BE} = 0.7 \ldots (\sim 1.0\,\mathrm{V})$	I_C, I_B, S-pars.

This maximum collector voltage is also used in the output-characteristic measurement and the base-collector depletion capacitance measurement, as can be seen in the table.

Reverse-Early measurement The measured base current in the reverse-Early measurement should be more or less constant, although it will eventually decrease due to the generation of avalanche and/or tunnelling currents in the reversed biased base-emitter junction. (Note that these currents are not described by Mextram.) The maximum reverse emitter voltage $V_{EB,max}$ may be obtained from the measurement by looking to the point where these effects start. Note that the maximum reverse emitter voltage is normally much lower then the maximum collector voltage due to the high doping concentrations in the base and emitter regions. The maximum reverse emitter voltage is also used in the base-emitter depletion capacitance measurement.

For advanced bipolar transistors the reverse base-emitter voltage may be lower than 0.5 V. The $\mathcal{V}_{EB}$-range can then be enlarged by biasing the base-emitter junction slightly in the forward ($\mathcal{V}_{EB} > -0.3$ V instead of $\mathcal{V}_{EB} > 0.0$ V).

Forward-Gummel and reverse-Gummel measurements In the next step the forward-Gummel and reverse-Gummel measurements are done. The forward junction bias varies from about 0.4 V up to 1.2 V. The reverse junction bias is 0 V to avoid the generation of avalanche/tunnelling currents and to prevent self-heating effects. In case of noise I_{sub} in the reverse measurement also I_C should be measured (see Sec. 2.5.12).

Output-characteristic measurement The output-characteristic is measured at least at three constant values of the base current. The value of the third base current (I_{Bset}) may be

©Koninklijke Philips Electronics N.V. 2001

obtained from the forward-Gummel measurement as the base current where the current gain is about the half of the maximum gain. This maximum will be at around $\mathcal{V}_{\mathrm{BE}} \approx 0.8$ V. A somewhat smaller $I_{B\mathrm{set}}$ is also possible, and is even recommended for SiGe transistors. The value of the first base current is $\frac{1}{4}I_{B\mathrm{set}}$ and that of the second base current is $\frac{1}{2}I_{B\mathrm{set}}$. The maximum collector voltage should be about $V_{\mathrm{CB,max}} + 1$ V. In this way the output characteristic normally exhibits sufficient quasi-saturation and/or high injection effect to extract the epilayer parameters and the knee current $\mathsf{I_k}$. The collector currents should not be far beyond the top of the f_T.

$\mathsf{R_E}$-flyback measurement In the $\mathsf{R_E}$-flyback measurement the transistor is biased in strong saturation to obtain the emitter resistance. The collector current should be 0A. In practice, however, it is better to supply a small but finite current ($< 1\mu$A). The applied base-emitter voltage is swept from about 1 V up to 1.5 V. The measured emitter current is plotted versus the measured collector voltage. The slope at high emitter currents (about 2 mA per μm^2 emitter area) should be more or less constant. This slope gives the emitter resistance.

$\mathsf{R_{Cc}}$-active measurement For the $\mathsf{R_{Cc}}$-active measurement the base-collector is forward biased with $\mathcal{V}_{\mathrm{BC}} = 0.6$ V. The base-emitter biased is then swept, also positive, from $\mathcal{V}_{\mathrm{BE}} = 0.7$ V to 1.3 V. In this case the collector current remains positive and reasonably large. The voltage drop over the collector resistance makes that internally the base-collector bias that drives the substrate current is increased even further than the externally applied 0.6 V. We measure the substrate current and use a simple model for this current to extract $\mathsf{R_{Cc}}$.

Depletion capacitance measurements Next the depletion capacitances are measured. The maximum reverse collector and emitter voltages are obtained from the forward-Early and reverse- Early measurements as explained before. The maximum substrate-collector voltage may be taken equal to the maximum collector-base voltage. The maximum forward junction voltage is usually taken as 0.4 V, since for higher forward biases diffusion charges start to play a role.

The capacitances can be measured using LCR-meters. This is the most straightforward way. Sometimes it is however time-consuming. An alternative is to determine the capacitances from special (off-state) S-parameter measurements. These measurements are done on the high-frequency structure at fixed frequency. The bias conditions are as in Table 1, where all biases except $\mathcal{V}_{\mathrm{B}}$ for C_{BE} and $\mathcal{V}_{\mathrm{C}}$ for C_{BC} and C_{SC} are zero. After de-embedding the S-parameters [4] and converting them to Y-parameters the capacitances can be found as $C_{BC} = -\mathrm{Im}Y_{12}/\omega$, $C_{BE} = \mathrm{Im}(Y_{12} + Y_{11})/\omega$, $C_{SC} = \mathrm{Im}(Y_{12} + Y_{22})/\omega$. (Note that the IC-CAP code as given by Agilent, named `MEXTRAM_stoc`, seems to use $C_{BC} = 1/(\omega\, \mathrm{Im}\, Y_{12}^{-1})$. This difference does not influence the results very much.)

The disadvantage of using the S-parameters to determine the capacitances is that it is much more sensitive to de-embedding errors or inaccuracies. Using the capacitances

 ©Koninklijke Philips Electronics N.V. 2001

extracted from LCR-meter measurements and looking at the rising part of the f_T (from on-state S-parameters) one can see directly whether the results from both measurements match or not (in which case at least one of the measurements or the previously extracted parameters are not accurate).

S-parameter measurement Finally the S-parameter measurement is done in the normal forward operation regime. De-embedding should be done according to Ref. [4]. The main quantity we need from this measurement is the cut-off frequency f_T. In this measurement the S-parameters are measured in the common emitter configuration. The base-emitter voltage $\mathcal{V}_{\rm BE}$ is swept from a low value of ~ 0.7 V to a maximum. This maximum $\mathcal{V}_{\rm BE}$ should be about the base-emitter bias corresponding the third curve (with $I_B = I_{B\rm set}$) in the output-characteristic measurement.

We take minimally three constant DC values of $\mathcal{V}_{\rm CB}$. The lowest $\mathcal{V}_{\rm CB}$ value should be 0 V or lower. The highest $\mathcal{V}_{\rm CB}$ value depends on the maximum supply voltage. it should be below $\rm BV_{ceo}$. The second $\mathcal{V}_{\rm CB}$-value should then be somewhere in between the other two.

As an alternative one could use three or more constant $\mathcal{V}_{\rm CE}$-values. When measuring more than three curves it is then useful to also include a low collector-emitter bias value (say $\mathcal{V}_{\rm CE} = 0.2$ V). This can help in the extraction of the reverse transit time $\tau_{\sf R}$.

2.2.1 What lay-out structure to be used

For a single transistor two different ways to connect to the bond-pads are in general available. Of course there is the normal structure where all four of the terminals (emitter, base, collector, and substrate) are connected to their individual bond-pads. However, for the high-frequency measurements a structure is needed where emitter and substrate are connected and grounded to increase the signal-to-noise ratio of the measurements. The disadvantage of this latter structure is that it can not be used for the reverse measurements. So in any case two structures are needed for a full parameter extraction. This also means that one must actually measure on two different transistors. To reduce the influence of process spread one should use two transistors close together on the same die and wafer.

The question now is, what measurements should one do on the DC-structure and what on the high-frequency structure.

• The measurements that *have* to be done on the DC-structure are the reverse-Early, the reverse-Gummel, the $\mathsf{R_E}$-flyback, and the $\mathsf{R_{Cc}}$-active measurements. Also all the capacitance measurements done with an LCR-meter should be done on the DC-structure.

• The measurements that *have* to be done on the high-frequency structure are of course the S-parameter measurements (and the capacitances when determined from S-parameters).

• This leaves three measurements from Table 1 that can be done on both structures. These are discussed below.

Both Early measurements should be done on the same transistor, since these are sensitive to the actual base profile. The forward-Early measurement should therefore be done on

the DC-structure, just as the reverse-Early measurement. When it is also measured on the high-frequency structure, it can be used as a check on the process-spread and its influence on the parameter extraction.

The current gain is also sensitive to the actual base doping profile. Since this current gain is needed in the extraction of the high-current parameters (that will be done mainly on the S-parameters and the currents that are measured along) it is logical to do the forward-Gummel measurement on the high-frequency structure. Since it is such a basic measurement it is probably best to do the measurement on both structures.

For the output-characteristic measurement, which also is used for the extraction of the high-current parameters, the same arguments as for the forward-Gummel measurement hold. It is useful to measure it on the high-frequency structure.

2.3 Initial parameter set

In many cases the extraction of a parameter means to minimise the difference between a measured curve and a simulated curve. This is done with some routine that optimises the value of the parameter. For those kinds of optimising routines the initial value of the parameter is important. If this initial value is good, the optimising process will be fast. Furthermore the chance of getting stuck in a local minimum with very unphysical values for the parameters is much smaller than it would be when one started with a random set of initial values.

In this section we describe a way to get an initial parameter set. We have to distinguish three categories of parameters. First, some parameters like LEVEL can immediately be given an initial value. Secondly, for some parameters the initial value can be directly extracted from measurements, without optimising. Thirdly, some parameters can be estimated on basis of physical quantities from the given process. The last category contains all the high-current parameters and for them it is especially important that the initial values are as close to the real value as possible.

2.3.1 Parameters that can immediately be given an initial value

Table 2 gives the parameters that can be set to a constant value. Some of them are somewhat process dependent. We will discuss this below. Note that the default reference temperature $\mathsf{T}_{\mathsf{ref}}$ for parameter extraction is 25 °C.

Diffusion voltages The diffusion voltages are in general difficult to determine from the depletion capacitance measurements. The reason is that one typically only measures up to a forward bias of about 0.4 V, whereas the diffusion voltage is between the 0.5 V and the 1 V. Apart from the collector-substrate diffusion voltage V_{dS}, these voltages determine the cross-over between junction charges and stored charges. Fitting them would lead to values that are generally too low. Hence one needs other ways to determine them. Only V_{dS} can be determined from fitting without much harm. It should however not be

 ©Koninklijke Philips Electronics N.V. 2001

Table 2: *Parameters that can be set to a constant as initial value. The parameters for temperature scaling are included since they might be needed when self-heating is included in the high-current parameter extraction (see Sec. 2.6.1).*

Parameter	value	remark
LEVEL	504	
T_{ref}	TEMP	The actual measurement temperature
dT_a	0	T_{ref} already describes the actual temperature
EXMOD	1	
EXPHI	1	
EXAVL	0	
m_{Lf}	2.0	
XI_{B_1}	0.0	
V_{Lr}	0.3	
X_{ext}	0.5	
a_{x_i}	0.3	
V_{d_E}	0.9	Somewhat depending on process
p_E	0.4	
C_{BEO}	0.0	
C_{BCO}	0.0	
m_τ	1.0	
τ_B	−1.0	See Sec. 2.6.3
τ_R	−1.0	See Sec. 2.6.3
dE_g	0.0	Unless for a SiGe transistor
X_{rec}	0.0	Effect not included in first order
$A_{Q_{B0}}$	0.3	
A_E	0.0	Somewhat depending on process
A_B	1.0	Somewhat depending on process
A_{ex}	0.5	Somewhat depending on process
A_{epi}	2.0	Somewhat depending on process
A_C	0.5	Somewhat depending on process
$dV_{g\beta f}$	0.05	
$dV_{g\beta r}$	0.05	
V_{g_B}	1.18	
V_{g_C}	1.18	
V_{g_j}	1.18	
$dV_{g\tau_E}$	0.0	
A_f	2.0	
K_f	20p	Rather arbitrary
K_{fN}	5μ	Rather arbitrary
V_{d_S}	0.6	Somewhat depending on process
p_S	0.3	
V_{g_S}	1.18	
A_S	2.0	Somewhat depending on process
R_{th}	0.0	
C_{th}	0.0	

©Koninklijke Philips Electronics N.V. 2001

smaller that about 0.5 V since this leads to very low (and possibly negative) values of this diffusion voltage at elevated temperatures. (Note that a low clipping value of 50 mV is recommended for all diffusion voltages [2].)

The emitter-base diffusion voltage $\mathsf{V_{d_E}}$ is typically 0.8 V for less advanced processes and 0.9–1.0 V for more advanced processes. This voltage is important for the determination of f_T. In principle it could therefore be determine by optimising it on the f_T-curve. However, $\mathsf{V_{d_E}}$ and $\mathsf{p_E}$ are strongly correlated. Changing the former means that the latter has to be extracted again, as well as many other parameters. Optimising the diffusion voltage would therefore lead to a very large optimising loop, which in general is not done. Instead it gets a set value (which might be changed by hand later on).

The collector-base diffusion voltage $\mathsf{V_{d_C}}$ is about 0.5 V for very low epilayer doping and can get up to 0.8 V for higher doping. It can be estimated from

$$\mathsf{V_{d_C}} \simeq 2\, V_T \ln(N_{\mathrm{epi}}/n_i), \tag{2.1}$$

(see also below).

Mobility exponents The mobility exponents $\mathsf{A_E}, \cdots, \mathsf{A_S}$ describe the temperature dependence of the (majority) mobility in the various regions of the collector. The general formula is [5, 6]

$$\mu \propto t_N^{-A}. \tag{2.2}$$

From a physical point of view [7, 8] the value of A should be between zero (for high doping levels) and 2.3 (for low doping levels). The values we have given in the table reflect the fact that the emitter is very high doped, the base and external collector are high doped and the epilayer is low doped. It is not always possible to extract them accurately which means that the estimates will determine the final value. See Chapter 3 for some more information.

2.3.2 Parameters estimated from measurements

Table 3 contains the list of parameters whose initial values can be obtained directly from measured data. We have also shown how to arrive at these values. Some more information about this direct extraction can be found in the sections where the extraction of the parameters is discussed. The last three quantities in the table are help-variables and not parameters.

2.3.3 Parameters to be calculated

At last we have some parameters whose initial values must be calculated from layout and technology data. The quantities that are needed are given in Table 4.

 ©Koninklijke Philips Electronics N.V. 2001

Table 3: *Parameters that can be extracted without optimising.*

Parm.	Way of extraction
C_{jE}	Zero bias value of base-emitter capacitance
C_{jC}	Zero bias value of base-collector capacitance
C_{jS}	Zero bias value of substrate-collector capacitance
R_{E}	Numerical derivative in R_{E}-flyback measurement
V_{er}	Numerical derivative in reverse-Early measurement
V_{ef}	Numerical derivative in forward-Early measurement
β_{f}	Maximum of forward current gain
β_{ri}	Maximum of internal reverse current gain
I_{s}	From (forward-Gummel) collector current without Early effect
I_{Ss}	From (reverse-Gummel) substrate current without Early effect
τ_{E}, τ_{B}	$1/[10\pi\ \max(f_T)]$
I_{B0}	Zero bias value of the base current in forward-Early measurement
I_{C0}	Zero bias value of the collector current in forward-Early measurement
I_{E0}	Zero bias value of the emitter current in reverse-Early measurement

Table 4: *The layout and process quantities needed.*

MULT	Number of transistors measured in parallel (the extracted parameter set will be for one transistor)
H_{em}	Emitter width (dimension on silicon)
L_{em}	Emitter stripe length (dimension on silicon)
$\rho_{\square}$	Pinched sheet resistance of the base
N_{base}	Number of base stripes
N_{epi}	Collector epilayer doping level
W_{epi}	Collector epilayer thickness

We need the following constants for the calculation

$$q = 1.602 \cdot 10^{-19}\,\mathrm{C}, \tag{2.3a}$$

$$k = 1.374 \cdot 10^{-23}\,\mathrm{J/K}, \tag{2.3b}$$

$$\varepsilon = 1.036 \cdot 10^{-10}\,\mathrm{C/Vm}, \tag{2.3c}$$

$$v_{\mathrm{sat}} = 8.0 \cdot 10^{4}\,\mathrm{m/s}. \tag{2.3d}$$

The quantities that can be directly calculated from the reference temperature are

$$V_T = \frac{k\mathsf{T}_{\mathsf{ref}}}{q}, \tag{2.4a}$$

$$n_i^2 = (9.61 \cdot 10^{32}\,\mathrm{cm}^{-6}\mathrm{K}^{-3}) \times {\mathsf{T}_{\mathsf{ref}}}^3\, e^{-\mathsf{V}_{\mathsf{gC}}/V_T}. \tag{2.4b}$$

Note that n_i^2 is needed for the epilayer parameters and is therefore the silicon value even when the base is SiGe.

©Koninklijke Philips Electronics N.V. 2001

From the layout data we can calculate the emitter surface and periphery

$$A_{\rm em} = H_{\rm em} \cdot L_{\rm em}, \tag{2.5a}$$
$$P_{\rm em} = 2\,(H_{\rm em} + L_{\rm em}). \tag{2.5b}$$

From the layout data and the direct extraction estimates we calculate

$$\mathsf{XC_{jE}} = \frac{P_{\rm em}}{P_{\rm em} + 6\,A_{\rm em}/\mu{\rm m}}, \tag{2.6a}$$
$$\mathsf{XC_{jC}} = \mathsf{XC_{jE}}\,\frac{\mathsf{V_{er}}}{\mathsf{V_{ef}}}\,\frac{\mathsf{C_{jE}}}{\mathsf{C_{jC}}}. \tag{2.6b}$$

The resistances can be estimated as

$$\mathsf{R_{Bv}} = \frac{H_{\rm em}\,\rho_{\square}}{3N_{\rm base}^2 L_{\rm em}}, \tag{2.7a}$$
$$\mathsf{R_{Bc}} = \mathsf{R_{Cc}} = \frac{300\,\Omega\,\mu{\rm m}}{L_{\rm em}}. \tag{2.7b}$$

The initial values of the knee currents and the non-ideal base currents are

$$\mathsf{I_k} = \frac{\mathsf{V_{er}}\,(1 - \mathsf{XC_{jE}})\,\mathsf{C_{jE}}}{\tau_{\mathsf{B}}}, \tag{2.8a}$$
$$\mathsf{I_{kS}} = (50\,\mu{\rm A}/\mu{\rm m}^2) \times {\rm A_{em}}, \tag{2.8b}$$
$$\mathsf{I_{Bf}} = 100\,\mathsf{I_s}, \tag{2.8c}$$
$$\mathsf{I_{Br}} = 100\,\mathsf{I_s}. \tag{2.8d}$$

The avalanche parameters can be given as

$$\mathsf{W_{avl}} = W_{\rm epi}, \tag{2.9a}$$
$$\mathsf{V_{avl}} = \frac{q\,N_{\rm epi}\,W_{\rm epi}^2}{2\varepsilon}. \tag{2.9b}$$

Note that $\mathsf{V_{avl}}$ can be expressed also as $\mathsf{V_{dC}}/\mathsf{X_p}^2$, when one uses the initial values calculated below. This latter formula gives a better idea of the value $\mathsf{V_{avl}}$ should have.

Now we turn to the various quantities that are related to the collector epilayer. The mobility in the epilayer can be calculated from [9]

$$\mu_0 = \mu_{\rm min} + \frac{\mu_{\rm max} - \mu_{\rm min}}{1 + (N_{\rm epi}/N_{\rm ref})^{\alpha}}, \tag{2.10}$$

where for NPN's we have

$$\mu_{\rm min} = 52\,{\rm cm^2/Vs}, \tag{2.11a}$$
$$\mu_{\rm max} = 1417\,{\rm cm^2/Vs}, \tag{2.11b}$$
$$N_{\rm ref} = 9.7 \cdot 10^{16}\,{\rm cm^{-3}}, \tag{2.11c}$$
$$\alpha = 0.68, \tag{2.11d}$$

 ©Koninklijke Philips Electronics N.V. 2001

and for PNP's we have

$$\begin{aligned} \mu_{\min} &= 45\,\text{cm}^2/\text{Vs}, && (2.12a)\\ \mu_{\max} &= 471\,\text{cm}^2/\text{Vs}, && (2.12b)\\ N_{\text{ref}} &= 2.2\cdot 10^{17}\,\text{cm}^{-3}, && (2.12c)\\ \alpha &= 0.72. && (2.12d) \end{aligned}$$

We also need some spreading parameters for the epilayer [10, 11]: α_l is the spreading angle at low current levels ($I_C < \mathsf{I_{hc}}$) while α_h is the spreading angle at high current levels. These quantities are process and geometry dependent. We can use the following values if we are only interested in generating an initial parameter set:

$$\begin{aligned} \tan\alpha_l &= 0.5, && (2.13a)\\ \tan\alpha_h &= 1.0, && (2.13b)\\ S_{Fl} &= \tan\alpha_l\; W_{\text{epi}}\left(\frac{1}{H_{\text{em}}}+\frac{1}{L_{\text{em}}}\right), && (2.13c)\\ \mathsf{S_{Fh}} &= \tfrac{2}{3}\tan\alpha_h\; W_{\text{epi}}\left(\frac{1}{H_{\text{em}}}+\frac{1}{L_{\text{em}}}\right). && (2.13d) \end{aligned}$$

The latter quantity is the current spreading factor for high injection, and is a parameter used in the high-current avalanche model (only when $\mathsf{EXAVL} = 1$). We can now calculate the epilayer parameters

$$\begin{aligned} \mathsf{V_{d_C}} &= V_T\;\ln(N_{\text{epi}}^2/n_i^2), && (2.14a)\\ \mathsf{R_{Cv}} &= \frac{W_{\text{epi}}}{q\mu_0 N_{\text{epi}} A_{\text{em}}}\,\frac{1}{(1+S_{Fl})^2}, && (2.14b)\\ \mathsf{I_{hc}} &= q N_{\text{epi}} A_{\text{em}} v_{\text{sat}}\,(1+S_{Fl})^2, && (2.14c)\\ \mathsf{SCR_{Cv}} &= \frac{W_{\text{epi}}^2}{2\varepsilon v_{\text{sat}} A_{\text{em}}}\,\frac{1}{(1+\mathsf{S_{Fh}})^2}, && (2.14d)\\ x_{d0} &= \sqrt{\frac{2\varepsilon\,\mathsf{V_{d_C}}}{q N_{\text{epi}}}} && (2.14e)\\ \mathsf{X_p} &= x_{d0}/W_{\text{epi}}, && (2.14f)\\ \mathsf{p_C} &= 0.3/(1-\mathsf{X_p}), && (2.14g)\\ \mathsf{m_C} &= (1-\mathsf{X_p})/2, && (2.14h)\\ \boldsymbol{\tau}_{\mathsf{epi}} &= \frac{W_{\text{epi}}^2}{4\,\mu_0\,V_T}, && (2.14i)\\ \boldsymbol{\tau}_{\mathsf{R}} &= (\boldsymbol{\tau}_{\mathsf{B}}+\boldsymbol{\tau}_{\mathsf{epi}})\,\frac{1-\mathsf{XC_{j_C}}}{\mathsf{XC_{j_C}}}. && (2.14j) \end{aligned}$$

The value of $\mathsf{X_p}$ should not be larger then 0.4. We refer to Section 2.6.3 for some more information about the initial values of the base, epilayer and reverse transit time.

Table 5: *A typical grouping of parameters in Mextram that can be used in the extraction procedure. The extraction procedure for each group is discussed in Section 2.5.*

Group	Parameters
Base-emitter depl. cap.	C_{jE}, p_E, (V_{d_E})
Base-collector depl. cap.	C_{jC}, p_C, X_p
Substrate-emitter depl. cap.	C_{jS}, p_S, (V_{d_S})
Forward-Early	W_{avl}, V_{avl}
Reverse-Early	V_{er}
Forward-Early	V_{ef}
Forward-Gummel	I_s
Forward-Gummel	β_f, I_{Bf}, m_{Lf}
R_E-flyback	R_E
R_{Cc}-active	R_{Cc}
Reverse-Gummel	I_{Ss}, (I_{ks})
Reverse-Gummel	β_{ri}, I_{Br}, V_{Lr}
Output-characteristic	R_{th}, I_k
Forward-Gummel	R_{Cv}, (V_{d_C})
Cut-off frequency	SCR_{Cv}, I_{hc}, τ_E, τ_{epi}, (τ_B, a_{x_i})
Reverse-Gummel	X_{ext}

2.4 Parameter extraction strategy

The general strategy for parameter extraction is to put the parameters in small groups (typically 1–3) and extract these parameters simultaneously out of measured data sensitive to these parameters. The composition of each individual group depends on the technology. However, it is possible to give general guidelines. A typical grouping of Mextram parameters is given in Table 5.

For many of the extractions one needs previously extracted parameters. This can only been done when one is careful about the sequence in which the extractions are performed. The sequence in the table is such that this has been taken care of.

In the next sections we will describe in detail how the parameters in each group should be extracted. We start with the depletion capacitances. Then we consider the other low-current parameters. Next the high-current parameters are extracted, taking self-heating into account. The self-heating capacitance is discussed separately later on.

2.5 Extraction of low current parameters

The extraction of the low current parameters (including the capacitances) should be no problem at all for any process. The depletion capacitances are fairly standard and can be extracted in almost any case from an almost ideal capacitance curve (with variable grading coefficient and possibly a constant part). Avalanche is straightforward and so are the Early voltages. The saturation current and forward current gain are also fairly standard. The reverse current gain and substrate saturation current need a bit more care, but are also not difficult. The collector series resistance extraction can be done without influence of other

 ©Koninklijke Philips Electronics N.V. 2001

parameters. For the emitter series resistance several methods are available, of which the flyback measurement (Giacoletto method) is probably the one most independent of other parameters.

For each step in the extraction we also show an example in a figure.

2.5.1 Base-emitter depletion capacitance

The measured base-emitter capacitance C_{BE} consists in principle of three contributions: a depletion capacitance, an overlap capacitance and a diffusion capacitance. As long as the base-emitter voltage is not too far in forward we can neglect the last contribution. We will therefore concentrate on the other two.

The base-emitter depletion capacitance can be calculated by adding the intrinsic and side-wall contributions of the depletion charge and taking the derivative w.r.t. the base-emitter voltage. Since no currents are flowing there is also no voltage drop over any resistors. The capacitance can be approximated by the (almost ideal) formula

$$C_{BE} \simeq \frac{\mathsf{C_{jE}}}{(1 - \mathcal{V}_{\rm BE}/\mathsf{V_{d_E}})^{\mathsf{p_E}}} + \mathsf{C_{BEO}}. \tag{2.15}$$

The constant capacitance $\mathsf{C_{BEO}}$ describes any overlap (peripheral) capacitances between base and emitter.

The expression above is an approximation of the base-emitter capacitance. The full expression is

$$C_{BE} = \frac{s_E\,\mathsf{C_{jE}}}{(1 - V_{j_E}/\mathsf{V_{d_E}})^{\mathsf{p_E}}} + \frac{(1 - s_E)\,\mathsf{C_{jE}}}{(1 - V_{FE}/\mathsf{V_{d_E}})^{\mathsf{p_E}}} + \mathsf{C_{BEO}}. \tag{2.16}$$

This formula describes a transition from a normal depletion capacitance (first term, when $s_E = 1$) to a constant capacitance (second term, $s_E = 0$). The constant part is a factor $a_{j_E} = 3$ larger than the zero-bias capacitance. In practice however one should not reach this constant part in the extraction of the depletion capacitances, because it only occurs when there is already a considerable amount of current flowing. Then the diffusion capacitance is already more important than the depletion capacitance.

The transition between the ideal and the constant part is described by the quantity s_E given by

$$s_E = \frac{1}{1 + e^{(\mathcal{V}_{\rm BE} - V_{FE})/0.1\,\mathsf{V_{d_E}}}}. \tag{2.17}$$

The point where the transition takes place is given by V_{FE}. It is defined using the quantity a_{j_E} discussed before: $V_{FE} = \mathsf{V_{d_E}}\,(1 - a_{j_E}^{-1/\mathsf{p_E}}) \simeq \mathsf{V_{d_E}}$. The voltage V_{j_E} that is actually used in the equation for the capacitance is

$$V_{j_E} = \mathcal{V}_{\rm BE} + 0.1\,\mathsf{V_{d_E}}\ln s_E. \tag{2.18}$$

©Koninklijke Philips Electronics N.V. 2001

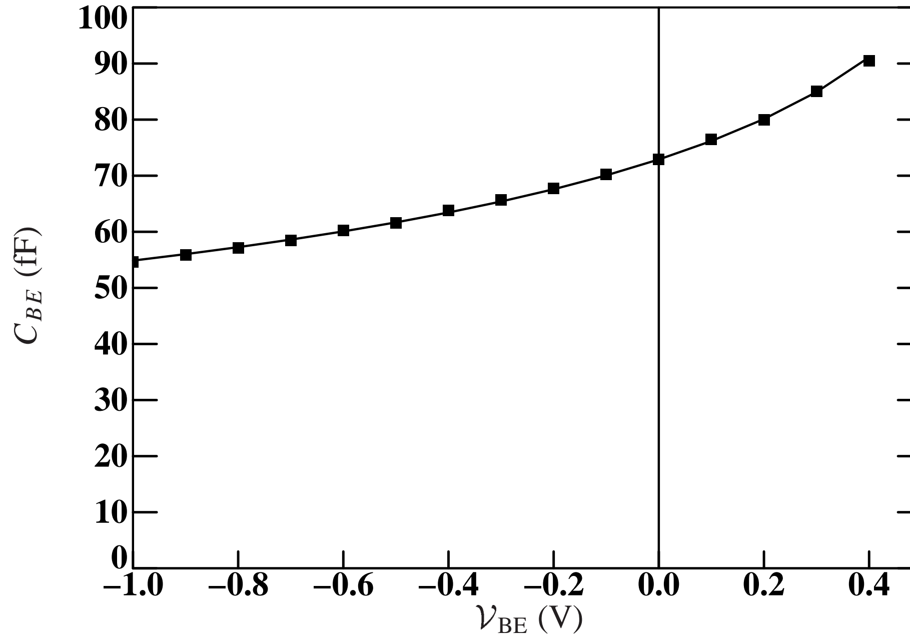

Figure 1: *Measured (markers) and simulated (line) base-emitter depletion capacitance.*

Note that $s_E = \mathrm{d}V_{j_E}/\mathrm{d}\mathcal{V}_{\mathrm{BE}}$. We then have the two cases

$$s_E \simeq 1, \qquad V_{j_E} \simeq \mathcal{V}_{\mathrm{BE}}, \qquad \text{when } \mathcal{V}_{\mathrm{BE}} < \mathsf{V_{d_E}}, \tag{2.19a}$$

$$s_E \simeq 0, \qquad V_{j_E} \simeq \mathsf{V_{d_E}}, \qquad \text{when } \mathcal{V}_{\mathrm{BE}} > \mathsf{V_{d_E}}. \tag{2.19b}$$

The parameters that can be extracted directly are the zero-bias capacitance $\mathsf{C_{j_E}}$ and the grading coefficient $\mathsf{p_E}$. It is in general not possible to extract the diffusion voltage $\mathsf{V_{d_E}}$ from the capacitance. Therefore in most cases one must choose a reasonable value (like $\mathsf{V_{d_E}} = 0.9$ V). This diffusion voltage might however have an influence on the top of the f_T curve.

The overlap capacitance $\mathsf{C_{BEO}}$ can be extracted simultaneously. Better is however to extract it from special structures, and take geometrical scaling into account.

Sometimes the zero-bias capacitance is extracted directly from the measurement at $\mathcal{V}_{\mathrm{BE}} = 0$ (using for instance the IC-CAP-function `MXT_cj0`). The grading coefficient is then extracted from the full curve. Although this is conceptually correct it has two disadvantages. First it is very sensitive to noise in the measurement at precisely $\mathcal{V}_{\mathrm{BE}} = 0$. Second it does not give the best fit overall. We therefore prefer not to do it this way here or for the other capacitances.

Extracted parameters	: $\mathsf{C_{j_E}}$, $\mathsf{p_E}$, ($\mathsf{C_{BEO}}$, $\mathsf{V_{d_E}}$)
IC-CAP-function	: `MXT_cbe`
Equations used from Ref. [2]	: (4.110)–(4.115)

 ©Koninklijke Philips Electronics N.V. 2001

2.5.2 Base-collector depletion capacitance

The extraction of the base-collector depletion capacitance is similar to that of the base-emitter capacitance. Now however the capacitance in Mextram has its own constant part (determined by the parameter $\mathsf{X_p}$). This constant part describes the fact that the collector epilayer has a finite thickness and hence the depletion region might run into the buried layer. The simplified expression now is

$$C_{BC} \simeq \frac{(1-\mathsf{X_p})\,\mathsf{C_{jc}}}{(1-\mathcal{V}_{\mathrm{BC}}/\mathsf{V_{dc}})^{\mathsf{p_C}}} + \mathsf{X_p}\,\mathsf{C_{jc}} + \mathsf{C_{BCO}}. \tag{2.20}$$

To get the more correct expression we must take the complete expression for the base-collector depletion charge and take the derivative. We can assume that the current is much smaller than $\mathsf{I_{hc}}$, which simplifies the expressions. We have $a_{jC} = 2.0$.

$$b_{jC} = (a_{jC} - \mathsf{X_p})/(1-\mathsf{X_p}), \tag{2.21a}$$

$$V_{FC} = \mathsf{V_{dc}}\,(1 - b_{jC}^{-1/\mathsf{p_C}}), \tag{2.21b}$$

$$s_C = \frac{1}{1+e^{(\mathcal{V}_{\mathrm{BC}}-V_{FC})/0.1\,\mathsf{V_{dc}}}}, \tag{2.21c}$$

$$V_{jC} = \mathcal{V}_{\mathrm{BC}} + 0.1\,\mathsf{V_{dc}}\ln s_C, \tag{2.21d}$$

$$C_{BC} = \frac{s_C\,(1-\mathsf{X_p})\,\mathsf{C_{jc}}}{(1-V_{jC}/\mathsf{V_{dc}})^{\mathsf{p_C}}} + \frac{(1-s_C)\,(1-\mathsf{X_p})\,\mathsf{C_{jc}}}{(1-V_{FC}/\mathsf{V_{dc}})^{\mathsf{p_C}}} + \mathsf{X_p}\,\mathsf{C_{jc}} + \mathsf{C_{BCO}}. \tag{2.21e}$$

The extraction is again straightforward. But due to the extra parameter $\mathsf{X_p}$ the constant part is overdetermined. Only by determining $\mathsf{C_{BCO}}$ from special structures or estimating it in some way one can make the extraction unambiguously. One can of course also take $\mathsf{C_{BCO}} = 0$. The diffusion voltage $\mathsf{V_{dc}}$ can again not be determined from the depletion capacitance. At this moment one needs to estimate it. $\mathsf{V_{dc}}$ does have a very strong influence on the h_{fe} roll-off in the high current regime. So it can be extracted later in the extraction procedure, but it will change only by a small amount. This means that for the extraction of the capacitance parameters an initial estimate for $\mathsf{V_{dc}}$ or an estimate from a previous extraction run suffices.

Extracted parameters	: $\mathsf{C_{jc}}$, $\mathsf{p_C}$, $\mathsf{X_p}$, ($\mathsf{C_{BCO}}$, $\mathsf{V_{dc}}$)
IC-CAP-function	: `MXT_cbc`
Equations used from Ref. [2]	: (4.116)–(4.135)

2.5.3 Collector-substrate depletion capacitance

The extraction of the collector-substrate capacitance is very similar to that of the base-emitter capacitance. The only differences are the names of the biases and the parameters and probably the range of the bias. The equations to use are (with $a_{jS} = 2.0$)

$$V_{FS} = \mathsf{V_{dS}}\,(1 - a_{jS}^{-1/\mathsf{p_S}}), \tag{2.22a}$$

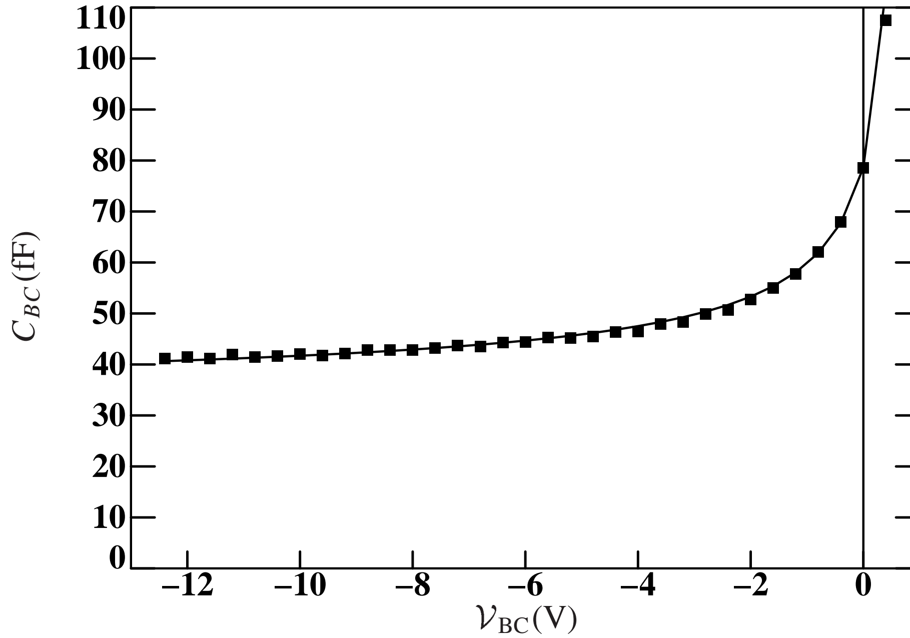

Figure 2: *Measured (markers) and simulated (line) base-collector depletion capacitance.*

$$s_S = \frac{1}{1+e^{(\mathcal{V}_{SC}-V_{FS})/0.1\,\mathsf{V_{dS}}}}, \tag{2.22b}$$

$$V_{jS} = \mathcal{V}_{SC} + 0.1\,\mathsf{V_{dS}}\ln s_S \tag{2.22c}$$

$$C_{SC} = \frac{s_S\,\mathsf{C_{jS}}}{(1-V_{jS}/\mathsf{V_{dS}})^{\mathsf{p_S}}} + \frac{(1-s_S)\,\mathsf{C_{jS}}}{(1-V_{FS}/\mathsf{V_{dS}})^{\mathsf{p_S}}} + C_{p,CS}. \tag{2.22d}$$

One can extract $\mathsf{C_{jS}}$ and $\mathsf{p_S}$ directly. The diffusion voltage $\mathsf{V_{dS}}$ is again difficult. But since it is not used in any other part of the model the combined extraction with the other parameter is no problem. It should however not be smaller that about 0.5 V since this leads to very low (and possibly negative) values of this diffusion voltage at elevated temperatures. (Note that a low clipping value of 50 mV is recommended for all diffusion voltages). The parasitic capacitance $C_{p,CS}$, which is not part of the Mextram model, is included only for convenience in the case of de-embedding problems. (For the base-emitter and base-collector capacitances one can use the overlap capacitances when needed.)

Extracted parameters	: $\mathsf{C_{jS}}$, $\mathsf{p_S}$, ($\mathsf{V_{dS}}$)
IC-CAP-function	: `MXT_csc`
Equations used from Ref. [2]	: (4.136)–(4.138)

2.5.4 Avalanche

The low current avalanche parameters are extracted from the base current in the forward-Early measurement. As long as there is no avalanche this base current is independent of the collector-base bias (for exceptions, see Sec. 2.8.2). When the collector-base bias gets larger avalanche becomes important and the base current drops (possibly to below zero).

 ©Koninklijke Philips Electronics N.V. 2001

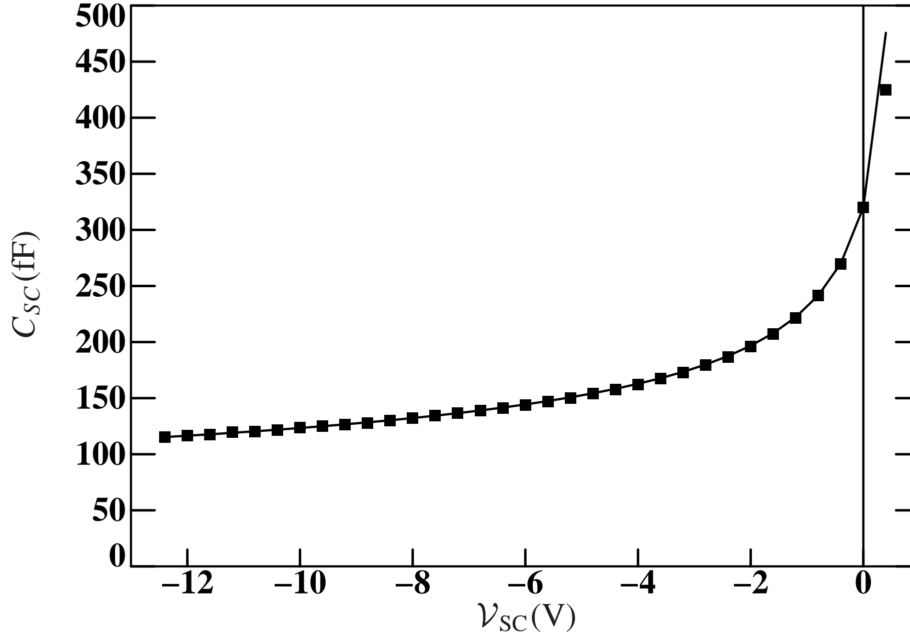

Figure 3: *Measured (markers) and simulated (line) collector-substrate depletion capacitance.*

The difference between the base current at $\mathcal{V}_{CB} = 0$ and at higher $\mathcal{V}_{CB}$ is the avalanche current. Hence we can extract $\mathsf{W_{avl}}$ and $\mathsf{V_{avl}}$ by fitting the measurements to the expression

$$I_B = I_{B0} - I_{avl}. \tag{2.23}$$

Here I_{B0} is a help-variable. We need it because we have not extracted any parameters that could give us the correct base current at $\mathcal{V}_{CB} = 0$. And even when we would have extracted the corresponding parameters, we need a very accurate description of this base current at zero $\mathcal{V}_{CB}$ to extract the avalanche parameters. The full model will not always give this accuracy, even after a full extraction. Therefore we make use of this help-variable.

The avalanche current itself can be found from the full expressions for this current with the approximation that the collector current is negligible. In that case the value of the model flag EXAVL is not important. We can express the avalanche current as

$$E_M = \frac{\mathsf{V_{d_C}} + \mathcal{V}_{CB} + 2\,\mathsf{V_{avl}}}{\mathsf{W_{avl}}} \sqrt{\frac{\mathsf{V_{d_C}} + \mathcal{V}_{CB}}{\mathsf{V_{d_C}} + \mathcal{V}_{CB} + \mathsf{V_{avl}}}}, \tag{2.24a}$$

$$\lambda_D = \frac{\mathsf{W_{avl}}^2}{2\,\mathsf{V_{avl}}}\, E_M, \tag{2.24b}$$

$$G_{EM} = \frac{A_n}{B_n}\, E_M\, \lambda_D \left\{ \exp\left[-\frac{B_n}{E_M}\right] - \exp\left[-\frac{B_n}{E_M}\left(1 + \frac{\mathsf{W_{avl}}}{\lambda_D}\right)\right]\right\}, \tag{2.24c}$$

$$I_{avl} = I_C\, G_{EM}. \tag{2.24d}$$

As one can see the avalanche current is proportional to the collector current. For the extraction of the avalanche parameters we use the measured collector current. The constants

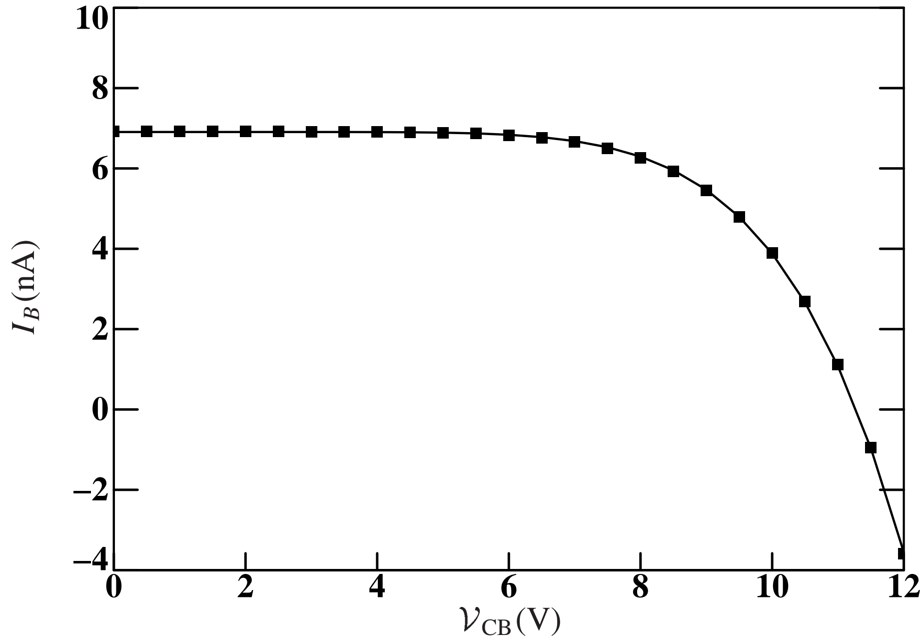

Figure 4: *Measured (markers) and simulated (line) base current in the forward-Early measurement for the extraction of the avalanche parameters.*

A_n and B_n are physical quantities (and also model constants) that depend on the polarity of the transistor (NPN or PNP). When the temperature of extraction is far from 300 K one needs to take the temperature rule of B_n into account.

The most important contribution to the avalanche current is the first exponential term, which is determined by the maximal electric field. For large collector-base biases this electric field is almost equal to $\mathcal{V}_{\rm CB}/\mathsf{W_{avl}}$. Therefore the effective thickness $\mathsf{W_{avl}}$ over which the electric field is appreciable is the most important parameter. The second parameter $\mathsf{V_{avl}}$ only determines the curvature of the avalanche current as function of bias.

Extracted parameters	:	$\mathsf{W_{avl}}$, $\mathsf{V_{avl}}$
Help-variable	:	I_{B0}
Approximations	:	$I_C < 0.01\,\mathsf{I_{hc}}$
IC-CAP-function	:	`MXT_veaf_ib`
Equations used from Ref. [2]	:	(4.66)–(4.74) and (4.79)–(4.83)

2.5.5 Reverse Early effect

In Mextram the forward and reverse Early effects are bias-dependent. The parameters $\mathsf{V_{er}}$ and $\mathsf{V_{ef}}$ are the values of these bias-dependent Early voltages when both the base-emitter and base-collector bias are zero. In that case we cannot measure anything. Therefore the bias dependence has to be taken into account in the extraction.

The reverse Early voltage parameter $\mathsf{V_{er}}$ is extracted from the reverse-Early measurement. We are not yet interested in the absolute value of the currents, but only in the variation with bias. We therefore need a help-variable I_{E0} which is the emitter current at $\mathcal{V}_{\rm BE} = 0$.

 ©Koninklijke Philips Electronics N.V. 2001

The emitter current can then be written as

$$I_E = I_{E0} \frac{1 + \dfrac{V_{t_C}}{\mathsf{V_{ef}}}}{1 + \dfrac{V_{t_E}}{\mathsf{V_{er}}} + \dfrac{V_{t_C}}{\mathsf{V_{ef}}}}. \tag{2.25}$$

The quantities V_{t_E} and V_{t_C} are directly related to the base-emitter and base-collector depletion charges. Therefore the parameters we extracted for the capacitances also influence the curvature of the actual Early voltages.

Furthermore, we can see that the emitter current depends also on the forward Early voltage parameter $\mathsf{V_{ef}}$. This means that to do the extraction for $\mathsf{V_{er}}$ properly one needs to have a reasonable good estimate of the $\mathsf{V_{ef}}$. We do this by extracting the Early voltages twice: first extract the reverse Early voltage, then the forward Early voltage, then redo the reverse Early voltage and at last redo the forward Early voltage. Normally one such iteration is enough. For the first time one can use the initial values that we discuss below.

For the calculation of the normalised charges V_{t_E} and V_{t_C} we again neglect the voltage drop over the resistances. We make use of previously given quantities and have

$$V_{t_E} = \frac{\mathsf{V_{d_E}}}{1 - \mathsf{p_E}} \left[1 - (1 - V_{jE}/\mathsf{V_{d_E}})^{1-\mathsf{p_E}} \right] + a_{j_E}(\mathcal{V}_{\mathrm{BE}} - V_{jE}), \tag{2.26a}$$

$$V_{t_C} = (1 - \mathsf{X_p}) \left(\frac{\mathsf{V_{d_C}}}{1 - \mathsf{p_C}} \left[1 - (1 - V_{jC}/\mathsf{V_{d_C}})^{1-\mathsf{p_C}} \right] + b_{jC}(\mathcal{V}_{\mathrm{BC}} - V_{jC}) \right) + \mathsf{X_p}\, \mathcal{V}_{\mathrm{BC}}. \tag{2.26b}$$

Note that the overlap capacitances $\mathsf{C_{BEO}}$ and $\mathsf{C_{BCO}}$ should not be included. Since the Early effect is present in many of the characteristics we will need V_{t_E} and V_{t_C} also in some of the following sections.

Apart from the emitter current it is sometimes also useful to look at the actual Early voltage. This is given by

$$V_{\mathrm{Rev-Early}} = I_E \left(\frac{\partial I_E}{\partial \mathcal{V}_{\mathrm{EB}}} \right)^{-1} = \frac{\mathsf{C_{jE}}\, \mathsf{V_{er}}}{C_{BE}} \left(1 + \frac{V_{t_E}}{\mathsf{V_{er}}} + \frac{V_{t_C}}{\mathsf{V_{ef}}} \right). \tag{2.27}$$

To determine the actual Early voltage from the measurements one must do a numerical differentiation. For comparison with the model one can use the equation given above, where one needs to use the full C_{BE} as given in Eq. (2.16) but with $\mathsf{C_{BEO}} = 0$. It is however more practical to use the same numerical differentiation on the I_E given in Eq. (2.25).

For the optimisation routine it is better to have a good initial estimate of the quantities it needs to optimise. I_{E0} can be estimated as the zero bias value of the measured I_E. $\mathsf{V_{er}}$ can be estimated as the zero bias value of the actual Early voltage calculated from the measurements (i.e. using a numerical differentiation of the first two points).

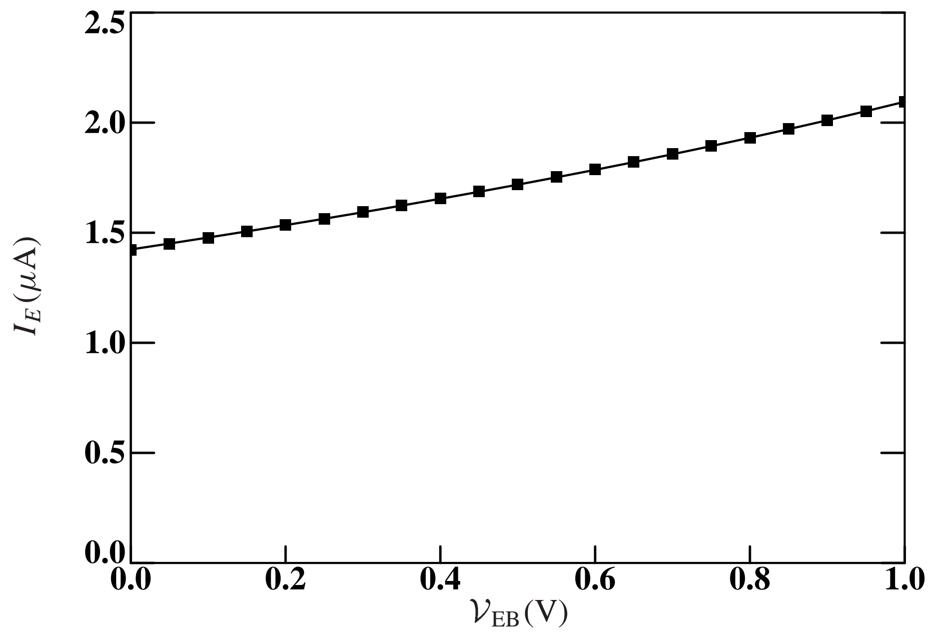

Figure 5: *Measured (markers) and simulated (line) emitter current in the reverse-Early measurement for the extraction of the reverse Early voltage.*

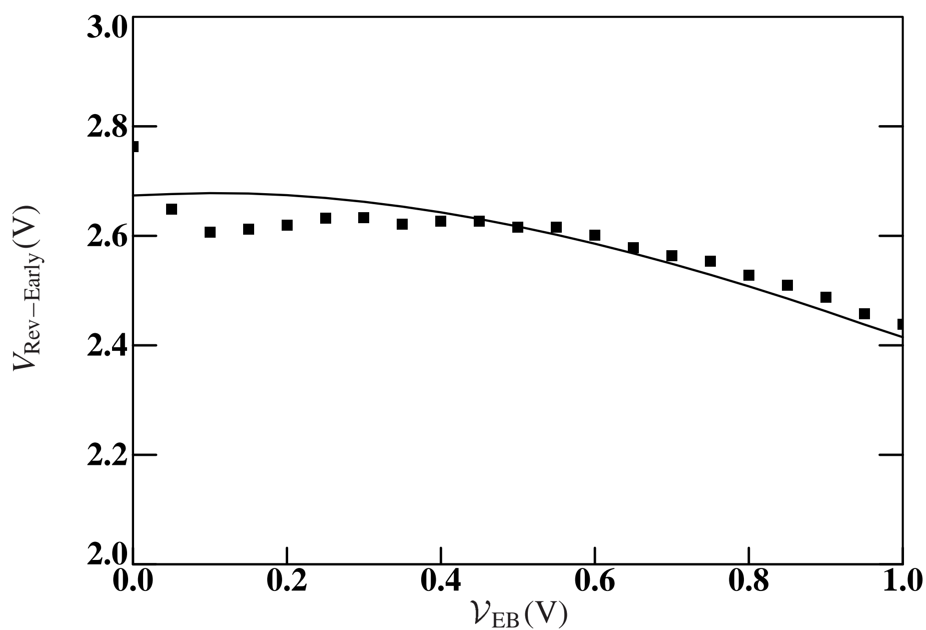

Figure 6: *Actual reverse Early voltage by numerical differentiation of the measured (markers) and simulated (line) emitter current in the reverse-Early measurement.*

 ©Koninklijke Philips Electronics N.V. 2001

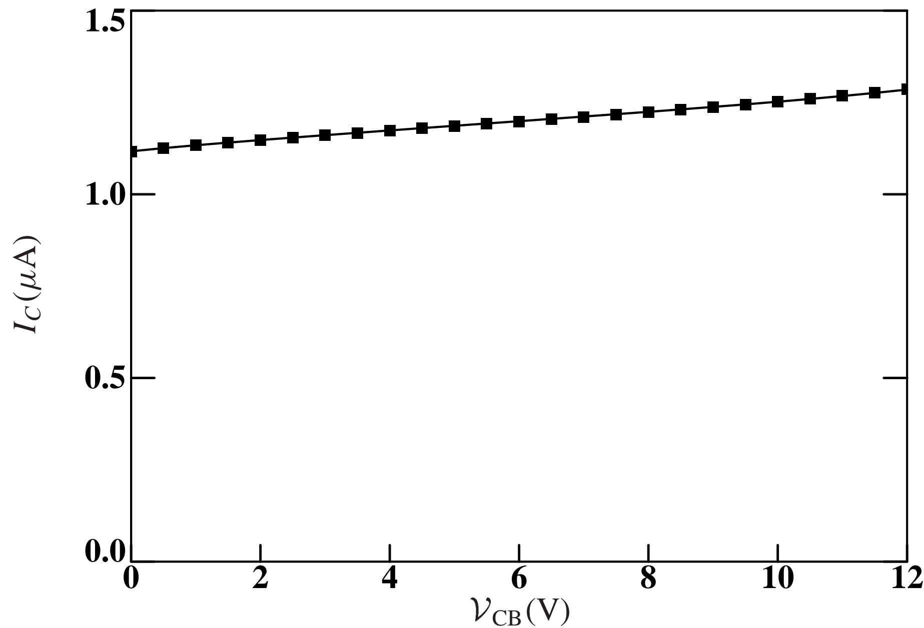

Figure 7: *Measured (markers) and simulated (line) collector current in the forward-Early measurement for the extraction of the forward Early voltage.*

Note that one must stay clear of any base-emitter breakdown effects at high $\mathcal{V}_{EB}$. These are not modelled in Mextram.

Extracted parameter	: $\mathsf{V_{er}}$
Help-variable	: I_{E0}
IC-CAP-function	: `MXT_vear_ie`, `derivative`
Equations used from Ref. [2]	: (4.53), (4.56), (4.112), (4.127), and (4.128)

2.5.6 Forward Early effect

The extraction of the forward Early voltage parameter $\mathsf{V_{ef}}$ is similar to the extraction of $\mathsf{V_{er}}$. Here the forward-Early measurement is used. The approximation for the collector current one can use is

$$I_C = I_{C0}\,\frac{1+\dfrac{V_{t_E}}{\mathsf{V_{er}}}}{1+\dfrac{V_{t_E}}{\mathsf{V_{er}}}+\dfrac{V_{t_C}}{\mathsf{V_{ef}}}} + I_{B0} - I_B\,. \tag{2.28}$$

The voltages V_{t_E} and V_{t_C} are defined as before, Eq. (2.26). We have added $I_{B0} - I_B = I_{\mathrm{avl}}$ to account for the avalanche current. The base current is best taken as the measured base current.

Again we can calculate the actual Early voltage:

$$V_{\mathrm{Forw-Early}} = I_C\,\left(\frac{\partial I_C}{\partial \mathcal{V}_{\mathrm{CB}}}\right)^{-1} = \frac{\mathsf{C_{jc}}\,\mathsf{V_{ef}}}{C_{BC}}\,\left(1+\frac{V_{t_E}}{\mathsf{V_{er}}}+\frac{V_{t_C}}{\mathsf{V_{ef}}}\right). \tag{2.29}$$

©Koninklijke Philips Electronics N.V. 2001

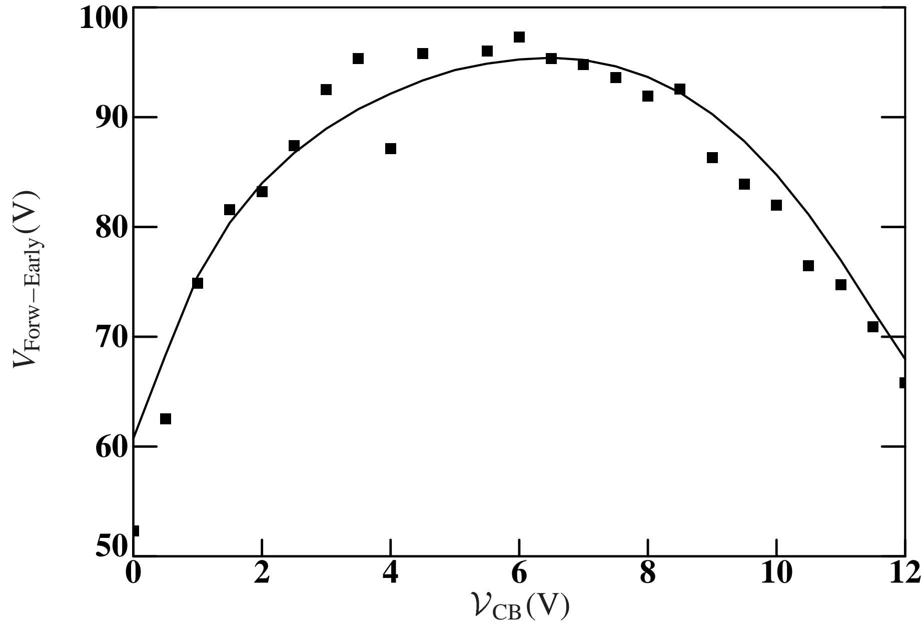

Figure 8: *Actual forward Early voltage by numerical differentiation of the measured (markers) and simulated (line) collector current in the forward-Early measurement.*

Again one can compare the numerical derivatives. When one wants to use the model C_{BC} is given in Eq. (2.21), taking $\mathsf{C_{BCO}} = 0$.

To do the extraction properly one should not include the high collector biases where avalanche becomes important. A practical range over which to optimise is $0 \ldots \frac{1}{2}\mathcal{V}_{\mathrm{CB,max}}$. When plotting the results we include avalanche to get a better idea of how correct the results are.

As before we can give estimates for the quantities we need to optimise. I_{C0} can be estimated as the zero bias value of the measured I_C. $\mathsf{V_{ef}}$ can be estimated as the zero bias value of the actual Early voltage calculated from the measurements (i.e. using a numerical differentiation of the first two points).

Extracted parameter	:	$\mathsf{V_{ef}}$
Help-variable	:	I_{C0}
IC-CAP-function	:	`MXT_veaf_ic`, `derivative`
Equations used from Ref. [2]	:	(4.53), (4.56), (4.112), (4.127), and (4.128)

2.5.7 Collector saturation current

We can now extract the saturation current $\mathsf{I_s}$ of the intrinsic transistor. A non-ideality factor is not needed since we have a good description of the Early effect. For the extraction of $\mathsf{I_s}$ we need the forward-Gummel measurement at small values of the base-emitter voltage ($0.4 < \mathcal{V}_{\mathrm{BE}} < 0.65$). At these small bias values high-injection, quasi-saturation and series resistance effects may be neglected. This gives us the simplified expression for

 ©Koninklijke Philips Electronics N.V. 2001

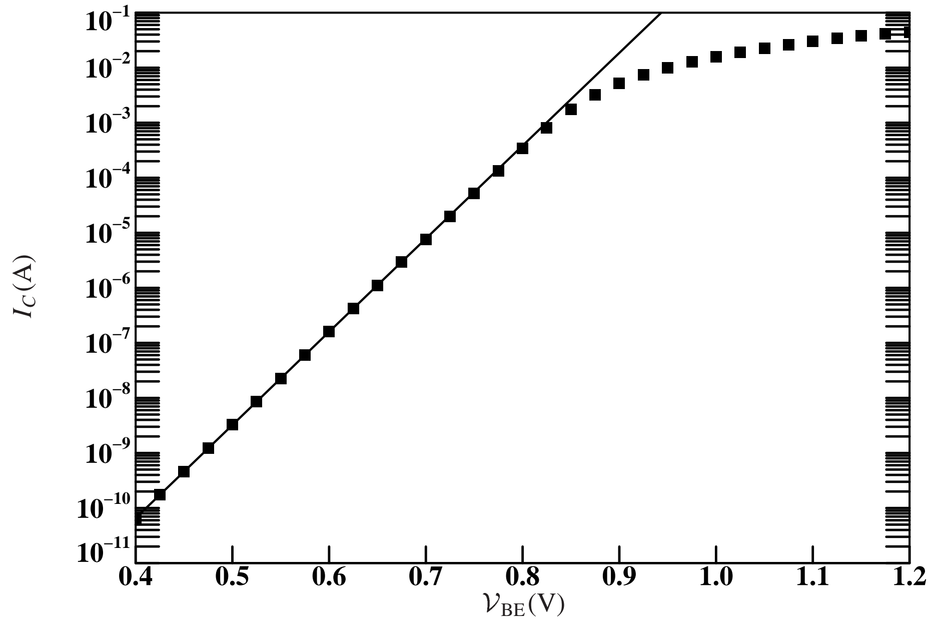

Figure 9: *Measured (markers) and simulated (line) collector current in the forward-Gummel measurement for the extraction of the saturation current.*

the collector current

$$I_C = \frac{\mathsf{I_s}\ e^{\mathcal{V}_{\rm BE}/V_T}}{1 + \dfrac{V_{t_E}}{\mathsf{V_{er}}} + \dfrac{V_{t_C}}{\mathsf{V_{ef}}}}. \tag{2.30}$$

Here $V_T = kT/q$ is the thermal voltage, which needs to be determined accurately from the actual absolute temperature. V_{t_E} and V_{t_C} have been defined in Eq. (2.26).

The initial estimate of $\mathsf{I_s}$ is simply using the first point of the measurement and writing $\mathsf{I_s} = I_C\ e^{-\mathcal{V}_{\rm BE}/V_T}/\mathsf{MULT}$.

Extracted parameter	:	$\mathsf{I_s}$
IC-CAP-function	:	`MXT_forward_ic`
Equations used from Ref. [2]	:	(4.51), (4.53), and (4.56)

2.5.8 Forward current gain

The parameters of the forward base current are extracted from the base current in the forward-Gummel measurements. We prefer to compare the current gain $h_{\rm fe}$ from measurements with a calculated $h_{\rm fe}$ because one can then better see how accurate the fit is. We use the same (measured) collector current for both.

The forward base current only depends on the internal base-emitter voltage $\mathcal{V}_{\rm B_2E_1}$, neglecting the voltage drop in the variable base resistance (for exceptions, see Sec. 2.8.2). When we take the internal bias equal to the external bias $\mathcal{V}_{\rm BE}$, like we did before, we must be sure that resistance effects are not important. For the optimisation of the forward

©Koninklijke Philips Electronics N.V. 2001

current gain $\boldsymbol{\beta}_{\mathsf{f}}$ we would like to be able to use the current gain h_{fe} up till the point where high-injection effects and quasi-saturation start (around $\mathcal{V}_{\mathrm{BE}} = 0.8\ldots0.9\,\mathrm{V}$). We must then correct for the resistances. This is done by using Eq. (2.30) for the collector current to calculate the internal bias:

$$\mathcal{V}_{\mathrm{B_2E_1}} = V_T\ \ln\left[\frac{I_C}{\mathsf{I_s}}\left(1+\frac{V_{t_E}}{\mathsf{V_{er}}}+\frac{V_{t_C}}{\mathsf{V_{ef}}}\right)\right]. \tag{2.31}$$

The external biases are used to calculate V_{t_E} and V_{t_C} given in Eq. (2.26). The ideal and non-ideal base currents are given by

$$I_{B_1} = \frac{\mathsf{I_s}}{\boldsymbol{\beta}_{\mathsf{f}}}\, e^{\mathcal{V}_{\mathrm{B_2E_1}}/V_T}, \tag{2.32a}$$

$$I_{B_2} = \mathsf{I_{Bf}}\,\left(e^{\mathcal{V}_{\mathrm{B_2E_1}}/\mathsf{m_{Lf}}V_T}-1\right) + G_{\mathrm{min}}\,(\mathcal{V}_{\mathrm{BE}}+\mathcal{V}_{\mathrm{BC}}). \tag{2.32b}$$

The minimal conductance G_{min} is needed in the circuit simulator to improve the convergency. It does have an influence on the low-bias current gain and therefore it is included here. The current gain now is

$$h_{\mathrm{fe}} = \frac{I_C}{I_{B_1}+I_{B_2}}, \tag{2.33}$$

where we use the measured collector current.

Normally the forward current gain β_f at zero base-collector bias is somewhat larger than the maximum of h_{fe}. This is due to the reverse Early effect (neglecting I_{B_2}):

$$h_{\mathrm{fe}} \simeq \frac{\boldsymbol{\beta}_{\mathsf{f}}}{1+\dfrac{V_{t_E}}{\mathsf{V_{er}}}}. \tag{2.34}$$

As an initial guess for $\boldsymbol{\beta}_{\mathsf{f}}$ one can therefore take the maximum of h_{fe}. In almost all cases one can take $\mathsf{m_{Lf}} = 2$. Only when the current gain increases slowly for several decades of current one might consider taking another value of $\mathsf{m_{Lf}}$ (possibly close to 1). The non-ideal base current I_{B_2} will then describe the base current over the whole bias range. I_{B_1} is no longer needed and $\boldsymbol{\beta}_{\mathsf{f}}$ will become large.

As an initial estimate for $\mathsf{I_{Bf}}$ one can take $100\,\mathsf{I_s}$.

Extracted parameters	: $\boldsymbol{\beta}_{\mathsf{f}}$, $\mathsf{I_{Bf}}$, $\mathsf{m_{Lf}}$
Approximations	: No high injection/saturation effects in I_C
IC-CAP-function	: `MXT_forward_hfe`
Equations used from Ref. [2]	: (4.57)–(4.59)

2.5.9 Emitter series resistances

One of the simplest way to extract the emitter resistance is from the Giacoletto method [12, 13]. We use the dedicated $\mathsf{R_E}$-flyback measurement. The collector current is kept

 ©Koninklijke Philips Electronics N.V. 2001

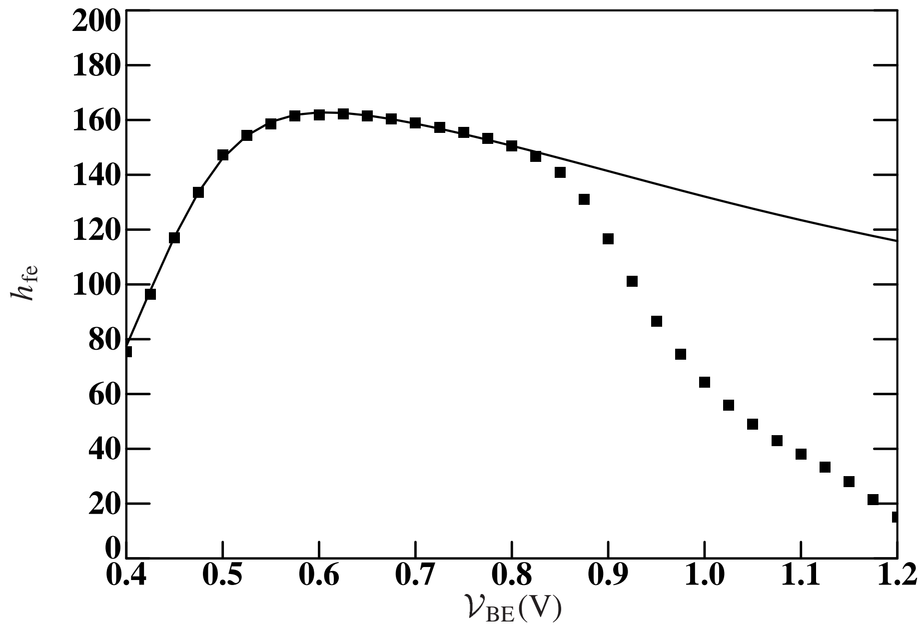

Figure 10: *Measured (markers) and simulated (line) current gain $h_{\rm fe}$ in the forward-Gummel measurement for the extraction of the forward base current parameters.*

zero and the base-emitter bias is increased. The collector-emitter voltage can be estimated as

$$\mathcal{V}_{\rm CE} \simeq I_E \, \mathsf{R_E} + \mathcal{V}_{\rm B_2E_1} - \mathcal{V}_{\rm B_2C_1}. \tag{2.35}$$

We must use the emitter current here and not the base current as originally described [12, 13], since in an IC-process the base current also contains the substrate current.

When we take the derivative of the collector voltage w.r.t. the emitter current we get the resistance

$$R = \frac{\partial \mathcal{V}_{\rm CE}}{\partial I_E}. \tag{2.36}$$

The emitter resistance $\mathsf{R_E}$ is the value of R for the highest emitter current (multiplied with MULT).

In general R will decrease as function of I_E. If it has reached a plateau, the value of R there will be the emitter resistance. If the plateau is not reached one will over-estimate $\mathsf{R_E}$. This is one of the disadvantages of this method. Another disadvantage is that it extracts $\mathsf{R_E}$ for very high currents. When the emitter resistance is current dependent this might not be the value one would like to have.

The emitter resistance extracted from the Giacoletto method can be used directly. We, however, prefer to use it as input for the following method. The most simple way to correct for series resistances is based on the observation of Ning and Tang [14] that there is a deviation in the base current (or collector current) from an ideal exponential curve

©Koninklijke Philips Electronics N.V. 2001

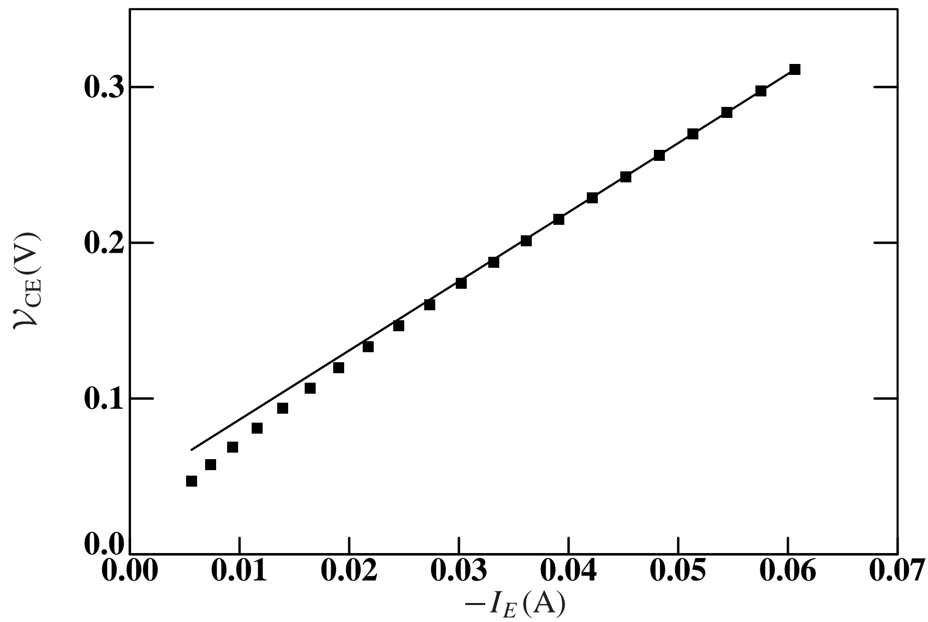

Figure 11: *Measured (markers) and simulated (line) collector voltage in the* $\mathsf{R_E}$*-flyback measurement for the extraction of the emitter series resistance.*

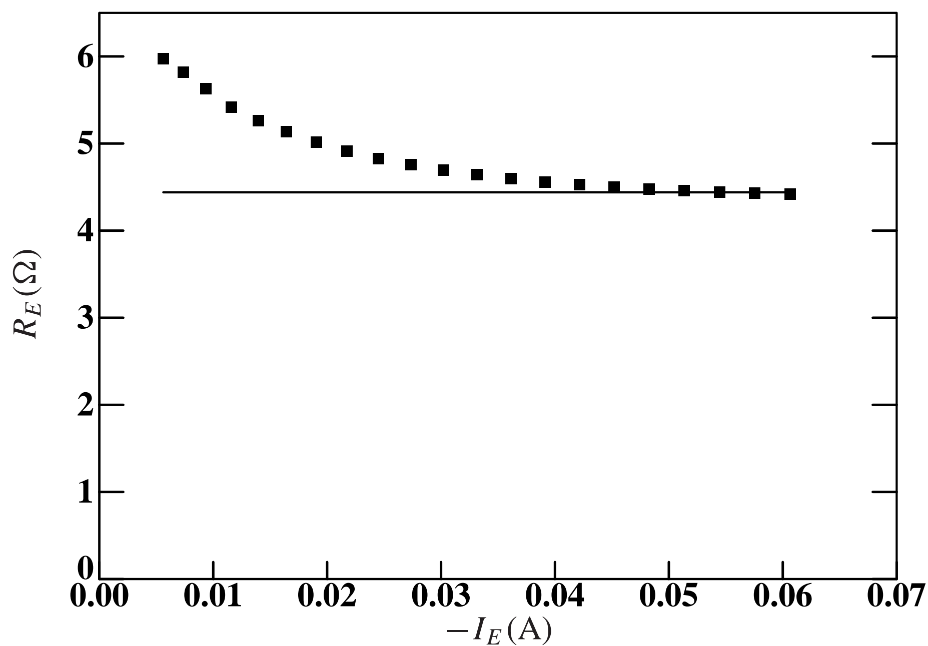

Figure 12: *Derivative of the measured (markers) and simulated (line) collector voltage w.r.t. the emitter current in the* $\mathsf{R_E}$*-flyback measurement for the extraction of the emitter series resistance.*

 ©Koninklijke Philips Electronics N.V. 2001

that can be used to extract the resistance. The external base-emitter bias is a sum of the internal junction bias and the voltage drop due to various series resistances:

$$\mathcal{V}_{\mathrm{BE}} = \mathcal{V}_{\mathrm{B_2E_1}} + \mathcal{V}_{\mathrm{B_1B_2}} + I_B\ \mathsf{R_{Bc}} + (I_C + I_B)\ \mathsf{R_E} + V_{\mathrm{off,Rb}}. \tag{2.37}$$

The internal junction bias $\mathcal{V}_{\mathrm{B_2E_1}}$ is solved iteratively using the measured base current and Eq. (2.32).

The voltage drop over the pinched resistance gives only a small contribution, but we do want to include the variation of the resistance due to charge modulation and current crowding. However, we must make some approximations. The charge modulation can be written as

$$R_{\mathrm{mod}} = \frac{\mathsf{R_{Bv}}}{q_B}, \tag{2.38}$$

where q_B is the normalised base charge. It is the same correction that is present in the collector current:

$$I_C = \frac{I_f - I_r}{q_B} \simeq \frac{\mathsf{I_s}\ \exp(\mathcal{V}_{\mathrm{B_2E_1}}/V_T)}{q_B}. \tag{2.39}$$

This is true only under the assumption that quasi-saturation is not very important which means that we can neglect I_r. (It is also not true when $\mathsf{dE_g} \neq 0$, see Sec. 2.8.1). We also assume that the non-ideal base current is negligible, which means that we can write $I_B = I_f/\boldsymbol{\beta}_{\mathsf{f}}$. The voltage drop is then

$$I_B\ R_{\mathrm{mod}} \simeq I_C\ \mathsf{R_{Bv}}/\boldsymbol{\beta}_{\mathsf{f}}. \tag{2.40}$$

To include also some current crowding effect and the fact that a part of the base current might go through the side-wall we write

$$\mathcal{V}_{\mathrm{B_1B_2}} = V_T\ \ln\left(1 + \frac{\mathsf{R_{Bv}}\ I_C\ (1 - \mathsf{XI_{B_1}})}{\boldsymbol{\beta}_{\mathsf{f}}\ V_T}\right). \tag{2.41}$$

The last non-trivial contribution is $V_{\mathrm{off,Rb}}$ which is a small but constant offset voltage added to correct for the difference between $\mathcal{V}_{\mathrm{BE}}$ and $\mathcal{V}_{\mathrm{B_2E_1}}$ at medium values of the base current. This difference may be due to the presence of the non-ideal base current and the approximation of the variable part of the base resistance. This offset voltage is optimised together with $\mathsf{R_E}$.

In theory the base resistance could be extracted in this way when the emitter resistance is known. However, in practice the influence of the emitter resistance is a factor h_{fe} larger (since the collector current goes through the emitter resistance). Any error in the emitter resistance will then heavily influence the extracted base resistance.

Some alternative methods are given in Refs. [15, 16]. A comparison between different methods is made in Ref. [17]. We think that these methods depend too much on the model one uses to be of general use.

Extracted parameter : $\mathsf{R_E}$
IC-CAP-function : `derivative/MXT_forward_vbe`

©Koninklijke Philips Electronics N.V. 2001

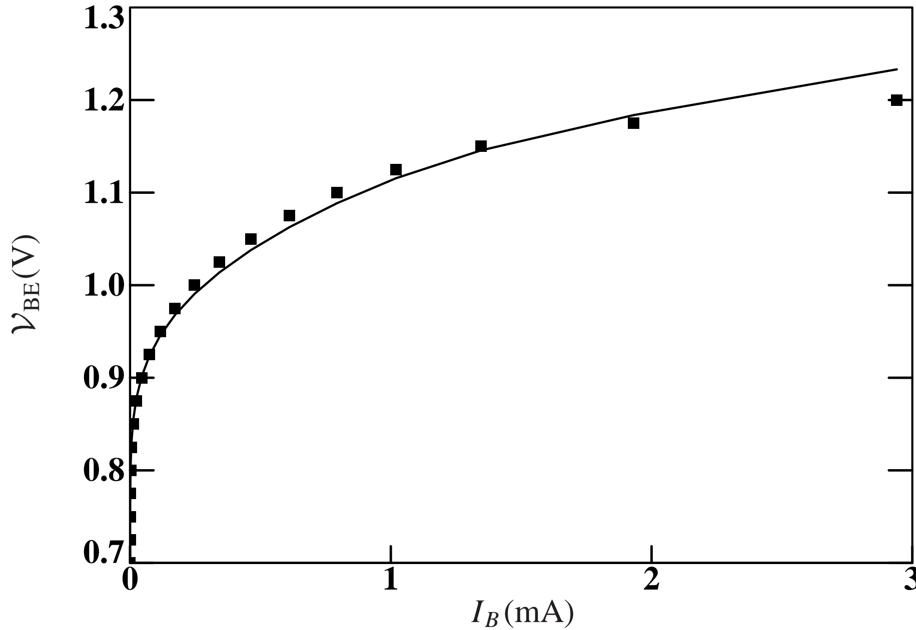

Figure 13: *Measured (markers) and simulated (line) base-emitter bias as function of the base current in the forward-Gummel measurement for the extraction of the emitter series resistance.*

2.5.10 Collector series resistances

The collector series resistance $\mathsf{R_{Cc}}$ can be extracted from the substrate current in the dedicated $\mathsf{R_{Cc}}$-active measurement. The substrate current can be described as

$$I_{\rm sub} = \frac{2\,\mathsf{I_{Ss}}\, e^{\mathcal{V}_{\rm B_1C_1}/V_T}}{1+\sqrt{1+4\,\frac{\mathsf{I_s}}{\mathsf{I_{ks}}}\,e^{\mathcal{V}_{\rm B_1C_1}/V_T}}}. \tag{2.42}$$

The value of the intrinsic base-collector bias can be found from

$$\mathcal{V}_{\rm B_1C_1} = \mathcal{V}_{\rm BC} - \mathsf{R_{Cc}}\, I_C \quad (+\,\mathsf{R_{Bc}}\, I_B). \tag{2.43}$$

Here the currents are from measurements. The last term describes a (small) correction for the constant base resistance. It should only be used when a reasonable estimate of the resistance is available.

The collector series resistance can now be found from the comparison of the simulated and measured substrate currents (as long as the measured one is above the noise level). The substrate saturation current $\mathsf{I_{Ss}}$ must be used as a help-parameter. Later it will be tuned to get the reverse current gain correct. Also the substrate knee current $\mathsf{I_{ks}}$ must be fitted along. (Note that $\mathsf{I_s}$ must already be known.) This knee current can be kept fixed from here on, or it can be tuned to describe the absolute values of the reverse currents later on.

 ©Koninklijke Philips Electronics N.V. 2001

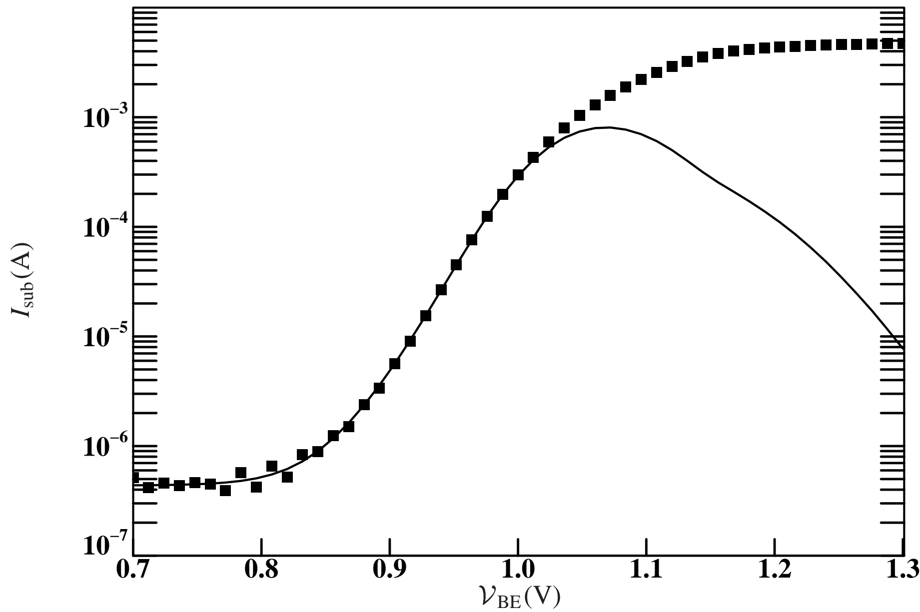

Figure 14: *Measured (markers) and simulated (line) substrate current in the* $\mathsf{R_{Cc}}$*-active measurement for the extraction of the collector series resistance and possibly the substrate knee current.*

Extracted parameters	: $\mathsf{R_{Cc}}$, ($\mathsf{I_{kS}}$)
Help-parameter	: $\mathsf{I_{Ss}}$
IC-CAP-function	: `MXT_hard_sat_isub`
Equations used from Ref. [2]	: (4.61)

2.5.11 Substrate saturation current

The substrate saturation current $\mathsf{I_{Ss}}$ is obtained from the reverse-Gummel measurement. In principle one can extract $\mathsf{I_{Ss}}$ directly from the equation

$$I_{\text{sub}} = \mathsf{I_{Ss}}\, e^{\mathcal{V}_{\text{BC}}/V_T}. \tag{2.44}$$

We will however *not* do this, because it might not give the correct total reverse current gain $h_{\text{fc,tot}}$. This reverse current gain is the ratio of the emitter current and base current $h_{\text{fc,tot}} = I_E/I_B$. The base current consists of the intrinsic base current and the substrate current. In most cases the latter is dominant. The emitter current from Mextram is already determined by parameters that have been extracted before. When the reverse Early modelling is not very accurate the modelled emitter current might differ from the measured emitter current. So when we extract $\mathsf{I_{Ss}}$ directly from the substrate current, we might have a less accurate current gain. To get the total current gain correct we will optimise both

$$h_{\text{fc,sub}} = \frac{I_E}{I_{\text{sub}}}, \tag{2.45}$$

and $I_E/I_{B,\text{intr}}$ (see next section).

©Koninklijke Philips Electronics N.V. 2001

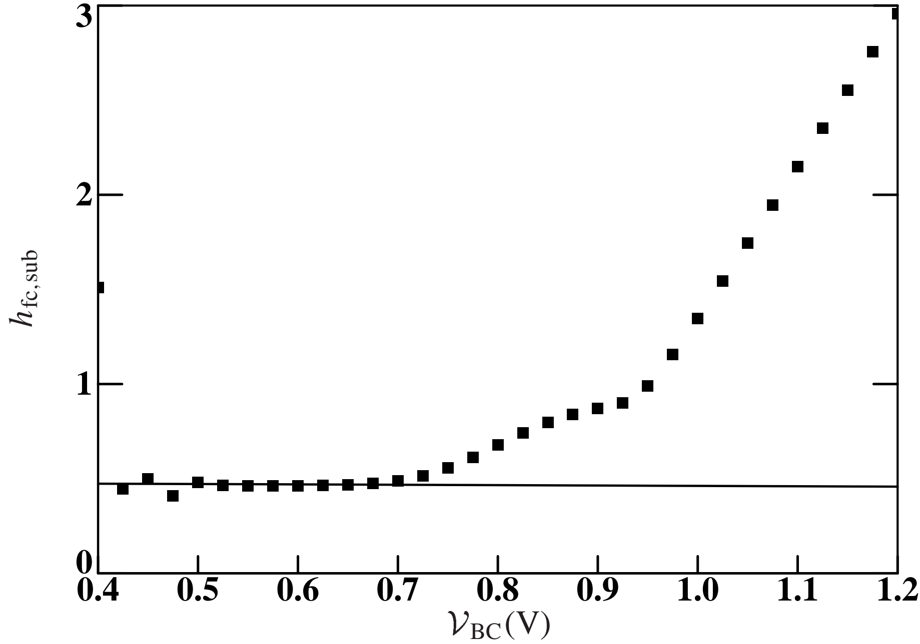

Figure 15: *Measured (markers) and simulated (line) $h_{\text{fc,sub}}$ in the reverse-Gummel measurement for the extraction of the substrate saturation current.*

The emitter current in the reverse-Gummel measurement at small values of $\mathcal{V}_{\text{BC}}$ (not including high injection effects) is

$$I_E = \frac{\mathsf{I_s}\; e^{\mathcal{V}_{\text{BC}}/V_T}}{1 + \dfrac{V_{t_E}}{\mathsf{V_{er}}} + \dfrac{V_{t_C}}{\mathsf{V_{ef}}}}. \tag{2.46}$$

Substituting the expressions for I_{sub} and I_E in the current gain we get

$$h_{\text{fc,sub}} = \frac{\mathsf{I_s}}{\mathsf{I_{Ss}} \left(1 + \dfrac{V_{t_E}}{\mathsf{V_{er}}} + \dfrac{V_{t_C}}{\mathsf{V_{ef}}}\right)}. \tag{2.47}$$

The external biases are used to calculate V_{t_E} and V_{t_C} given in Eq. (2.26).

The substrate saturation current should be extracted from the low bias regime, where the current gain is constant.

The initial estimate of $\mathsf{I_{Ss}}$ is simply using the first point of the measurement and writing $\mathsf{I_{Ss}} = -I_{\text{sub}}\; e^{-\mathcal{V}_{\text{BC}}/V_T}/\mathsf{MULT}$. Note the minus sign which implies a substrate current coming out of the transistor.

When $h_{\text{fc,sub}}$ is plotted as function of I_E also an estimate for $\mathsf{I_{ks}}$ can be given: it is approximately the emitter current where $h_{\text{fc,sub}}$ starts to rise.

 ©Koninklijke Philips Electronics N.V. 2001

Extracted parameter	: $\mathsf{I_{Ss}}$
Approximations	: No high injection effects in I_E and I_{sub}
IC-CAP-function	: `MXT_reverse_hfc_sub`
Equations used from Ref. [2]	: (4.52), (4.53), (4.56), and (4.61)

2.5.12 Reverse current gain

The extraction of the reverse base current parameters is done in mainly the same way as for the forward base current. We compare the measured h_{fc} and calculated h_{fc}. In the reverse-Gummel measurement the base-collector is forward biased. This means that the external base current contains not only the internal base current but also the substrate current. To calculate the internal current gain we must correct for this. Hence we get from the measurements

$$h_{\text{fc}} = \frac{|I_E|}{|I_B| - |I_{\text{sub}}|}. \tag{2.48}$$

One needs to be careful with the signs of the currents here, hence the absolute signs. Since one is subtracting two currents the result can be noisy. Some smoothing is perhaps necessary.

The internal base-collector bias $\mathcal{V}_{\text{B}_1\text{C}_1}$ is calculated using Eq. (2.46) as

$$\mathcal{V}_{\text{B}_1\text{C}_1} = V_T \ \ln\left[\frac{I_E}{\mathsf{I_s}}\left(1 + \frac{V_{t_E}}{\mathsf{V_{er}}} + \frac{V_{t_C}}{\mathsf{V_{ef}}}\right)\right]. \tag{2.49}$$

The external biases are used to calculate V_{t_E} and V_{t_C} given in Eq. (2.26). The ideal and non-ideal reverse base currents are given by

$$I_{\text{ex}} = \frac{\mathsf{I_s}}{\beta_{\mathsf{ri}}}\, e^{\mathcal{V}_{\text{B}_1\text{C}_1}/V_T}, \tag{2.50a}$$

$$I_{B_3} = \mathsf{I_{Br}}\, \frac{e^{\mathcal{V}_{\text{B}_1\text{C}_1}/V_T}}{e^{\mathcal{V}_{\text{B}_1\text{C}_1}/2V_T} + e^{\mathsf{V_{Lr}}/2V_T}} + G_{\text{min}}\, (\mathcal{V}_{\text{BE}} + \mathcal{V}_{\text{BC}}). \tag{2.50b}$$

The simulated internal current gain then is

$$h_{\text{fc}} = \frac{I_E}{I_{\text{ex}} + I_{B_3}}, \tag{2.51}$$

where the measured emitter current is used.

Again one needs to concentrate only on that part of the current gain below the point where high-injection and quasi-saturation effects start. When the current gain shows a clear low level plateau, an increase, a high level plateau and a drop (for increasing bias) the parameter $\mathsf{V_{Lr}}$ should get the value of $\mathcal{V}_{\text{BC}}$ where the initial plateau ends. Otherwise it should have a low value (and it doesn't need to be extracted anymore).

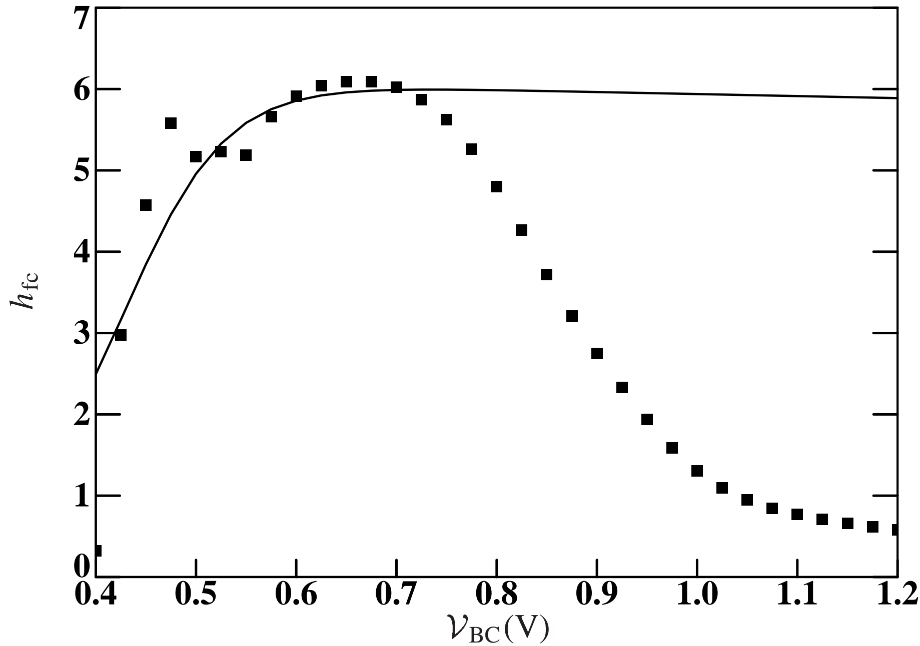

Figure 16: *Measured (markers) and simulated (line) intrinsic current gains in the reverse-Gummel measurement for the extraction of the reverse base current parameters.*

Sometimes the low current part is very noisy. One of the main reasons for this noise is the noise-floor of the substrate current. This might be higher than that of the other currents, due to the background noise of the whole wafer. This is especially so when the substrate current has a long path between intrinsic transistor and substrate bond-pad, for instance due to deep trench isolation. To reduce this noise one might try to calculate the substrate current from all other currents: $I_{sub} = -I_C - I_B - I_E$ (note that I_C and I_E as measured have a different sign). If this does not help the parameters $\mathsf{I_{Br}}$ and $\mathsf{V_{Lr}}$ can be extracted directly from I_B if the non-ideal part is large enough (i.e. I_B must be large enough compared to I_{sub}).

An initial value for the reverse current gain β_{ri} is the maximum of h_{fc}. As an initial estimate for $\mathsf{I_{Br}}$ one can take 100 $\mathsf{I_S}$.

Extracted parameters	: β_{ri}, $\mathsf{I_{Br}}$, $\mathsf{V_{Lr}}$
Approximations	: No high injection effects in I_E and I_{ex}
IC-CAP-function	: `MXT_reverse_hfc`
Equations used from Ref. [2]	: (4.60) and (4.63)–(4.65)

 ©Koninklijke Philips Electronics N.V. 2001

2.6 High current parameters

The extraction of the high-current parameters is not so straightforward as that of the low current parameters. This section is therefore ordered in another way.

First self-heating is discussed. Note that for taking self-heating into account one must have the values of the temperature parameters, or at least some good estimates. The extraction of these parameters is treated in Chapter 3.

Next we show how one can calculate the collector current for the Gummel plot or output-characteristic and how we calculate the cut-off frequency. Then we discuss quasi-saturation, what parameters influence it, and how we can observe this in the measurements. This discussion will be focused on parameter extraction.

Only when we have done that we turn to the parameter extraction methodology of the high-current parameters. We close with the extraction of $\mathsf{X}_{\mathsf{ext}}$ from the high currents in reverse.

2.6.1 Self-heating

To be able to extract the high-current parameters correctly, it is important to take self-heating into account. This means that one must determine the thermal resistance R_{th}. We believe that one must do this, even when one does not plan to include self-heating in the circuit simulations for design. This is the only way to ensure that one does not try to explain certain physical effects (self-heating) with parameters that are meant to describe other physical effects (quasi-saturation).

It is important to realize that the thermal resistance for a transistor in a packaged device can be much lower than the thermal resistance measured on-wafer. Here we will of course only consider the one relevant for parameter extraction.

Due to self-heating the temperature of the transistor will rise with an amount given by

$$\Delta T = \mathsf{R}_{\mathsf{th}}\,(I_B\,\mathcal{V}_{\mathrm{BE}} + I_C\,\mathcal{V}_{\mathrm{CE}}). \tag{2.52}$$

The collector part is obviously the most important contribution to the self-heating. Typical values of R_{th} are 100–500 °C/W but higher values are becoming more common due to oxide isolation instead of junction isolation and due to SOI processes.

The thermal resistance is extracted from the base-emitter voltage in the output-characteristic measurement, for which the base current is constant. For negligible self-heating a constant base current implies a constant internal base-emitter voltage. (For exceptions in SiGe processes, see Sec. 2.8.2). When self-heating can not be neglected the saturation current I_s increases with increasing power dissipation. The base-emitter voltage then decreases to keep the base-current constant. From this decrease we extract R_{th}.

For high currents we have approximately

$$I_B \simeq \frac{\mathsf{I}_{\mathsf{sT}}}{\beta_{\mathsf{fT}}}\, e^{\mathcal{V}_{\mathrm{B_2E_1}}/V_T}, \tag{2.53}$$

©Koninklijke Philips Electronics N.V. 2001

from which we calculate the internal junction voltage $\mathcal{V}_{B_2E_1}$. This leads to an external base-emitter voltage of

$$\mathcal{V}_{BE} \simeq V_T \ \ln \frac{I_B \ \beta_{fT}}{I_{sT}} + I_C \, R_{ET}, \tag{2.54}$$

where one can use the measured currents. Note that from here on we use the parameters *after* temperature scaling [2], denoted by an extra subindex T.

Since R_E is also present in Eq. (2.54) we need to know its value accurately. Since this is not always the case it is better to consider R_E a help-parameter here and extract it together with R_{th}. So before the extraction one must remember the old value of R_E, then do the extraction which gives R_{th} and R_E, and then set R_E to the previously extracted and remembered value. (As an alternative, one can of course decide to extract R_E just from this measurement [18]. It does not have all the disadvantages of the Giacoletto method.) More elaborate ways to extract R_{th} have been given in Refs. [19, 20].

For better accuracy of Eq. (2.54) one needs to take other effects into account also. The most important effect is that of the non-ideal base current I_{B_2}, but also the voltage drop over the base resistances can be calculated. When including these effects it is no longer possible to calculate the quantities directly: one has to solve the internal junction voltages, as calculated for the output characteristic (see next subsection). Details are given in Section 5.1.21.

The temperature parameter that has the most influence on this extraction is V_{g_B} which determines the temperature behaviour of I_s. When this parameter is not extracted yet, at least an estimate should be given. The value of R_{th} will depend only slightly on V_{g_B}.

Extracted parameter	: R_{th}
Help-parameter	: R_E, (V_{g_B})
Approximations	: No avalanche ($I_{avl} \ll I_B$)
	: No hard saturation (I_{ex}, $I_{sub} \ll I_B$)
IC-CAP-function	: `MXT_ic_vce`
Equations used from Ref. [2]	: (4.57)–(4.59), (4.37) and others.

2.6.2 Output-characteristics and forward-Gummel

In this section we will only discuss how one can calculate the collector current in the output-characteristic measurement. In the same way we can calculate the collector current in the forward-Gummel measurement, or in the forward Gummel results that are also measured along with the *S*-parameters. The actual parameter extraction procedure is discussed in Section 2.6.5.

Up till now we have calculated the Mextram simulation results using simplifications of the full Mextram equations and without iteratively solving internal biases. This was possible since high-current effects could be neglected, which from now on is no longer true. We also need to take more of the Mextram equations into account (either all those belonging to the forward mode, or all those of reverse mode). This also means that we need to actually solve for some internal biases, since we can no longer use the external ones.

 ©Koninklijke Philips Electronics N.V. 2001

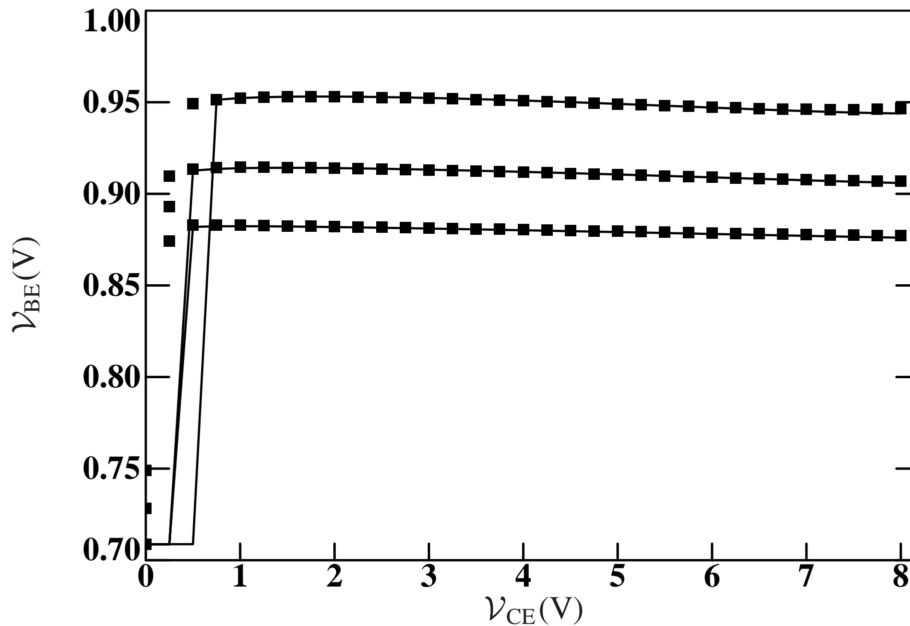

Figure 17: *Measured (markers) and simulated (line) base-emitter voltage in the output-characteristic measurement for the extraction of the thermal resistance. Note that in the left-part of the figure auto-ranging is used, which makes the value of the calculated $\mathcal{V}_{\mathrm{BE}}$ equal to the minimum of the measured $\mathcal{V}_{\mathrm{BE}}$.*

The most straightforward way to do this is making use of a circuit simulator. For the output-characteristic this is a good option. We will see that it is not so good an option for the cut-off frequency (see also Sec. 5.3). Furthermore, not everyone has a link to a circuit simulator. Therefore we will now describe how one can calculate the collector current. Some of the details are given in Section 5.1.21.

We need to calculate the collector current as function of the base current I_B and the collector-emitter bias $\mathcal{V}_{\mathrm{CE}}$. When we have done this, we can use it not only in the output-characteristic, but also in the Gummel plot. The advantage of using I_B instead of $\mathcal{V}_{\mathrm{BE}}$ is that the internal base-emitter voltage $\mathcal{V}_{\mathrm{B_2E_1}}$ is then much better determined (it does not depend on the emitter resistance for instance). This gives a better description of I_C when the resistances are not very well known.

The first step is to calculate the internal base-emitter bias from the base current. Since the non-ideal base current can become dominant even for higher base currents (e.g. when $\mathsf{m_{Lf}}$ is close to 1), we need to solve a non-linear equation

$$I_B = I_{B_1}(\mathcal{V}_{\mathrm{B_2E_1}}) + I_{B_2}(\mathcal{V}_{\mathrm{B_2E_1}}). \tag{2.55}$$

The assumption here is that the avalanche currents and reverse base currents can be neglected. This also means that it is not possible to include the part of the output-characteristic where avalanche is important.

The internal base-collector bias can now be calculated as

$$\mathcal{V}_{\mathrm{B_2C_1}} = \mathcal{V}_{\mathrm{B_2E_1}} + I_C\ \mathsf{R_{CcT}} + (I_B + I_C)\ \mathsf{R_{ET}} - \mathcal{V}_{\mathrm{CE}}. \tag{2.56}$$

©Koninklijke Philips Electronics N.V. 2001

Here we use the measured currents I_B and I_C. The error we make here is not very large, especially when the simulated and measured collector currents are close to each other. The advantage is that the procedure is more robust.

Next we have to solve for $I_{C_1C_2}$ using the equation

$$I_{C_1C_2} = I_N = \mathsf{I_{sT}} \, \frac{e^{\mathcal{V}_{\mathrm{B_2E_1}}/V_T} - e^{V^*_{B_2C_2}/V_T}}{q_B}. \tag{2.57}$$

The internal base-collector bias $V^*_{B_2C_2}$ can be calculated from the current $I_{C_1C_2}$ and the bias $\mathcal{V}_{\mathrm{B_2C_1}}$ by calculating first x_i/W_{epi} and p_0^*. The base charge q_B can also be given once $\mathcal{V}_{\mathrm{B_2E_1}}$, $\mathcal{V}_{\mathrm{B_2C_1}}$, and $I_{C_1C_2}$ are known (also $V^*_{B_2C_2}$ will be needed.) So Eq. (2.57) is a non-linear equation in $I_{C_1C_2}$ that can be solved iteratively. The (external) collector current is then of course equal to $I_{C_1C_2}$.

In the approach above we first calculate $\mathcal{V}_{\mathrm{B_2E_1}}$ from the measured base current and next we iteratively solve $I_{C_1C_2}$. This has the disadvantage that the expression for the base current can not depend on the collector current $I_{C_1C_2}$ (either directly or indirectly via $\mathcal{V}^*_{\mathrm{B_2C_2}}$). This means that neutral base recombination (see Sec. 2.8.2) and avalanche can not be included. To include both effects one needs to solve $\mathcal{V}_{\mathrm{B_2E_1}}$ and $I_{C_1C_2}$ simultaneously from Eqs. (2.55) and (2.57). For more detail see Section 5.1.21.

IC-CAP-function	:	`MXT_ic_vce`
Approximations	:	No hard saturation (I_{ex}, $I_{\mathrm{sub}} \ll I_B$)
Equations used from Ref. [2]	:	(4.51)–(4.59), (4.94)–(4.104), T-scaling and others

2.6.3 Cut-off frequency

In this section we will discuss how one can calculate the cut-off frequency f_T from measurements and from simulations. The actual parameter extraction procedure is discussed in Section 2.6.5.

The cut-off frequency is defined as the frequency where the current gain h_{fe} becomes unity. In almost all cases the current gain as function of frequency f shows ideal-first order roll-off up to f_T or even beyond:

$$h_{\mathrm{fe}} = \frac{h_{\mathrm{fe,0}}}{1 + j\, h_{\mathrm{fe,0}}\; f/f_T}. \tag{2.58}$$

The current gain itself can be expressed in terms of Y-parameters as

$$h_{\mathrm{fe}} = h_{21} = \frac{Y_{21}}{Y_{11}}. \tag{2.59}$$

We want to have the cut-off frequency as function of collector current. Normally not for every bias point a complete frequency sweep is done. Hence we need to determine f_T at a single frequency point.

 ©Koninklijke Philips Electronics N.V. 2001

There are two ways to calculate the cut-off frequency. The first one is simply

$$f_T = f\ |h_{\rm fe}|. \tag{2.60}$$

This is correct only at sufficient high frequencies such that $h_{\rm fe,0}\, f/f_T \gg 1$. In practice the ideal form in Eq. (2.58) is no longer correct close to f_T. Since $h_{\rm fe,0}$ is of the order of 100, this leaves only a limited frequency range where this method is accurate. When f_T varies as function of collector current it is important to make sure that the frequency at which one does the measurement is in this range for all currents.

A better method is

$$f_T = \frac{f}{\mathrm{Im}\ (1/h_{\rm fe})}. \tag{2.61}$$

This method can also be used for intermediate frequencies. The only limitation is that the frequency must be sufficiently high to measure this imaginary part accurately. (Hence $h_{\rm fe,0}\, f/f_T$ must be measurable accurately compared to 1. It doesn't need to be much larger.)

It is instructive to use both methods and see what the difference is in practical cases.

The simulated cut-off frequency is determined in another way:

$$\frac{1}{2\pi\ f_T} = \tau_T = \left.\frac{\mathrm{d}Q}{\mathrm{d}I_C}\right|_{\mathcal{V}_{\rm CE}}. \tag{2.62}$$

Here τ_T is the total emitter-collector transit time. It is related to the differential charge $\mathrm{d}Q$ that has to be supplied by the base and to the differential current $\mathrm{d}I_C$, both under the restraint of a constant collector-emitter bias $\mathcal{V}_{\rm CE}$. Note that also the depletion charges between base and collector add to the total differential charge, as well as the overlap charges related to $\mathsf{C_{BEO}}$ and $\mathsf{C_{BCO}}$.

The calculation is now done in three steps. First we must determine the DC operating point, just as we did for the output-characteristic. This means iteratively solving for the three independent quantities $\mathcal{V}_{\rm B_2E_1}$, $\mathcal{V}_{\rm B_2C_1}$, and $I_{C_1C_2}$ (where the last simply equals the given collector current.)

Second, we must determine the small signal variations. This means that we must calculate for instance the variation of I_N as function of variations in the three independent quantities. By using the fact that $\mathcal{V}_{\rm CE}$ is constant and that we have current conservation ($I_N = I_{C_1C_2}$) we find

$$\mathrm{d}\mathcal{V}_{\rm CE} = \frac{\partial \mathcal{V}_{\rm CE}}{\partial \mathcal{V}_{\rm B_2E_1}}\,\mathrm{d}\mathcal{V}_{\rm B_2E_1} + \frac{\partial \mathcal{V}_{\rm CE}}{\partial \mathcal{V}_{\rm B_2C_1}}\,\mathrm{d}\mathcal{V}_{\rm B_2C_1} + \frac{\partial \mathcal{V}_{\rm CE}}{\partial I_{C_1C_2}}\,\mathrm{d}I_{C_1C_2} = 0, \tag{2.63a}$$

$$\mathrm{d}I_N = \frac{\partial I_N}{\partial \mathcal{V}_{\rm B_2E_1}}\,\mathrm{d}\mathcal{V}_{\rm B_2E_1} + \frac{\partial I_N}{\partial \mathcal{V}_{\rm B_2C_1}}\,\mathrm{d}\mathcal{V}_{\rm B_2C_1} + \frac{\partial I_N}{\partial I_{C_1C_2}}\,\mathrm{d}I_{C_1C_2} = \mathrm{d}I_{C_1C_2}. \tag{2.63b}$$

By solving these two equations we can calculate $\mathrm{d}\mathcal{V}_{\rm B_2E_1}/\mathrm{d}I_{C_1C_2}$ and $\mathrm{d}\mathcal{V}_{\rm B_2C_1}/\mathrm{d}I_{C_1C_2}$, both under the condition that $\mathcal{V}_{\rm CE}$ is constant.

©Koninklijke Philips Electronics N.V. 2001

The third step is to calculate the transit time using Eq. (2.62). The differential charge can be calculated similar to differential voltage and current above:

$$\mathrm{d}Q = \frac{\partial Q}{\partial \mathcal{V}_{\mathrm{B_2E_1}}}\,\mathrm{d}\mathcal{V}_{\mathrm{B_2E_1}} + \frac{\partial Q}{\partial \mathcal{V}_{\mathrm{B_2C_1}}}\,\mathrm{d}\mathcal{V}_{\mathrm{B_2C_1}} + \frac{\partial Q}{\partial I_{C_1C_2}}\,\mathrm{d}I_{C_1C_2}. \tag{2.64}$$

In this way we can calculate the cut-off frequency f_T as function of the collector current I_C and the collector-emitter bias $\mathcal{V}_{\mathrm{CE}}$. Again it is useful to use the collector current as input, rather than the base-emitter voltage. The collector current gives a much more direct way to determine the internal biases of the transistor. Using the external base-emitter voltage would make one very dependent on the series resistances, which are not always accurately known. So, even when the absolute value of the collector current as function of bias is not very good described (yet), it is possible to give a good description of f_T as function of I_C.

Initialisation of parameters Just as for the other parameters, we need an estimate of the initial values of the transit time parameters (see also Sec. 2.3). For the emitter and base transit time we can use the maximum of the measured f_T:

$$\tau_{\mathrm{E}} = \tau_{\mathrm{B}} = \frac{1}{10\,\pi\ \max(f_T)}. \tag{2.65}$$

For the transit time of the epilayer and the reverse transit time we can use

$$\tau_{\mathrm{epi}} = \frac{W_{\mathrm{epi}}^2}{4\,\mu_0\,V_T}, \tag{2.66a}$$

$$\tau_{\mathrm{R}} = (\tau_{\mathrm{B}} + \tau_{\mathrm{epi}})\,\frac{1 - \mathrm{XC_{jC}}}{\mathrm{XC_{jC}}}. \tag{2.66b}$$

In the implementation of the calculation of f_T that we use (see Sec. 5.1.22), we have an extra feature that makes use of the physical relation of various parameters. Whenever one of the three parameters τ_{B}, τ_{epi}, and τ_{R} is set to a negative value, its value in further calculations will be given by the following initialisation formulas:

$$\tau_{\mathrm{B}} = \frac{\mathrm{V_{er}}\,(1 - \mathrm{XC_{jE}})\,\mathrm{C_{jE}}}{\mathrm{I_k}}, \tag{2.67a}$$

$$\tau_{\mathrm{epi}} = \tau_{\mathrm{B}}\,\frac{\mathrm{I_s}\,\mathrm{I_k}\,\mathrm{R_{Cv}}^2}{4\,V_T^2}\,e^{\mathrm{V_{d_C}}/V_T}, \tag{2.67b}$$

$$\tau_{\mathrm{R}} = (\tau_{\mathrm{B}} + \tau_{\mathrm{epi}})\,\frac{1 - \mathrm{XC_{jC}}}{\mathrm{XC_{jC}}}. \tag{2.67c}$$

These formulas are based on the derivation of the charge contributions [11] at the reference temperature. (For SiGe transistors the formulas do not hold. They should be corrected for bandgap narrowing in the base. But there is no parameter available for this.)

 ©Koninklijke Philips Electronics N.V. 2001

The use of these automatically calculated initial values has several advantages.
• It is the first order extraction, since using these values leaves only τ_E to be extracted on f_T.

• It makes it possible to extract other high-current parameters even when the transit times are not yet optimised.

• When the extraction is overdetermined, it gives the possibility to fix one or more of the transit time parameters in a physical way. The others can then be optimised.

Of course, the actual parameter value, and not the negative dummy value, must be given when using a circuit simulator since negative τ's are not physical and are therefore not allowed in the simulators. The actual value that is used can be found, for instance, using the function `MXT_show_parms`.

IC-CAP-function	:	`MXT_ft`
Approximations	:	No avalanche ($I_{\mathrm{avl}} \ll I_B$)
	:	No hard saturation (I_{ex}, $I_{\mathrm{sub}} = 0$)
Equations used from Ref. [2]	:	Many, including the temperature rules.

2.6.4 Quasi-saturation

The extraction of high current parameters is not always easy. It helps if one has an understanding of the physics behind the transistor behaviour. Quasi-saturation is one of the more difficult physical effects. We will discuss it now.

In the normal forward mode the base-emitter is forward biased. Externally the base-collector is reverse biased. The base-collector junction should therefore not be open. There is however a voltage drop between the external collector and the internal collector. This drop is a result of the constant collector resistance $\mathsf{R_{Cc}}$ and, even more important, the voltage drop over the collector epilayer. When the internal base-collector bias[1] $\mathcal{V}_{\mathrm{B_2C_2}}$ is forward biased due to the voltage drop, we speak of quasi-saturation. To be more specific, with forward biased we mean a forward bias of around $\mathsf{V_{d_C}}$ or more.

There are two physical effects that can lead to quasi-saturation. The first effect is simply an ohmic voltage drop over the epilayer due to its resistance. We call this ohmic quasi-saturation. This resistance is modelled with the parameter $\mathsf{R_{Cv}}$ (the variable Collector Resistance). The second effect is well known under the name Kirk effect. The voltage drop is now not due to an ohmic resistance, but due to a space-charge resistance. This resistance is modelled with the parameter $\mathsf{SCR_{Cv}}$ (Space Charge Resistance of the Collector, also variable). In general the space charge resistance is a few times the ohmic resistance: $\mathsf{SCR_{Cv}} > \mathsf{R_{Cv}}$. The cross-over between the two regimes is governed by the parameter $\mathsf{I_{hc}}$ (hot carrier current).

The onset of quasi-saturation It is important for a compact model to accurately predict where the onset of quasi-saturation is. In Mextram quasi-saturation starts when the

[1] In Mextram 504 the actual value that should be used is not $\mathcal{V}_{\mathrm{B_2C_2}}$, but $V^*_{B_2C_2}$ [1, 2]. The difference between the two is of no importance for the present discussion and will therefore be neglected.

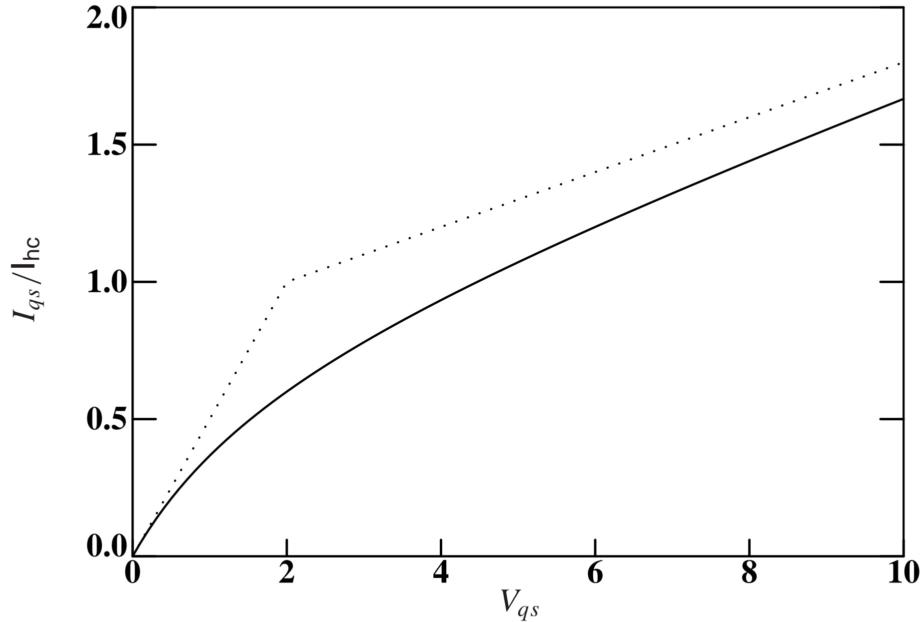

Figure 18: *The current I_{qs} where quasi-saturation starts as function of the voltage drop over the epilayer $V_{qs} = \mathsf{V_{dC}} - \mathcal{V}_{\mathrm{B_2C_1}}$. The low-voltage limit $I_{qs} = V_{qs}/\mathsf{R_{Cv}}$ and the high-voltage limit $I_{qs} = V_{qs}/\mathsf{SCR_{Cv}} + \text{constant}$ are also shown (dotted). The values used are* $\mathsf{I_{hc}}\,\mathsf{R_{Cv}} = 2\,\mathrm{V}$ *and* $\mathsf{I_{hc}}\,\mathsf{SCR_{Cv}} = 10\,\mathrm{V}$.

epilayer current is equal to I_{qs}, given by

$$V_{qs} = \mathsf{V_{dC}} - \mathcal{V}_{\mathrm{B_2C_1}}, \tag{2.68a}$$

$$I_{qs} = \frac{V_{qs}}{\mathsf{SCR_{Cv}}}\,\frac{V_{qs} + \mathsf{I_{hc}}\,\mathsf{SCR_{Cv}}}{V_{qs} + \mathsf{I_{hc}}\,\mathsf{R_{Cv}}}. \tag{2.68b}$$

In Fig. 18 we show how I_{qs} varies with V_{qs}. How do we interpret this equation? When quasi-saturation starts the internal base-collector bias $\mathcal{V}_{\mathrm{B_2C_2}}$ equals $\mathsf{V_{dC}}$, as mentioned before. This means that $V_{qs} = \mathcal{V}_{\mathrm{B_2C_2}} - \mathcal{V}_{\mathrm{B_2C_1}} = \mathcal{V}_{\mathrm{C_1C_2}}$ is the voltage drop over the epilayer, at the onset of quasi-saturation. For low external base-collector bias (low V_{qs}) the current that runs through the epilayer is then $I_{qs} = V_{qs}/\mathsf{R_{Cv}}$, just Ohm's law. For high external base-collector bias (high V_{qs}) we have simply $I_{qs} = V_{qs}/\mathsf{SCR_{Cv}}$. This is also Ohm's law, but with a different resistance. We now see that as long as there is no quasi-saturation, i.e. $I_{C_1C_2} < I_{qs}$, the resistance of the epilayer is somewhere between $\mathsf{R_{Cv}}$ and $\mathsf{SCR_{Cv}}$, its value depending on whether $I_{C_1C_2}$ is smaller or larger than $\mathsf{I_{hc}}$.

How do we observe this onset of quasi-saturation in measurements? When the transistor is in quasi-saturation, the performance degrades dramatically. This can be seen in the current gain h_{fe} and the cut-off frequency f_T, which start to decrease. As an example we look at $\mathcal{V}_{\mathrm{CB}}$-dependence of the current gain in Fig. 19. We took the ratio between $\mathsf{SCR_{Cv}}$ and $\mathsf{R_{Cv}}$ rather large. For small $\mathcal{V}_{\mathrm{CB}}$ the resistance is low which means that the points where the current gain starts to drop are far apart. For higher $\mathcal{V}_{\mathrm{CB}}$ the space charge resistance becomes more important. The curves are now closer together. Basically the same holds for the cut-off frequency (see Fig. 20). For lower $\mathcal{V}_{\mathrm{CB}}$ the curves are further apart then for

 ©Koninklijke Philips Electronics N.V. 2001

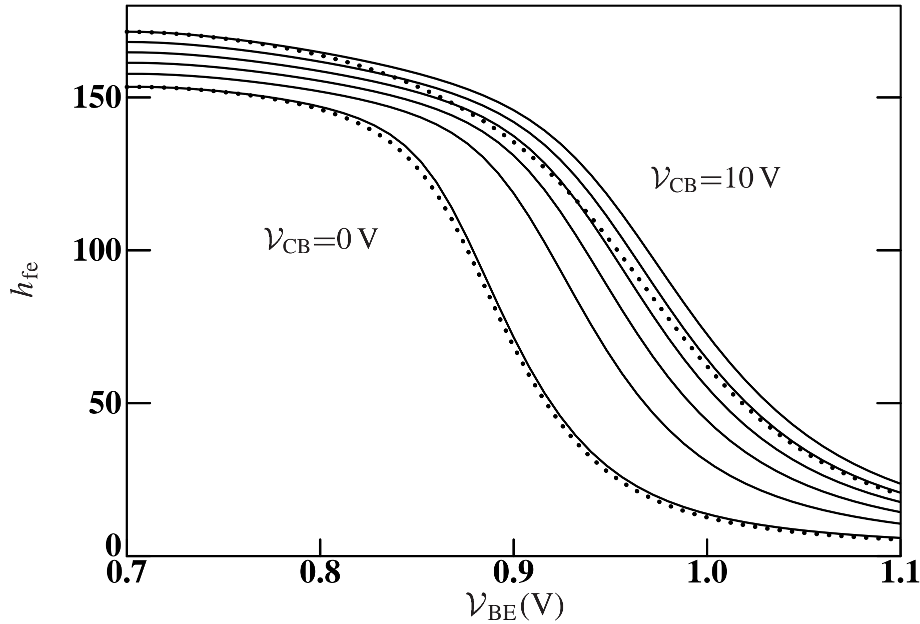

Figure 19: *The current gain as function of the base-emitter bias for* $\mathcal{V}_{CB} = 0$*, 2, 4, 6, 8, and* 10 V *for a hypothetical transistor to show the* $\mathcal{V}_{CB}$*-dependence of the onset of quasi-saturation. The parameters used are the default parameters from Ref. [2], but with* $V_{d_C} = 0.8$ V, $I_k = 1$ A, $I_{hc} = 20$ mA, $R_{Cv} = 150\,\Omega$*, and* $SCR_{Cv} = 2\,k\Omega$*, to enlarge the effect. The dotted lines are with a more realistic knee current of* $I_k = 0.1$ A *for the lowest and highest* $\mathcal{V}_{CB}$.

higher $\mathcal{V}_{CB}$. The maximum of f_T depends very much on the point where quasi-saturation starts. Again one can in general observe that the maxima are closer together for higher $\mathcal{V}_{CB}$. The same holds when the cut-off frequency is plotted versus the collector current, which is normally done.

It is also interesting to know that in general the top of the f_T is around or even before the point where the current gain starts to decrease (see Figs. 19 and 20).

The transistor in quasi-saturation We also need to know how we can influence the behaviour of the model when the transistor is in quasi-saturation. One of the parameters that has the most influence on the decrease of the current gain is the diffusion voltage V_{d_C}. We will therefore extract this parameter from the current gain. Another parameter that has influence is R_{Cv}.

For the decrease of the cut-off frequency the parameters that are important are related to the charges that are present only in quasi-saturation. These charges are Q_{BC} (with main parameter τ_B) and Q_{epi} (with main parameter τ_{epi}). It depends somewhat on the process which parameter has the most influence. Note however that the top of the f_T is mainly determined by τ_E and again τ_B. In practice we therefore have one parameter too much. In that case one should fix one of them (for instance using the initial values of Section 2.6.3).

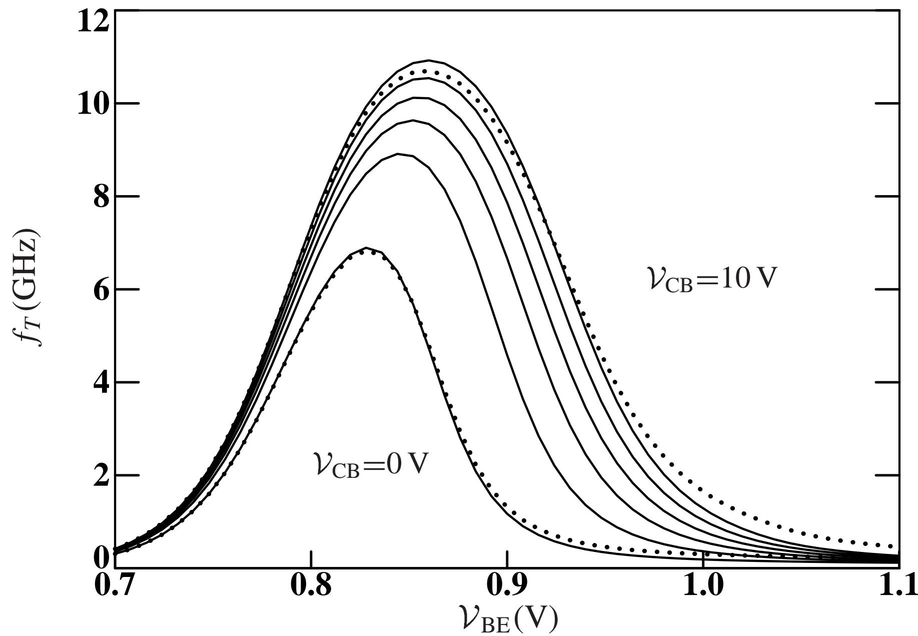

Figure 20: *The cut-off frequency for the same simulation as in Fig. 19.*

The influence of the knee current The more advanced bipolar transistors are getting, the higher the base doping level and therefore also the knee current $\mathsf{I_k}$. In many cases $\mathsf{I_k}$ becomes even larger than the hot-carrier current $\mathsf{I_{hc}}$. In older compact models like the much-used Gummel-Poon model quasi-saturation is not modelled and as a consequence the knee current is used to describe current gain degradation. In Mextram performance degradation is mainly described by quasi-saturation effects. Nevertheless, a knee current $\mathsf{I_k}$ is present in Mextram. Its influence is of minor importance, since current degradation is described already. The value of the parameter is therefore not always good defined, nor is it always as physical as one would like. The influence of $\mathsf{I_k}$ can be seen in Fig. 19 (dotted lines). It decreases the collector current a little bit, just at the point where the current gain starts to decrease. It can therefore be extracted from the forward-Gummel measurement or from the current gain measured in the *S*-parameter measurement. Alternatively $\mathsf{I_k}$ can be extracted from the collector current in the output-characteristic measurement, especially at higher collector voltage where quasi-saturation is not important.

The knee current $\mathsf{I_k}$ does not have a large influence on the cut-off frequency versus bias (or versus collector current), as can be seen from the dotted lines in Fig. 20.

Quasi-saturation in the output-characteristic For ideal ohmic quasi-saturation, e.d. without velocity saturation and Kirk effect, the output characteristic looks like the one in Fig. 21. The quasi-saturation region is the one between hard-saturation, where the current rises steeply, and the almost flat region at higher collector voltages.

In this ohmic case $I_C < \mathsf{I_{hc}}$ mainly the parameter $\mathsf{I_k}$ determines the level of the flat region. The parameter $\mathsf{I_{hc}}$ has only a small indirect influence via the current dependence of the base-collector depletion charge. The parameter $\mathsf{R_{Cv}}$ determines the onset of quasi-

 ©Koninklijke Philips Electronics N.V. 2001

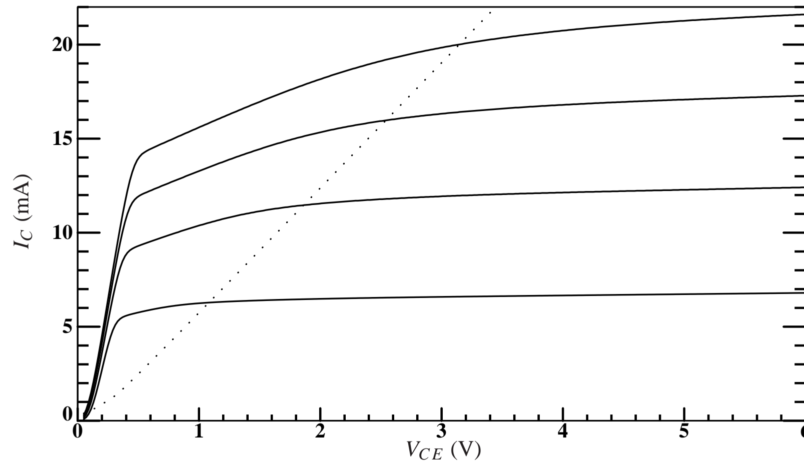

Figure 21: *Output characteristic for the ohmic case where is no velocity saturation and Kirk effect. Three regions can be clearly observed: hard saturation, quasi-saturation and normal region. The dotted line (I_{qs}) shows the transition between the latter two regions.*

saturation, i.e. the transition from the flat region to the quasi-saturation region, which is given by I_{qs} (dotted line in Fig. 21). The parameter $\mathsf{V_{dC}}$ determines the slope of the current in the quasi-saturation region.

In practice the transition from one region to the other is not as clear as in the example. This is due to the influence of the Kirk effect. The output characteristic is almost the same, but the transitions are more rounded. For $I_C > \mathsf{I_{hc}}$ mainly $\mathsf{SCR_{Cv}}$ determines the onset of quasi-saturation. The slope is now determined by both $\mathsf{R_{Cv}}$ as well as $\mathsf{V_{dC}}$. This illustrates that these two parameters are correlated (see next section).

2.6.5 Extraction of high-current parameters

In the initialisation part of the parameters we have calculated initial values for $\mathsf{I_{hc}}$, $\mathsf{R_{Cv}}$ and $\mathsf{SCR_{Cv}}$. The initial values of $\mathsf{I_{hc}}$ and $\mathsf{R_{Cv}}$ are stored and called $I_{\rm crit}$ and $R_{\rm epi}$. During parameter extraction these quantities are used to define lower and upper bound values for $\mathsf{I_k}$, $\mathsf{I_{hc}}$, $\mathsf{R_{Cv}}$ and $\mathsf{SCR_{Cv}}$. First $\mathsf{I_k}$ is extracted from the collector current at high $\mathcal{V}_{\rm CE}$ using the output-characteristic measurements. At sufficient high $\mathcal{V}_{\rm CE}$ the transistor comes out of quasi-saturation and therefore the epilayer resistance becomes of minor importance. The maximum allowed collector voltage is limited by avalanche multiplication. By extracting first $\mathsf{I_k}$ the average absolute value of I_C should be correct. The output conductance (bias dependency with $\mathcal{V}_{\rm CE}$) may be still bad. When $\mathsf{I_k}$ becomes unrealisticly large (upper boundary is set to 100 $I_{\rm crit}$) the initially calculated collector series resistances may be too large.

In the next step the ohmic resistance $\mathsf{R_{Cv}}$ is extracted from the decrease of the current gain in the forward-Gummel measurement (or from the $\mathcal{V}_{\rm CB} = 0$ curve measured along with S-parameters). In Mextram the decrease of the gain due to quasi-saturation is also affected by the diffusion voltage $\mathsf{V_{dC}}$ of the collector and both parameters $\mathsf{R_{Cv}}$ and $\mathsf{V_{dC}}$ are strongly correlated. It is therefore difficult to extract these two parameters simultaneously.

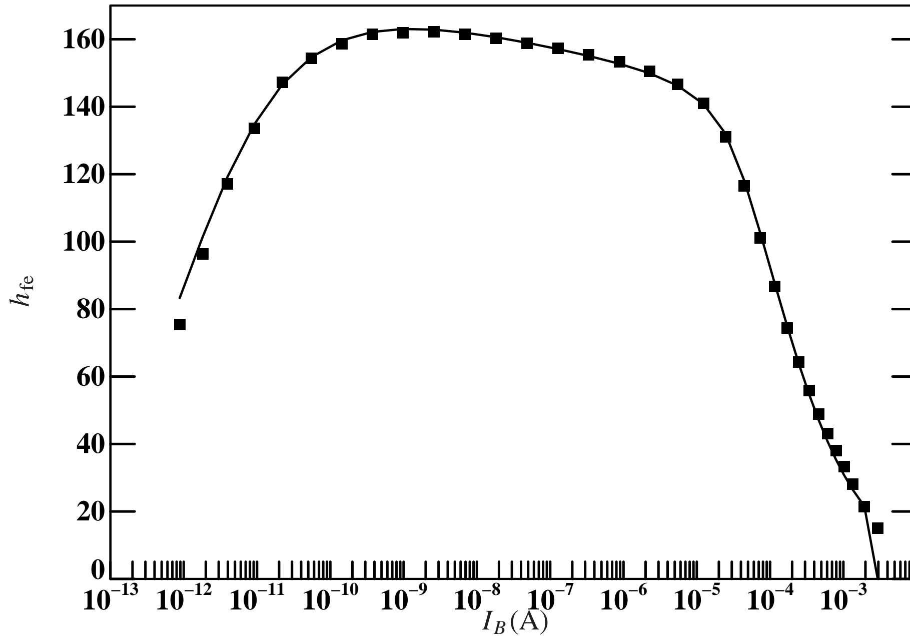

Figure 22: *Measured (markers) and simulated (lines) forward current gain as function of the measured base current in the forward-Gummel measurement for the extraction of the high-current parameters.*

In practice we fix the diffusion voltage V_{d_C}, based on the doping level of the epilayer. For advanced transistors with a thin and highly doped epilayer R_{Cv} becomes small and its precise value is of minor importance and the initial calculated value may be sufficiently accurate.

Now we repeat the extraction of I_k because R_{Cv} changes the absolute value of I_C in the output characteristic. The output conductance should be modelled now much better and can be still improved during the following steps. It is important to have the final value of I_k before we start with the extraction of the transit time parameters. The reason is that in general we do not extract the base transit time τ_B and the reverse transit time τ_R. Then the value of both parameters depends on I_k, see Section 2.6.3.

In the final step we extract the remaining transit time and epilayer parameters simultaneously from the f_T measurements. The maximum f_T at high $\mathcal{V}_{CB}$ is used to set the emitter transit time τ_E. From the degradation of f_T with increasing I_C and decreasing $\mathcal{V}_{CB}$ we extract τ_{epi}, I_{hc} and SCR_{C_v}. The smoothing parameter a_{x_i} mainly effects the lower $\mathcal{V}_{CB}$ curves. In many cases, however, the influence is not sufficient large and the correlation with the other parameters too strong to extract a_{x_i}. The f_T drops more abruptly with decreasing a_{x_i}. The lower limit of a_{x_i} is about 0.1 to keep the characteristics monotonic and the maximum realistic value is about 0.5.

The three steps above are repeated at least once to reach the final parameter values. The output conductance should now be modelled sufficiently accurately.

Normally process spread should not be very large. One can imagine however that for the extraction of the high-current parameters one would like to have all measurements that one

 ©Koninklijke Philips Electronics N.V. 2001

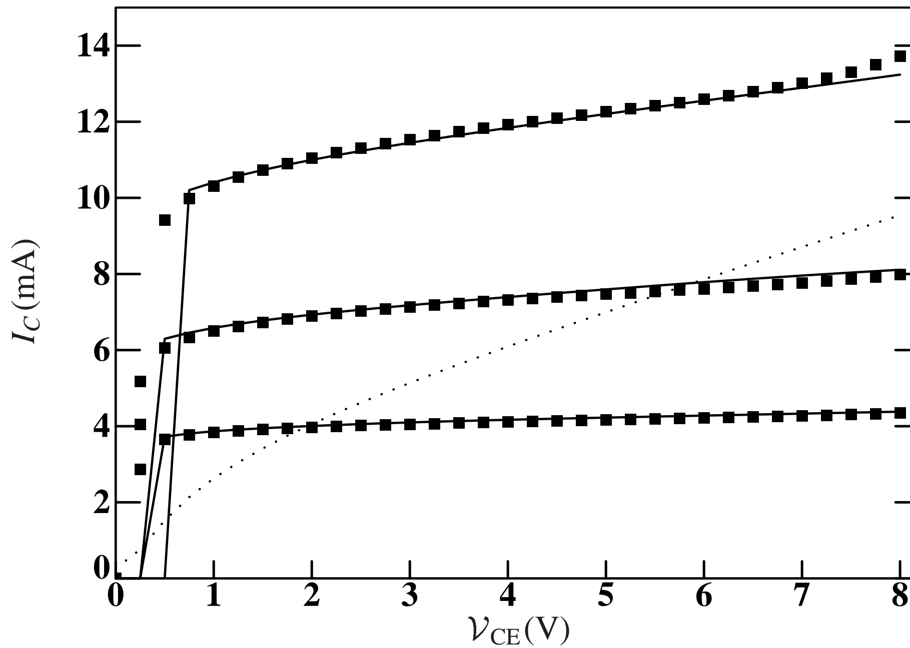

Figure 23: *Measured (markers) and simulated (line) collector current in the output-characteristic measurement for the extraction of the high-current parameters. The dotted line is I_{qs}, the current at which quasi-saturation start (which is almost independent of the base current).*

needs to be done on the same device. In that case the Gummel plot of the S-parameters should be used instead of the one done on the DC-structure. Also the output-characteristic measurement should be (re-)done on the high-frequency structure.

The use of the output-characteristic measurement for the extraction of the high-current parameters has a disadvantage: it is normally measured at currents that are higher than where the top of the f_T is. This might be beyond the region of interest. An alternative way to extract the high current parameters is to use only the currents as measured in the S-parameter measurement (these are Gummel measurements). The advantage is that all parameters are now extracted using the same bias conditions. The disadvantage is that we have less control over the output conductance due to the larger influence of self heating. (The output-characteristic measurement is done at constant base current which reduces the influence of self-heating. The S-parameters are voltage controlled measurements.) The extraction is then done by optimising simultaneously $\mathsf{I_k}$ and $\mathsf{R_{Cv}}$ from the Gummel plot. In the next step τ_{E}, τ_{epi}, $\mathsf{I_{hc}}$ and $\mathsf{SCR_{Cv}}$ are extracted from f_T.

In all description above τ_{B} is calculated from other parameters and m_τ is kept constant (and equal to 1). Only when the results from the extraction procedure gives cause for a different approach should one consider to fit τ_{B} and m_τ along.

Extracted parameters : $\mathsf{R_{Cv}}$, ($\mathsf{V_{d_C}}$), $\mathsf{I_k}$, $\mathsf{SCR_{Cv}}$, ($\mathsf{I_{hc}}$), τ_{E}, τ_{epi}, (τ_{B}, $\mathsf{a_{xi}}$, m_τ)
IC-CAP-functions : `MXT_ic_vce` and `MXT_ft`

©Koninklijke Philips Electronics N.V. 2001

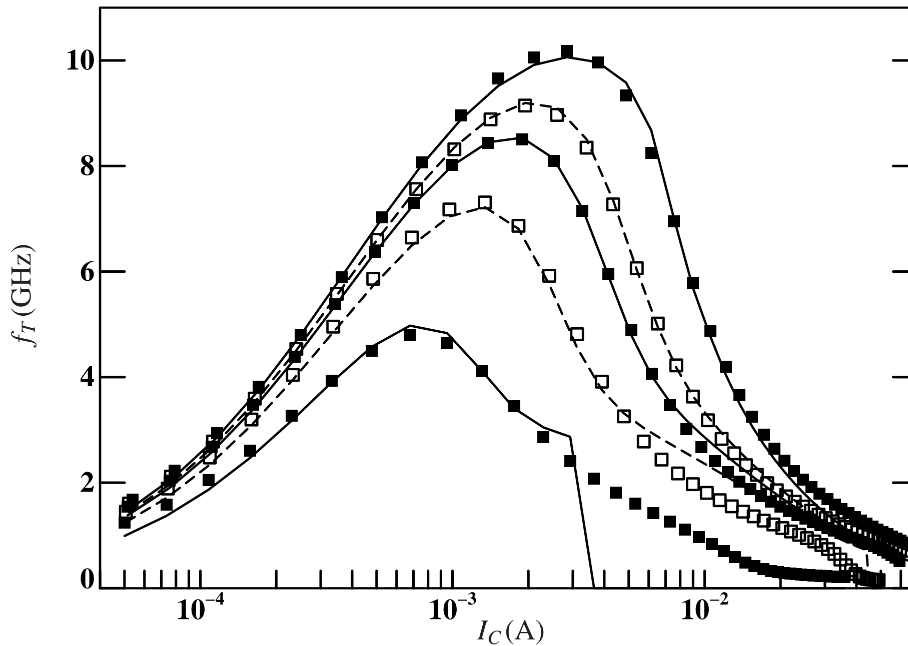

Figure 24: *Measured (markers) and simulated (line) cut-off frequency in the S-parameter measurement for the extraction of the high-current parameters.*

2.6.6 Avalanche at high currents

Extracting the high-current spreading parameter for avalanche is only necessary when in the final parameter set extended avalanche is used ($\mathsf{EXAVL} = 1$). One must fully realise that this can have consequences for the convergence of circuits in a circuit simulator. Hence this should only be done with a special purpose in mind. This purpose would then also lead to an idea in what kind of bias-setting the extended avalanche is needed. It seems therefore logical to let that purpose define how one should extract $\mathsf{S_{Fh}}$.

In general one can of course extract $\mathsf{S_{Fh}}$ from the collector current in the output-characteristic measurement at high voltages and high currents. Only there $\mathsf{S_{Fh}}$ will have an influence. All other high-current parameters should have their final value before one starts to look at high-current avalanche. (Note that self-heating is very important in the same bias regime). Even then, one should not spent too much time extracting this parameter.

Extracted parameter	:	$\mathsf{S_{Fh}}$
IC-CAP-function	:	`MXT_ic_vce`
Equations used from Ref. [2]	:	Almost all equations for forward mode.

2.6.7 Reverse currents at high injection

When all the high-current parameters have been extracted it is possible to extract $\mathsf{X_{ext}}$ from the absolute values of the reverse currents I_B, I_E en $I_{\mathrm{sub,ext}}$ in the high-current regime (the subindex ‘ext’ is used here to denote the difference between the external substrate current and the substrate current in the Mextram model between nodes B_1 and

 ©Koninklijke Philips Electronics N.V. 2001

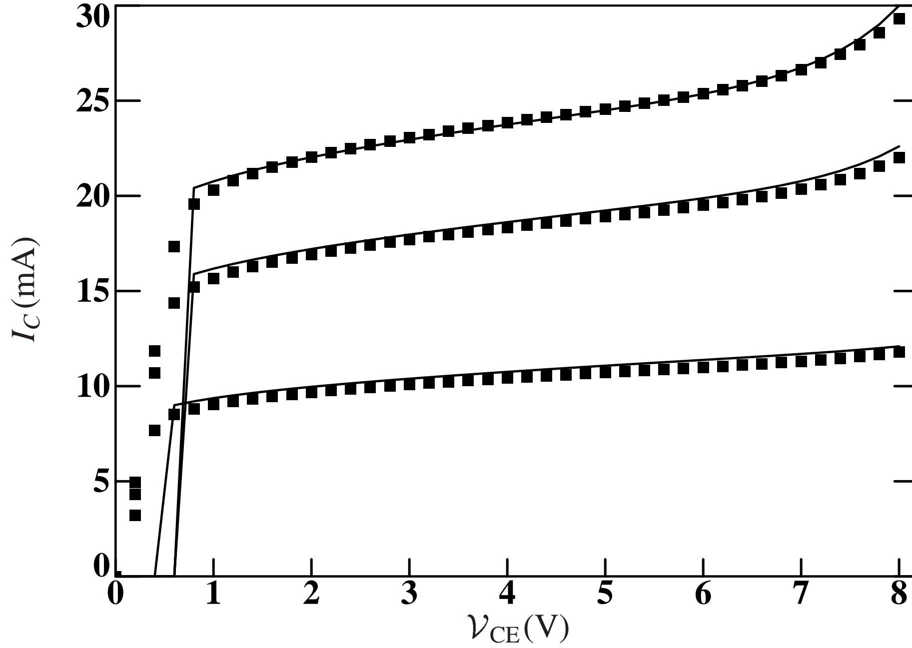

Figure 25: *Measured (markers) and simulated (line) collector current in the output-characteristic measurement for the extraction of the high-current spreading parameter* $\mathsf{S_{Fh}}$ *for avalanche.*

C_1). $\mathsf{X_{ext}}$ can only be extracted if $\mathsf{EXMOD} = 1$, because otherwise the currents do not depend on EXMOD. This also means that $\mathsf{R_{Bc}}$ must be known, since it is the resistance over which the reverse base-currents are split in a part with $\mathsf{X_{ext}}$ and a part with $(1-\mathsf{X_{ext}})$.

The reverse currents have to be calculated iteratively. As a free variable we use $\mathcal{V}_{\rm B_2C_2}$. We then calculate $\mathcal{V}_{\rm BC}$ as shown below and optimise $\mathcal{V}_{\rm B_2C_2}$ such that the calculated $\mathcal{V}_{\rm BC}$ matches the input. We start with the internal base emitter voltage that can be given as

$$\mathcal{V}_{\rm B_2E_1} = \mathcal{V}_{\rm BE} + I_N\ \mathsf{R_{ET}} - (I_{\rm ex} + I_{\rm sub} + I_{B_3})\ \mathsf{R_{BcT}}, \tag{2.69}$$

where I_N, $I_{\rm ex}$ and $I_{\rm sub}$ are currents from the Mextram model that have been calculated in the previous iteration. (The input I_E is used in the initial estimation.) Note that $\mathcal{V}_{\rm B_1B_2} = 0$ since in reverse mode there is no current flowing from B_2 to B_1, because all reverse base-current components are positioned at the extrinsic base-collector junctions. Since the current is not yet known, we neglect the current modulation in the base-collector depletion charge (i.e. we take $I_{\rm cap} = 0$). This has only a minor influence on the final curves. The main current can then be found from

$$I_N = \mathsf{I_{sT}}\ \frac{e^{\mathcal{V}_{\rm B_2C_2}/V_T}}{q_B(\mathcal{V}_{\rm B_2E_1}, \mathcal{V}_{\rm B_2C_2})}. \tag{2.70}$$

Next we need to solve (iteratively) the junction voltage $\mathcal{V}_{\rm B_2C_1} = \mathcal{V}_{\rm B_1C_1}$ using the relation

$$I_{C_1C_2}(\mathcal{V}_{\rm B_2C_1}, \mathcal{V}_{\rm B_2C_2}) = I_N, \tag{2.71}$$

©Koninklijke Philips Electronics N.V. 2001

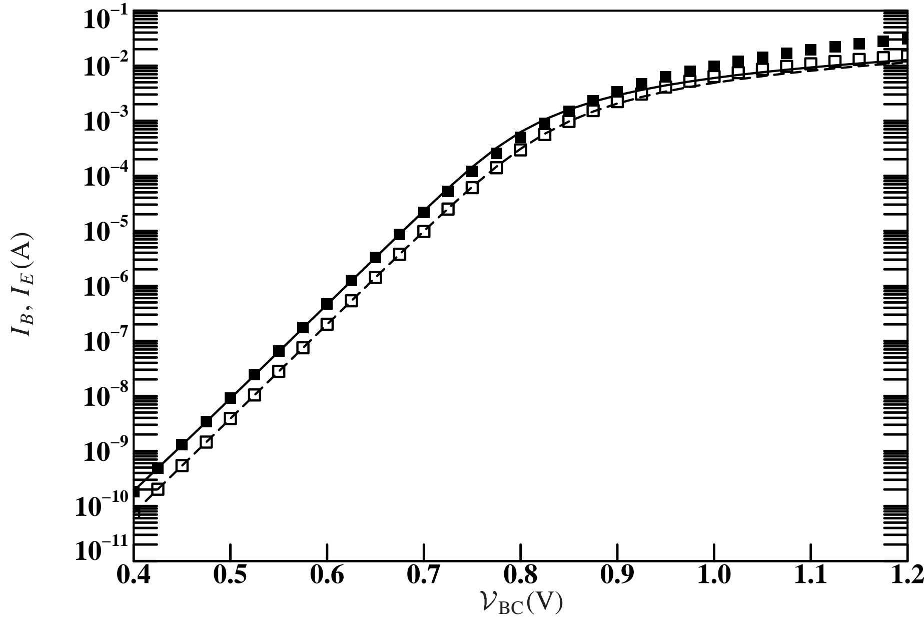

Figure 26: *Measured (markers) and simulated (line) reverse emitter (filled markers) and base currents (open markers) in the reverse-Gummel measurement for the extraction of the external region splitting parameter* $\mathsf{X_{ext}}$ *and possibly the substrate knee current. Note that no non-ideal reverse base current is present in these measurements.*

where in reverse $I_{C_1C_2}$ is a relatively simple function of the biases (Mextram uses the Kull model in reverse). We can now calculate the currents I_{ex}, I_{sub}, and I_{B_3} from the equations in Ref. [2]. The last junction voltage we need is

$$\mathcal{V}_{BC_1} = \mathcal{V}_{B_1C_1} + (I_{ex} + I_{sub} + I_{B_3})\ \mathsf{R_{BcT}}, \tag{2.72}$$

which is used for the calculation of XI_{ex} and XI_{sub}.

With all the results we can calculate the external base-collector bias $\mathcal{V}_{BC} = \mathcal{V}_{BC_1} + (I_{B_3} + I_{ex} + XI_{ex} + I_N)\ \mathsf{R_{CcT}}$. As mentioned before the internal junction bias $\mathcal{V}_{B_2C_2}$ must now be iterated such that the calculated external base-collector bias equals the bias as given in the inputs.

When the iteration loop is finished, we find the following currents

$$I_E = I_N, \tag{2.73a}$$
$$I_B = I_{ex} + XI_{ex} + I_{sub} + XI_{sub} + I_{B_3}, \tag{2.73b}$$
$$I_{sub,ext} = -I_{sub} - XI_{sub}. \tag{2.73c}$$

Extracted parameters	:	$\mathsf{X_{ext}}$, ($\mathsf{I_{ks}}$)
Approximations	:	No current modulation in BC-depletion charge
IC-CAP-function	:	`MXT_reverse_currents`
Equations used from Ref. [2]	:	(4.60)–(4.65), (4.153)–(4.163) and others.

 ©Koninklijke Philips Electronics N.V. 2001

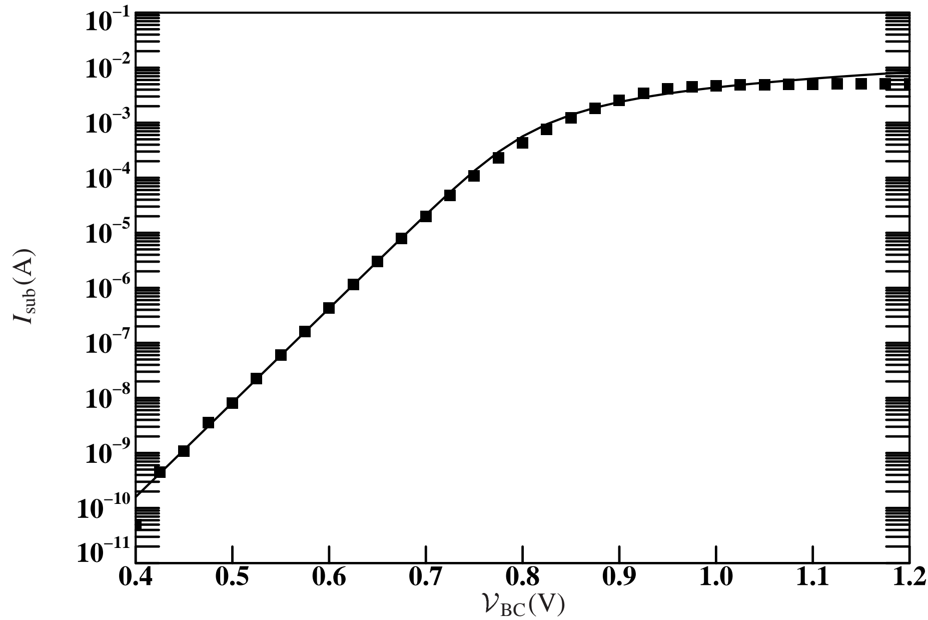

Figure 27: *Measured (markers) and simulated (line) substrate current in the reverse-Gummel measurement for the extraction of the external region splitting parameter* X_{ext} *and possibly the substrate knee current.*

2.6.8 Reverse transit time

For an accurate determination of the reverse transit time τ_R one should have measurements of the f_T in reverse. This is not normally done because it requires special structures on silicon (with collector and substrate connected).

The reverse transit time does have an influence on the f_T measured in normal forward operation for low V_{CE} (say below 0.5 V). Extracting τ_R from the forward f_T however is inaccurate since the inaccuracy of the other parameters has a large influence. In practice it is best to calculate τ_R from Eq. (2.67).

2.7 Some alternative ways to extract parameters

2.7.1 No substrate present

In some cases there is no substrate present (discrete transistors, transistors in SOI processes). One can then use the three-terminal version of Mextram. As an alternative one can set $I_{Ss} = 0$ and $C_{jS} = 0$, which has the same effect. All the extractions for the substrate part are then no longer needed. The extraction of the collector resistance is however more difficult. We discuss this next.

2.7.2 Collector resistance when no substrate is present

When there is no substrate present, and hence no substrate current, the extraction of the collector resistance from the R_{Cc}-active measurement is no longer possible. One then needs to do something else. There are three options.

First, one can extract the collector resistance in the same way as the emitter resistance, using the Giacoletto method (R_{Cc}-flyback). Now however the transistor has to be operated in reverse. New measurements have to be performed, similar to the R_E-flyback measurement. This means taking $I_E \simeq 0$, $\mathcal{V}_{BC} = 1.0 \ldots 1.5\,V$ and extracting R_{Cc} from the derivative of $\mathcal{V}_{EC}$ versus I_C.

Second, one can optimise the collector resistance together with X_{ext} from the high currents in the reverse-Gummel measurement. These high currents are sensitive to both parameters.

Third, one can extract R_{Cc} from the on-resistance in the output-characteristic measurement (saturation region). To do this an accurate modelling of the reverse gain is important. The simulated data can only be obtained via an interface to a circuit simulator.

2.7.3 Reverse Early voltage without reverse measurements

The high frequency S-parameter measurements are performed on a structure where emitter and substrate are shorted. This is done to reduce the noise-limit of these sensitive measurements. The reverse measurements are not possible on this structure. When no other structure is available, one must work with only the forward measurements.

Some of the parameters can not be extracted. The reverse current gain β_{ri} is one of them. Also the collector resistance is difficult (see previous section). The most important parameter that we normally extract from the reverse measurements is the reverse Early voltage V_{er}. We need this parameter, since it influences many forward characteristics as well. Its extraction must then be done on the collector current in the forward-Gummel measurement, together with I_s (see Sec. 2.5.7). To see the result of the extraction it is useful to plot $I_C/(I_s\, e^{\mathcal{V}_{B_2E_1}/V_T})$, which looks similar to the current gain h_{fe} (but is a factor β_f lower). Note that no correction for series resistance, quasi-saturation or high injection effects is taken into account.

2.7.4 Grading coefficients from Early measurements

As mentioned before it is very difficult to extract the overlap capacitances C_{BEO} and C_{BCO} from a single transistor. There is a way of doing it, but it might not be the most accurate one. To extract them in an accurate way one needs to look at geometric scaling (see Chapter 4).

The Early voltage is not constant as function of bias. The voltage dependence is determined by the voltage dependence of the depletion charge (either Q_{t_E} or Q_{t_C}). This voltage dependence is mainly determined by the grading coefficient (p_E or p_C). It is

 ©Koninklijke Philips Electronics N.V. 2001

therefore possible to extract the grading coefficient from the curvature of the Early voltages. In practice the collector and emitter current in the reverse-Early and forward-Early measurements are used to fit the model.

Once the grading coefficients are known one can turn to the capacitance measurements. Since the grading coefficients are fixed, the only parameter left to extract is $\mathsf{C_{jE}}$ (or $\mathsf{C_{jC}}$), together with the overlap capacitance $\mathsf{C_{BEO}}$ (or $\mathsf{C_{BCO}}$). It might be clear that the result does not necessarily give the correct physical value of the overlap capacitances, due to the rather indirect determination.

2.7.5 Base and emitter series resistances

Although there are various ways to extract emitter and base series resistances, these resistances are notoriously difficult to extract, especially from measurements at only one transistor. We will say something about the extraction methods here, although we will not go into detail. For geometric scaling of the resistances see Section 4.3.11.

The extraction of the emitter resistance was already discussed in Section 2.5.9. We will only discuss the emitter resistance here in as far as it has influence on the extraction of base resistances.

For the determination of the base series-resistance we think it best to determine it from calculations based on known process parameters. The variable base-resistance is the effective resistance of the pinched base. One must take care to take geometrical effects into account. This includes the numerical factor that describes the fact that not all of the current needs to go through all of the base. For a single sided base contact, for instance, with the emitter width H_{em} much smaller than its length L_{em}, this factor is $1/3$ since we have

$$\mathsf{R_{Bv}} = \frac{H_{\mathrm{em}}}{3\,L_{\mathrm{em}}}\,\rho_{\square}, \tag{2.74}$$

where $\rho_{\square}$ is the sheet resistance of the pinched based. It is important to realize that when one tries to calculate the base resistance from geometrical considerations, also the emitter plug effect has to be taken into account.

The external part of the base resistance can also be calculated, depending very much on the technology, and is modelled with the constant resistance $\mathsf{R_{Bc}}$. The methods we describe below are meant as various ways to check the calculated resistances (if possible for different geometries). If there are no big differences one can keep the calculated values. If the differences are larger one is probably not taking all resistances into account (possibly due to problems in the technology).

One of the ways to check the results for the base resistances (as well as the emitter resistance) is given in Ref. [21]. The (total) base resistance can be calculated as function of bias using both the two-port method and the circle impedance method. Note that in contrast to common believe the last method can also be used when the measurements have been done only at one frequency (together with some DC results). It is *not* necessary to do a frequency sweep. Results from the S-parameter measurements can therefore be used.

©Koninklijke Philips Electronics N.V. 2001

In order to get reasonable accurate values of the total base resistance one must be careful to correct for the emitter resistance. Also an alternative way to extract the emitter resistance is given in Ref. [21], based on the DC-curves, just as in Section 2.5.9. The results should be almost equal. Note however that the measurements are possibly done on different structures (DC-structures versus high-frequency structures) and the probes one uses might also be different. It is easily possible to get a difference in the emitter resistance of 1 Ω due to these effects.

It is well known that the base-resistance is important for the determination of the noise figure of a bipolar transistor. It seems therefore logical to extract the base-resistance also from noise measurements [22, 23]. This does have a few problems however. First of all noise is difficult to measure. When the measurements have been done it is important to have a very good idea of the total circuit that is measured [24] (including the external sources, the wires to the device, the parasitics of bond-pads and finally the transistor itself). It is therefore difficult to interpret the results. As is the case of base-resistance determination from S-parameters, one must carefully correct for the influence of the emitter resistance (which is also difficult to determine).

2.8 SiGe parameter extraction

The most important remark we have to make here is that in many cases the extraction of a SiGe transistor can be done in the same way as that of a pure-Si transistor. The two extra features discussed below might not be needed. One must realise, however, that the modelling of the bias-dependency of the Early voltages will not be as accurate as for pure Si-transistors.

What changes in parameters can we expect? One of the parameters that might change is $\mathsf{a}_{\mathsf{x_i}}$. For SiGe transistors it might be smaller, due to the abrupt degradation of the cut-off frequency and the current gain. Also the collector diffusion voltage $\mathsf{V}_{\mathsf{d_C}}$ might be larger for the same reason. The emitter resistance might be larger when an emitter epilayer is present between the high dopes of the emitter and the base.

2.8.1 Gradient in the Ge-profile

For some SiGe processes the Ge-profile is graded. Mextram contains a special formulation to describe this. The parameter $\mathsf{dE_g}$ of this formulation is the difference of the bandgap over the neutral base (as it is for zero bias):

$$\mathsf{dE_g} = E_g(0) - E_g(W_B). \tag{2.75}$$

This results in a difference of intrinsic electron concentrations

$$\frac{n_i^2(W_B)}{n_i^2(0)} = e^{\mathsf{dE_g}/kT}. \tag{2.76}$$

 ©Koninklijke Philips Electronics N.V. 2001

We assume a linear profile of the Germanium concentration. For the case of no Ge at the emitter and a high concentration of Ge at the collector $\mathsf{dE_g}$ is positive. Another thing to note is that $\mathsf{dE_g}$ should be given in electron-Volts. This implies that for calculations we need to correct with a factor $1.6 \cdot 10^{-19}$, the value of the unit charge in Coulomb. In the formal documentation we therefore find $q\,\mathsf{dE_g}/kT = \mathsf{dE_g}/V_T$ instead of $\mathsf{dE_g}/kT$.

The most direct way to determine $\mathsf{dE_g}$ is by using process knowledge. In this way $\mathsf{dE_g}$ gets a fixed value. This can be done before any other parameters are extracted.

There is also another way of extracting this parameter [25], although we have no experience here. Two dedicated measurements are needed. We take a forward bias V_F, preferably the same as used in the forward-Early and reverse-Early measurements. The first measurement consists of measuring the collector current $I_{C,f}$ and the forward output conductance $g_{\mathrm{out,f}} = \mathrm{d}I_C/\mathrm{d}\mathcal{V}_{\mathrm{CB}}$ as function of temperature at fixed $\mathcal{V}_{\mathrm{BE}} = V_F$. The second measurement consists of measuring the emitter current $I_{E,r}$ and the reverse output conductance $g_{\mathrm{out,r}} = \mathrm{d}I_E/\mathrm{d}\mathcal{V}_{\mathrm{EB}}$ as function of temperature at fixed $\mathcal{V}_{\mathrm{BC}} = V_F$. This is the reverse measurement of the first measurement, at the same forward bias.

The bandgap difference can now be found from the relation

$$\mathsf{dE_g} = kT \left(\ln \frac{g_{\mathrm{out,r}}}{g_{\mathrm{out,f}}} - 2\,\ln \frac{I_{E,r}}{I_{C,f}} - \ln \frac{C_{BE,r}}{C_{BC,f}} \right). \tag{2.77}$$

Note that $\mathsf{dE_g}$ should be given in electron-Volt for the parameter list. The last term with the capacitances is an extra correction term. The base-emitter depletion capacitance should be measured together with the reverse measurement, the base-collector depletion capacitance with the forward measurements. In practice it is rather time-consuming to measure them. As an alternative one can use the capacitances as predicted by Mextram (once these are known).

When one extracts the parameter in this way the result is not quite the bandgap difference over the neutral base in zero bias, but rather $\Delta E_g = E_g(0_r) - E_g(W_{B,f})$, where the actual boundaries of the neutral base are used. The error is small however.

It is important to check afterwards if the value taken for $\mathsf{dE_g}$ is not too high. If it is, the collector-bias dependence of the cut-off frequency as given by the model is too large. One should then decrease $\mathsf{dE_g}$ and redo the extraction of the other parameters. Note that the actual Early voltages can be much larger or smaller than the corresponding Early voltage parameter when $\mathsf{dE_g} \neq 0$.

Although the model formulation was intended for graded Ge-profiles only, we found that it can be useful also for other Ge-profiles. ($\mathsf{dE_g}$ might even become negative.)

Extracted parameters	:	$\mathsf{dE_g}$
IC-CAP-function	:	None
Equations used from Ref. [2]	:	None

2.8.2 Neutral base recombination

When recombination of electrons and holes in the base leads to a significant contribution of the base current, one must make use of an extra feature of Mextram that describes this effect. The corresponding parameter $\mathsf{X}_{\mathsf{rec}}$ can be extracted from the same measurement as the avalanche parameters: the base current in the forward-Early measurement. The base current at small $\mathcal{V}_{\text{CB}}$ will no longer be constant. Instead it will decrease with $\mathcal{V}_{\text{CB}}$. At higher collector-base voltages the decrease will be even more pronounced. This latter effect is, as before, due to avalanche. The parameter for the neutral base recombination therefore has to be extracted from the smaller $\mathcal{V}_{\text{CB}}$'s [26]. The equation for the base current that one can use is

$$I_{B_1} = I_{B0}\left[1 + \mathsf{X}_{\mathsf{rec}}\,(1 - \mathsf{XI}_{\mathsf{B}_1})\,\frac{V_{tC}}{\mathsf{V}_{\mathsf{ef}}}\right] - I_{\text{avl}}. \tag{2.78}$$

This equation must be used in e.g. `MXT_veaf_ib` and `MXT_forward_hfe`.

The extraction has to be done after that of the Early voltages, since V_{ef} is needed. The base current I_{B0} at $\mathcal{V}_{\text{CB}} = 0$ is the same help-variable that has been used for the extraction of the avalanche parameters.

When the forward base current depends on the collector voltage, some of the assumptions we made for the extraction of some other parameters are no longer valid. In some extraction routines this has been taken into account, in other routines it has been neglected.

Note that in quasi-saturation $\mathsf{X}_{\mathsf{rec}}$ also influences the forward base current, which can be seen in the Gummel plot. When the effect as modelled is too large, one must reduce $\mathsf{X}_{\mathsf{rec}}$.

Extracted parameters	:	$\mathsf{X}_{\mathsf{rec}}$, ($\mathsf{W}_{\mathsf{avl}}$, $\mathsf{V}_{\mathsf{avl}}$)
IC-CAP-function	:	`MXT_veaf_ib`
Equations used from Ref. [2]	:	(4.173)

2.9 Some left over extraction issues

2.9.1 Thermal capacitance

The thermal capacitance can only be extracted when either time-resolved or frequency dependent measurements are performed. We will discuss both ways, although we do not have experience in either method. It is important to realize that having only a single thermal resistance and thermal capacitance means having only one time-constant. The actual response of the transistor will in general be more complicated (more time constants). To model this one needs to make use of the node dT of the thermal network [2] and model the thermal behaviour externally. Of course the extraction will become more difficult.

The first method is the time-resolved measurement [19, 20]. In a similar way as we used to extract R_{th} we can make use of the base-current and the emitter-base bias to make a temperature sensor: for fixed $\mathcal{V}_{\text{BE}}$ the base current will increase as function of temperature. When we now use a time-dependent measurement where the base-emitter

 ©Koninklijke Philips Electronics N.V. 2001

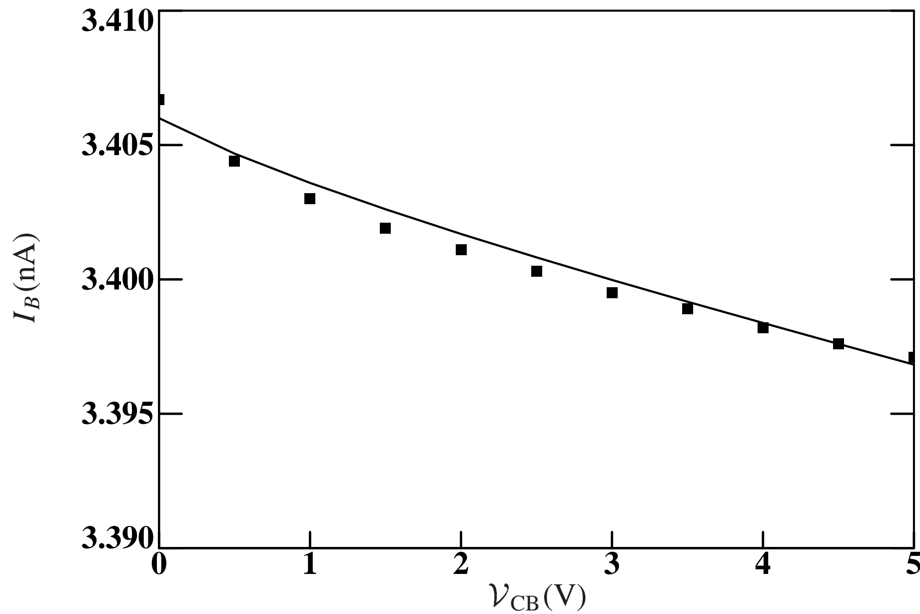

Figure 28: *Base current in the forward-Early measurement for the extraction of the neutral base recombination parameter* $\mathsf{X_{rec}}$. *Markers are Medici simulations, lines are Mextram simulations. Normally avalanche would be present also, but this has not been included in the Medici simulations.* $\mathsf{X_{rec}}$ *is in this example still small (*~ 0.05*).*

voltage is stepped abruptly to a high value, the base-current will increase as function of time due to self-heating. After some time it will saturate. The corresponding time constant of the rise of I_B is the thermal time constant $\mathsf{R_{th}}\,\mathsf{C_{th}}$. It will be of the order of 1 μs. The experiment can be done for various collector-emitter biases.

The alternative way of determining the thermal capacitance is by doing frequency depending output-conductance measurements. This is the same technique as used for MOSFET's [27, 28]. The collector current in the output-characteristic measurement increases with increasing $\mathcal{V}_{CE}$. This is the Early effect. When self-heating is important this increase will be larger (or in some cases smaller, depending on the temperature behaviour of h_{fe}). Also the derivative of the collector current w.r.t. $\mathcal{V}_{CE}$ will therefore be larger. This derivative is the low-frequency output conductance. For higher frequencies the self-heating effect is too slow to follow the variations in bias. The temperature of the device will therefore be constant. The high-frequency output conductance is then the derivative of the collector current at the fixed but elevated temperature. It only contains the Early effect. In general it will be smaller than the low-frequency output conductance. Measuring the output conductance as function of frequency will therefore show a certain value at low frequencies, followed by a smaller value at high frequencies. The transition frequency is directly related to the time constant $\mathsf{R_{th}}\,\mathsf{C_{th}}$. By comparing measurements with simulations and using the known thermal resistance we can extract the thermal capacitance.

©Koninklijke Philips Electronics N.V. 2001

2.9.2 Verification of Y-parameters

For the verification of the Y-parameters it is necessary to measure the Y parameters also over frequency. One can then plot the real and imaginary parts of all the Y-parameters and compare these to the results of the Mextram model. (To do this an external simulator is needed.)

In Fig. 29 we show a general small-signal circuit for bipolar transistors. This circuit can be used up to intermediate current levels and frequencies to get an idea what parts of the model are most important for the various Y-parameters. When we take the lowest two orders in the frequency expansion of the four Y-parameters (and assume $g_m\, r_B/\beta \ll 1$) we get

$$Y_{11} = g_m/\beta + j\omega\,[C_{\text{ex}} + C_{\text{in}} + C_{BE}]\,, \tag{2.79a}$$

$$Y_{21} = g_m - j\omega\,[C_{\text{ex}} + C_{\text{in}}(1{+}g_m\, r_B) + C_{BE}\, g_m\, r_B] \tag{2.79b}$$

$$Y_{12} = -\omega^2 r_B C_{\text{in}}\,[C_{\text{in}}{+}C_{BE}] - j\omega\,[C_{\text{ex}} + C_{\text{in}}]\,, \tag{2.79c}$$

$$Y_{22} = g_{\text{out}} + j\omega\,[C_{\text{ex}} + C_{\text{in}}(1{+}g_m\, r_B) + C_{SC}]\,. \tag{2.79d}$$

One can therefore find the different capacitance contributions from the Y-parameters at low frequencies. For higher frequencies the circuit of Fig. 29 can still be used but the equations above have to be modified. For higher currents, however, the full equivalent circuit of Mextram has to be taken into account.

Note that it is very important that the actual operating point of the measured and simulated transistor are the same. In practice this means that the collector currents must be the same. This is not always the case when the transistors have the same external biases and the modelling of the resistances is not completely accurate.

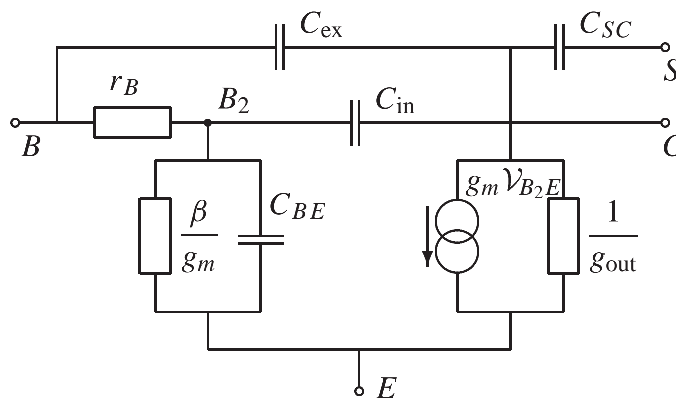

Figure 29: *Small-signal equivalent circuit describing the approximate behaviour of the Mextram model at small currents. Note that in the S-parameter measurement the nodes S and E are connected.*

One of the other things that needs to be taken into account is the fact that the link between emitter and emitter bond-pad contributes a self-inductance. This self-inductance

 ©Koninklijke Philips Electronics N.V. 2001

should be de-embedded using the short structure [4]. This structure is however not always present. The self-inductance then adds effectively to the emitter resistance. The inductance can be estimated by multiplying the length of this link by 1 nH/mm. This extra impedance has an influence on the Y-parameters at higher current levels, as well as on the base-resistance extraction.

©Koninklijke Philips Electronics N.V. 2001

3 Temperature scaling

In this chapter the extraction of the parameters in the temperature scaling rules are treated. The Mextram model has 14 parameters dealing with temperature scaling. There are 43 electrical parameters to describe the characteristics at the reference temperature of which 16 are temperature independent. So there are more electrical parameters that scale with temperature then there are parameters for that.

To extract the parameters and to verify the scaling rules measurements should be done preferably both at lower and higher temperatures with respect to the reference temperature. One should include the temperatures at the limits of the specifications (say $-40°C$ and $125°C$). On-wafer measurements are, however, difficult for temperatures below freezing. For high temperatures ($> 125°C$) one must realize that due to oxide formation between probe tips and contact pads the contact resistance will increase rapidly with time.

3.1 The temperature parameters and their influence

In Table 6 the cross reference between the temperature parameters and the electrical parameters is listed. As is clear from this table certain temperature parameters, especially those related to the active base like $A_{Q_{B0}}$, A_B and V_{g_B}, occur in many other electrical parameters. This implies that a one way extraction of the temperature parameters is not possible. Furthermore, not all temperature parameters, especially those of the series resistances, can be accurately extracted from transistor characteristics. We need to keep this in mind while doing the parameter extraction.

Table 6: *Summary of the occurrence of the temperature parameters in the temperature scaling rules of the electrical parameters. Especially temperature parameters related to the intrinsic base occur in many electrical parameters.*

1	$A_{Q_{B0}}$	V_{er}	V_{ef}	I_s	β_f	R_{Bv}	τ_B	τ_R	I_{ks}	dE_g
2	A_E	R_E	β_f							
3	A_B	R_{Bv}	β_f	I_s	I_k	τ_E	τ_B	τ_R	I_{ks}	
4	A_{epi}	R_{Cv}	τ_{epi}	τ_R						
5	A_{ex}	R_{Bc}								
6	A_c	R_{Cc}								
7	$dV_{g\beta f}$	β_f								
8	$dV_{g\beta r}$	β_{ri}								
9	V_{g_B}	I_s	C_{j_E}	V_{d_E}	V_{er}	I_{ks}				
10	V_{g_C}	C_{j_C}	V_{d_C}	X_p	I_{Br}	V_{ef}				
11	V_{g_j}	I_{Bf}								
12	$dV_{g\tau_E}$	τ_E								
13	V_{g_S}	I_{Ss}	I_{ks}	C_{j_S}	V_{d_S}					
14	A_S	I_{Ss}	I_{ks}							

The resistances normally increase with temperature. Their dependence is mainly deter-

 ©Koninklijke Philips Electronics N.V. 2001

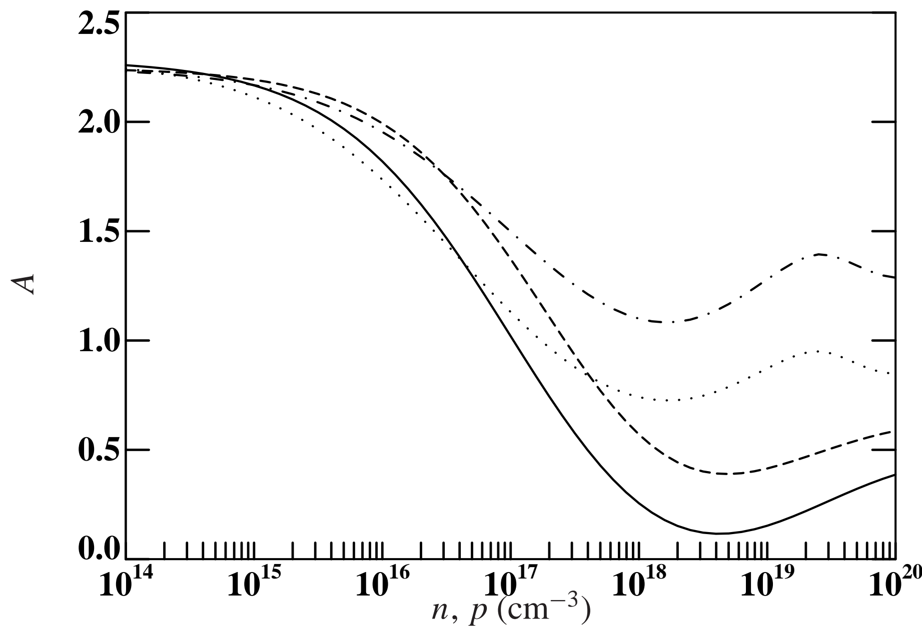

Figure 30: *The mobility exponents* A *versus doping concentration for majority electrons (solid line), majority holes (dashed line), minority electrons (dotted line), and minority holes (dashed-dotted line). The numbers have been found by fitting the model of Ref. [8] to* $\mu = T^{-A}$ *over a temperature range between* $T = 200°\mathrm{C}$ *and* $T = 500°\mathrm{C}$.

mined by the doping level of the corresponding region. The doping level determines the mobility temperature coefficient A which is needed to describe the mobility as function of temperature: $\mu \sim T^{-A}$. When the doping levels of the emitter, base and collector regions are known one can obtain from literature the mobility temperature coefficients $\mathrm{A_E}$, $\mathrm{A_B}$, $\mathrm{A_{epi}}$, $\mathrm{A_{ex}}$, $\mathrm{A_C}$ and $\mathrm{A_S}$. This procedure to determine the mobility coefficients significantly reduces the amount of extraction work. Results based on Ref. [8] are presented in Fig. 30. In most cases the majority mobility exponent needs to be used. The mobility exponent $\mathrm{A_B}$ is used for both majority and minority mobility in the Mextram description. An intermediate value is then an option.

All the remaining temperature parameters, except $\mathrm{dV_{g\tau_E}}$, can be extracted from transistor characteristics measured at small and medium current levels. The extraction of the Mextram low current parameters like the Early voltages $\mathrm{V_{er}}$, $\mathrm{V_{ef}}$, the saturation currents $\mathrm{I_s}$, $\mathrm{I_{Ss}}$ and $\mathrm{I_{Bf}}$ is simple and in most cases accurate values can be obtained at the various temperatures. Also the temperature dependence of the forward and reverse current gain is clearly seen from measurements.

The extraction of the high current related parameters like $\mathrm{I_k}$ and the collector epilayer parameters $\mathrm{R_{Cv}}$, $\mathrm{SCR_{Cv}}$ and $\mathrm{I_{hc}}$ is hampered due to self-heating. To be able to account for self-heating we need to know the temperature rise. This temperature rise can be calculated from the dissipated power and the temperature dependence of the collector and base current. As argued before the temperature dependence of both the collector and base current can be extracted from measurements at small current level over temperature. Therefore the best place to extract the temperature parameters is before starting with the high current

©Koninklijke Philips Electronics N.V. 2001

Table 7: *Extraction sequence to obtain the temperature parameters. The third column indicates the preferred choice from the list of electrical parameters to extract accurately the temperature parameters. In brackets some alternatives are indicated.*

1	$A_{Q_{B0}}$	V_{er} (V_{ef})
2	V_{g_B}	I_s
3	V_{g_C}	I_{Br} (C_{j_C})
4	V_{g_j}	I_{Bf}
5	$dV_{g\beta f}$	β_f
6	$dV_{g\beta r}$	β_{ri}
7	$dV_{g\tau_E}$	τ_E
8	V_{g_S}	I_{Ss}

parameter extraction. Then we have accurate temperature parameters to take into account self-heating at high current densities.

There are more electrical parameters then temperature parameters (see Table 6). Therefore, for each temperature parameter, we choose an electrical parameter from which we will extract the temperature parameter. (This is easier than doing a fit over all the electrical parameters and it gives more control.) The sensitivity of the electrical parameters with respect to temperature (large sensitivity gives an easy extraction) and the importance of some characteristics define the choices. The advised choices are listed in Table 7.

The bandgap voltages of the base, collector and substrate can be extracted from the increase of the saturation currents I_s, I_{Bf}, I_{Br} and I_{Ss} with temperature. Due to the large sensitivity of a saturation current with temperature an accurate extraction is possible. The extraction of the non-ideal reverse base current parameter I_{Br} may be difficult when the substrate current dominates the total reverse base current. As an alternative the temperature dependence of the base-collector depletion capacitance C_{j_C} at zero bias can be used. Because depletion capacitances only slightly increase with temperature accurate capacitance measurements are needed to extract reliable bandgap voltages from those measurements. (This is also true for C_{j_E} and C_{j_S}. Their bandgap voltages can, however, be accurately obtained from the temperature dependence of I_s and I_{Ss}.)

The temperature coefficient $A_{Q_{B0}}$ for the neutral base charge Q_{B0} can be extracted from the reverse and/or forward Early voltage. The temperature dependence of the forward and reverse current gain is given by $dV_{g\beta f}$ and $dV_{g\beta r}$. Usually the cut-off frequency f_T decreases with temperature and this can be characterised by $dV_{g\tau_E}$.

3.2 Different extraction procedures for temperature parameters

Different extraction over temperature procedures are possible for IC transistors and discrete transistors. In an IC process one has transistors with different dimensions and the electrical parameters at the reference temperature are calculated using geometric scaling rules. The temperature parameters are always taken geometry-independent. Therefore

 ©Koninklijke Philips Electronics N.V. 2001

only for one transistor (the reference transistor) the temperature parameters are extracted. No attempt is made to have the best fit for all geometries over temperature. This of course reduces also considerably the measurement effort.

For a discrete transistor one has just one geometry and therefore it is more viable to strive for the best fit over temperature. This will of course lead to a less than optimal result at the reference temperature itself. All electrical parameters now have to be extracted at each temperature. Both the parameter value at the reference temperature and its temperature scaling parameter are extracted from the all measurements. For temperature independent parameters the average value over temperature can be taken.

Different methods can be used to extract temperature parameters depending on the desired accuracy.

1. The simplest way to extract temperature parameters is to use only a limited data set at one elevated temperature, together with the data at the reference temperature. First we extract the parameters at the reference temperature. Then we repeat the extraction at a high temperature (e.g. 100°C). Instead of extracting the electrical parameter (column 3 in Table 7) from the measurements at the elevated temperature, we extract the corresponding temperature parameter (as shown in column 2 in Table 7). The main advantage is that no additional software is needed because we can use the standard extraction routines of the single transistor which contains the temperature scaling rules for all electrical parameters.

   As an example we look at the saturation current $\mathsf{I_S}$ and its temperature parameter $\mathsf{V_{g_B}}$. Both are extracted from the collector current in the forward Gummel plot. $\mathsf{I_S}$ is extracted using the measurement at the reference temperature. Using the already extracted saturation current $\mathsf{I_S}$ and the temperature scaling rule of $\mathsf{I_S}$, we extract $\mathsf{V_{g_B}}$ from the measurement at the elevated temperature. The extraction conditions for $\mathsf{V_{g_B}}$ are the same as for $\mathsf{I_S}$ (no high injection, no quasi-saturation, negligible voltage drop over base and emitter resistance).

   Because we use only one high temperature the accuracy of this method depends upon the reliability of the extraction at this temperature point (i.e. it must not be an outlier).

   The temperature parameters are extracted before the extraction of the high current related parameters, because we can then accurately correct for self heating due to power dissipation. The extracted parameters at the reference temperature are copied to the file containing the high temperature measurements. Here we do the extraction of the temperature parameters as depicted in Table 7. When we are finished the parameter list is copied back to the file with the measurements at the reference temperature and we can proceed with the extraction of the high current related parameters and the cut-off frequency f_T.

2. We can improve the overall accuracy of the previous method by using the characteristics at all temperatures for which data is available. The main advantage of this procedure is that one can check the correctness of the temperature scaling rules by

©Koninklijke Philips Electronics N.V. 2001

looking at the plots with extracted and simulated parameters as function of temperature. This procedure is accurate for the extraction of the temperature parameters in an IC process. We need additional software containing the Mextram temperature scaling rules to convert the parameter set at the reference temperature to all other temperatures. Also additional extraction and plot routines for the parameters over temperature are required.

We start with the extraction of the capacitance and the low and medium current levels related parameters at the reference temperature. We use this parameter set together with initial temperature parameters to create the parameter sets for all other temperatures. In all of these generated parameter sets we put the reference temperature T_{ref} to the elevated device temperature TEMP. For each of the temperatures we then do the extraction for the electrical parameters mentioned in Table 7. Since they all have there reference temperature equal to the actual temperature, the temperature scaling rules of the extraction routines are not used during these extractions. Note that the temperature independent electrical parameters are the same for all temperatures when the above procedure is followed, because we have set them to the values extracted at the reference temperature, and have not extracted them at elevated temperatures.

Next the extracted electrical parameters as function of temperature are collected as target data for optimisation. The value of the electrical parameter at the reference temperature and its temperature parameter as listed in Table 7 are optimised together. By extracting simultaneously the electrical parameter and temperature parameter we get the correct slope with temperature. The value of the electrical parameter should then be set back to the original extracted value at the reference temperature (the value that will ultimately be determined by geometric scaling), before continuing with the extraction of the high-current parameters.

Next we proceed with the high current related parameter extraction at the reference temperature including the cut-off frequency. After finishing the extraction at the reference temperature the parameter set is converted to all other temperatures and copied to the respective files to extract the last temperature parameter $dV_{g\tau_E}$. From the maximum of the cut-off frequency f_T the neutral emitter transit time parameter τ_E is extracted for all temperatures. Finally the extracted values of τ_E are plotted versus temperature to extract $dV_{g\tau_E}$.

3. In the third method we try to find the best fit for all measured data over temperature. This can be an extraction strategy for a discrete transistor.

   One way to achieve this is by simultaneously optimisation of all data over temperature. This is not recommended for reasons we now discuss. Look for instance at the base-emitter capacitance. One can extract C_{j_E} and p_E using the data from all temperatures. While doing this we keep V_{d_E} and V_{g_B} (estimated before from I_S) at their predefined values. The extracted parameters C_{j_E} and p_E then yield the minimum error between measured and simulated data. The disadvantage of this method is that we do not extract the individual parameters at each temperature. When there are unexpected differences between the Mextram model simulations and measured

 ©Koninklijke Philips Electronics N.V. 2001

data you do not know whether it is due to shortcomings in the electrical model (bias dependency) or in the temperature model (temperature dependency). Also we are not sure that the best physical parameter set is found. For instance, suppose that we extracted for each individual curve a constant grading coefficient $p_E = 0.5$. The capacitance at zero bias, however, does not follow properly the scaling rule of C_{jE}. To compensate for this non-ideal behaviour of C_{jE} a grading coefficient unequal to 0.5 will be extracted when doing the optimisation of all temperatures as mentioned before. Mainly for these two reasons we will not optimise simultaneously all data.

The method we prefer, is to do a complete parameter extraction at each temperature as performed at the reference temperature. As done in the previous method the total parameter extraction procedure is split into two parts. In the first part the capacitance parameters, the parameters at low and medium current levels and the temperature parameters are extracted. In the second part the parameters from the high current regime and the cut-off frequency f_T are considered. The extracted parameters are plotted versus temperature. There are three possible cases:

- A parameter has a temperature scaling rule and the corresponding temperature parameter should be extracted using this rule (e.g. V_{g_B} from I_s). These are the parameters listed in Table 7. We extract simultaneously the electrical parameter at the reference temperature and the temperature parameter. These parameters should be extracted first to have accurate temperature parameters for the following case.
- A parameter has a temperature scaling rule and the corresponding temperature parameter is not extracted using this rule (like V_{g_B} and C_{jE} and the series resistances). Now we extract only the electric parameter at the reference temperature to get the best fit over temperature.
- A parameter is temperature independent. In this case we take the average extracted value over temperature.

At this stage we have a first parameter set. This set still needs to be improved.

- We repeat the extraction of p_C from the base collector capacitance with a predefined value for X_p according to the scaling rule. The reason is that p_C and X_p are correlated.
- The avalanche parameter W_{avl} is extracted with a constant value for V_{avl} over temperature. Because V_{avl} is constant also the extracted values for W_{avl} will vary less with temperature.
- The forward and reverse Early voltage extraction is repeated because p_E, X_p and p_C slightly effect V_{er} and V_{ef}.
- The extraction of the parameter value at the reference temperature has to be repeated for p_C, W_{avl}, V_{er} and V_{ef}.

Now we proceed with the extractions of the knee current I_k, the epilayer and the transit time parameters at each temperature. The over temperature scaled parameter

©Koninklijke Philips Electronics N.V. 2001

set is used instead of the initially extracted parameters. Self heating of the device can taken accurately into account because we know already all temperature parameters except $dV_{g\tau_E}$. The thermal resistance R_{th} may be extracted at each temperature or a constant average value can be taken. Note that Mextram does not have a scaling rule for it.

After finishing this parameter extraction the obtained parameters are plotted versus temperature. The parameter value at the reference temperature is extracted to achieve the best fit over temperature for I_k, R_{Cv}, SCR_{Cv}, I_{hc}, τ_{epi}, τ_B, τ_E and $dV_{g\tau_E}$. Then we recompute all the electrical parameters and repeat the optimisation of f_T with only τ_E as parameter to improve the dependence of the maximum of f_T with temperature. In the final step τ_E and $dV_{g\tau_E}$ are refined from the new τ_E values.

In summary three different extraction strategies for the temperature parameters are explained. The first method can be used for a fast but less accurate temperature parameter extraction, the second method can by applied to an IC transistor, and the third method to a discrete transistor.

3.3 Experimental examples

In this section experimental results of the extracted and simulated electrical parameters listed in Table 7 are shown as function of temperature.

The temperature coefficients of the series resistances are difficult to extract from transistor characteristics. Usually the sheet resistance of a certain layer is obtained from special test structures. The same structures can be used to determine the temperature coefficient. In this example we take $A_E = 0$, $A_B = 0.9$, $A_{ex} = 0.5$, $A_C = 1$ and $A_S = A_{epi} = 2.5$.

In Figs. 31 and 32 the reverse and forward Early voltages V_{er} and V_{ef} are plotted. The temperature parameter $A_{Q_{B0}}$ may be extracted using both Early voltages. The parameters V_{g_C} and V_{g_B} to be extracted in the following steps have only a slight influence on the extracted value of $A_{Q_{B0}}$. Therefore reasonable initial values for V_{g_C} and V_{g_B} are in general sufficient. The extracted value for $A_{Q_{B0}}$ is 0.131.

From the forward Gummel plot the collector saturation current I_s, the non-ideal base current I_{Bf} and the forward current gain β_f are extracted. The plots are shown in Figs. 33, 34 and 35. The saturation currents are strongly temperature dependent and therefore the corresponding temperature parameters are easy and accurate to extract. The extracted values are: $V_{g_B} = 1.15\,V$, $V_{g_j} = 1.07\,V$ and $dV_{g\beta f} = 25.8\,mV$. As seen in Fig. 34 the parameter value at the reference temperature β_f is extracted simultaneously with the corresponding temperature parameter $dV_{g\beta f}$ to get the correct temperature dependence. Would we have fixed β_f at the reference temperature the temperature dependence would have become too small, due to the low value of β_f at $T = 25°C$. Afterwards β_f may be set back to the original value as extracted at the reference temperature. The same procedure is followed in the other cases.

From the reverse Gummel plot the substrate saturation current I_{Ss}, the reverse gain β_{ri} of

 ©Koninklijke Philips Electronics N.V. 2001

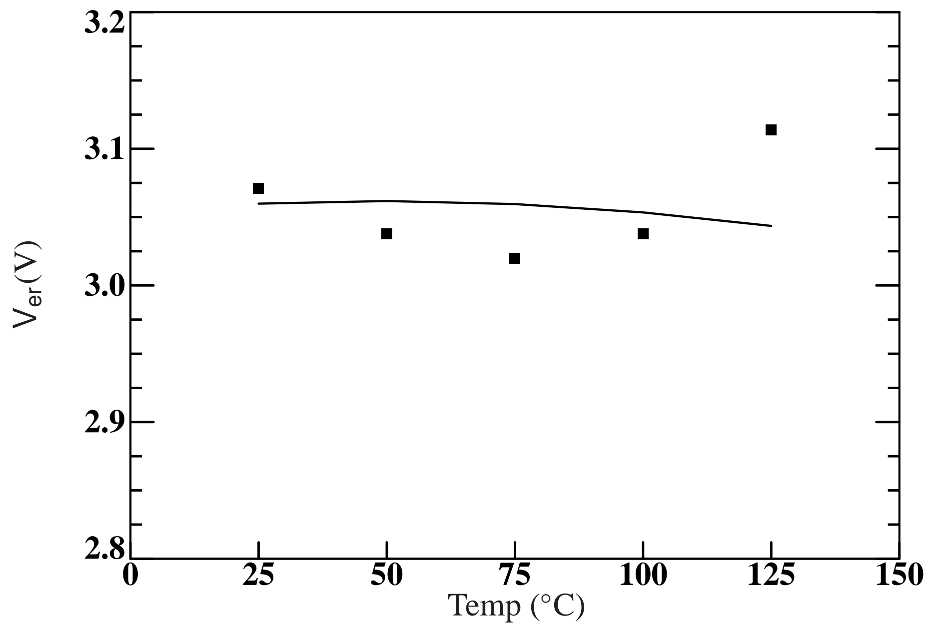

Figure 31: *Extracted (markers) and simulated (line) values of the reverse Early voltage.*

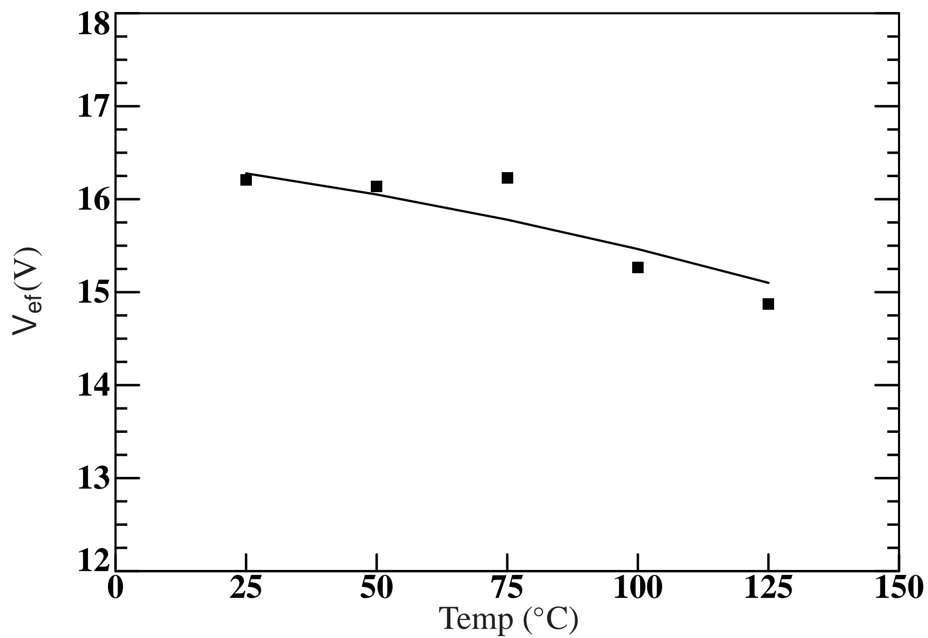

Figure 32: *Extracted (markers) and simulated (line) values of the forward Early voltage.*

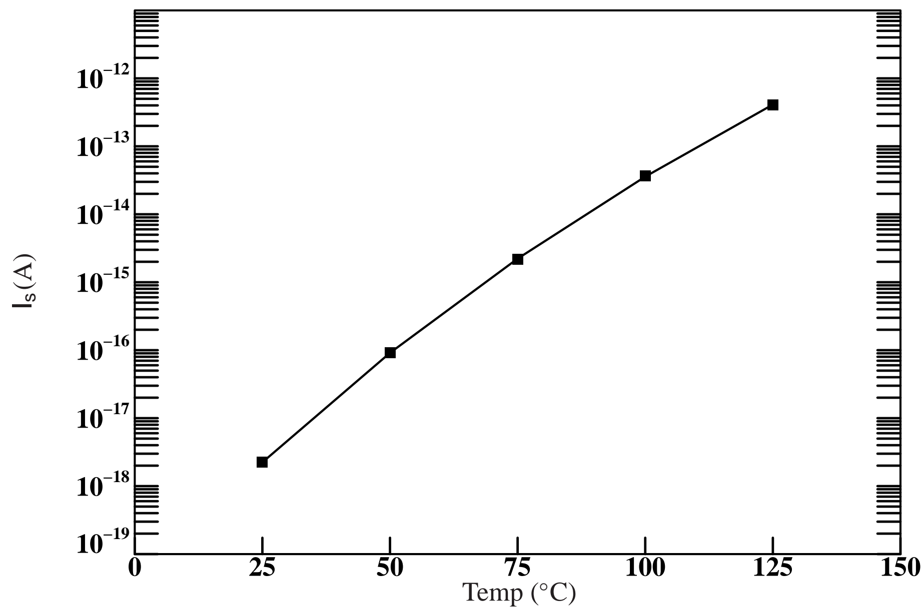

Figure 33: *Extracted (markers) and simulated (line) values of the collector saturation current.*

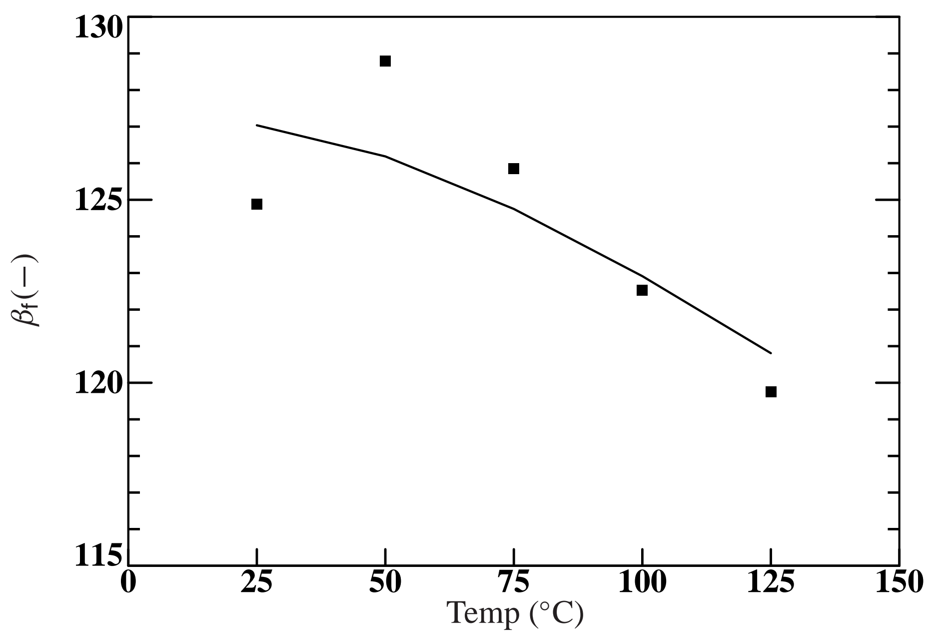

Figure 34: *Extracted (markers) and simulated (line) values of the forward current gain.*

 ©Koninklijke Philips Electronics N.V. 2001

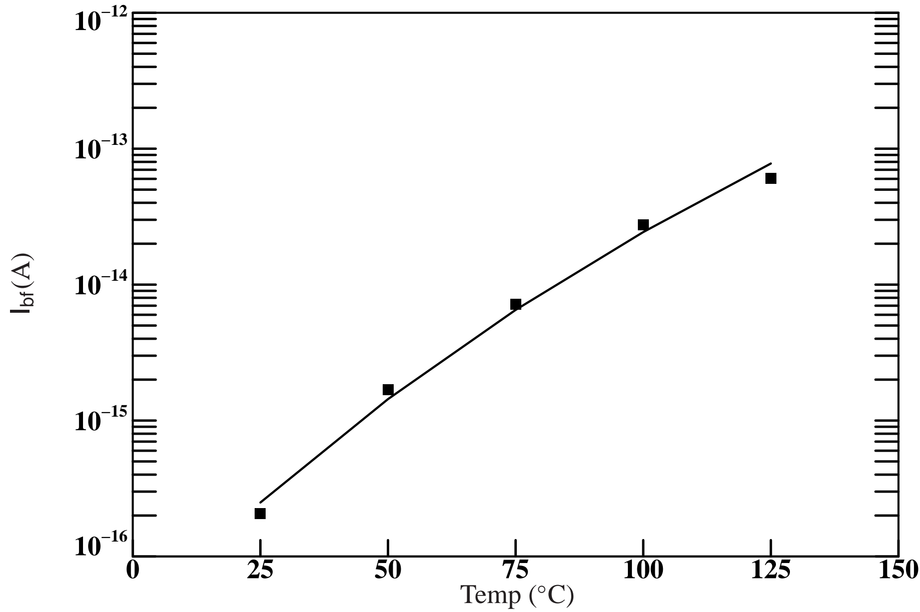

Figure 35: *Extracted (markers) and simulated (line) values of the non-ideal forward base current.*

the intrinsic NPN transistor and the non-ideal reverse base current I_{Br} are used to determine the reverse temperature parameters. The plots are shown in Figs. 36, 37 and 38. The extracted parameter values are: $V_{g_S} = 1.17$ V, $V_{g_C} = 1.18$ V and $dV_{g\beta r} = 24.6$ mV.

From the maximum of the cut-off frequency f_T the emitter transit time parameter τ_E is extracted and the results are shown in Fig. 39. The cut-off frequency slightly decreases with temperature. The extracted parameter value for $dV_{g\tau_E}$ is 36 mV.

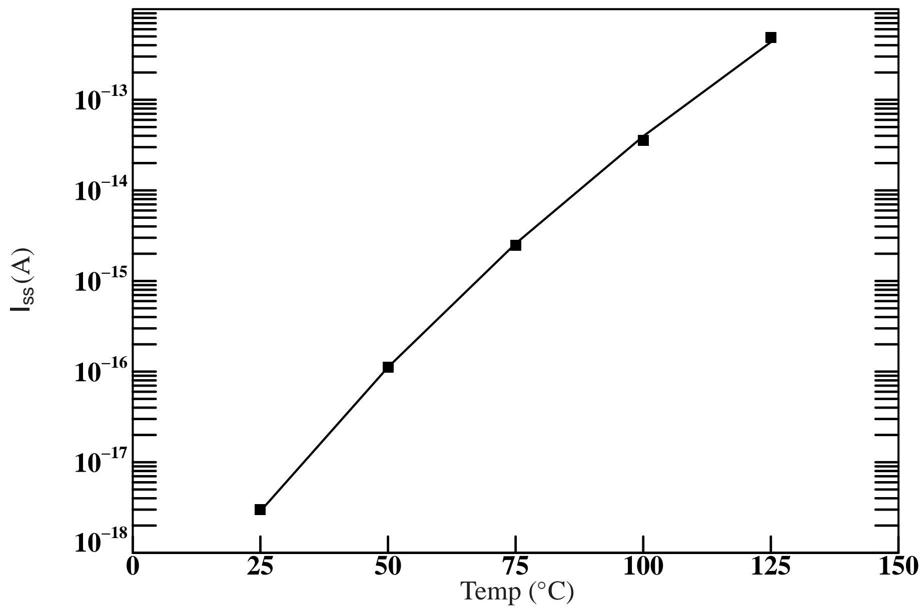

Figure 36: *Extracted (markers) and simulated (line) values of the substrate saturation current.*

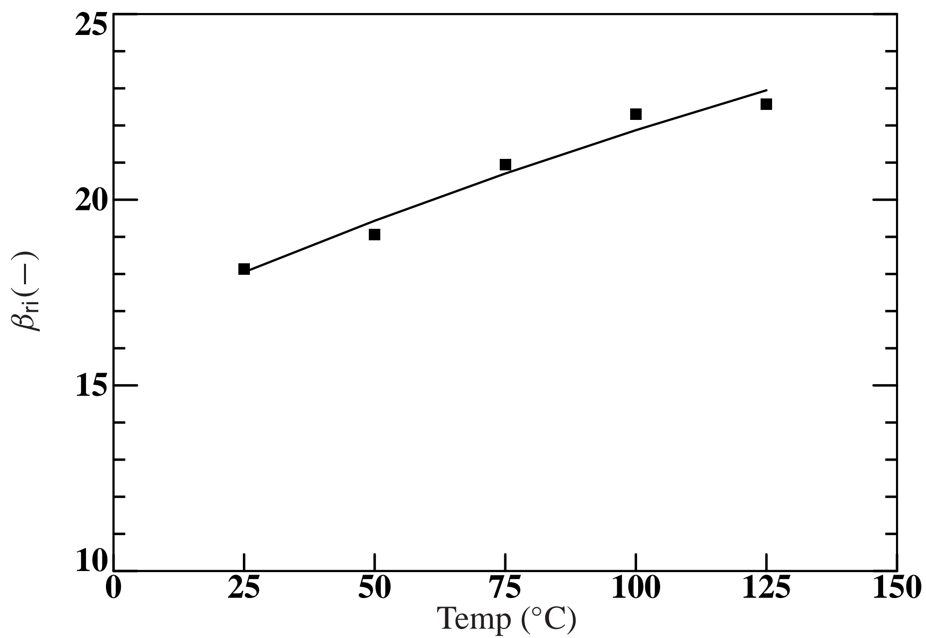

Figure 37: *Extracted (markers) and simulated (line) values of the reverse current gain of the intrinsic NPN transistor.*

 ©Koninklijke Philips Electronics N.V. 2001

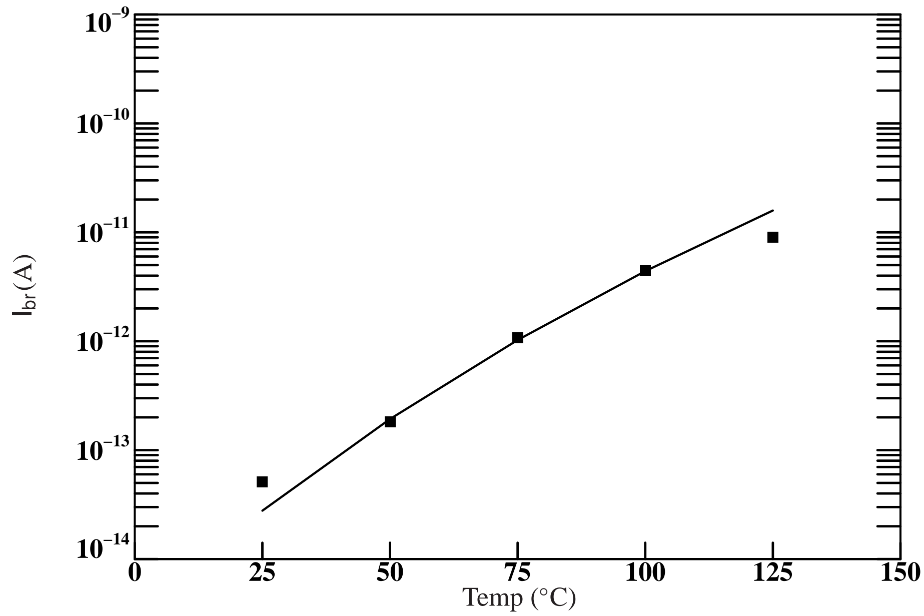

Figure 38: *Extracted (markers) and simulated (line) values of the non-ideal reverse base current.*

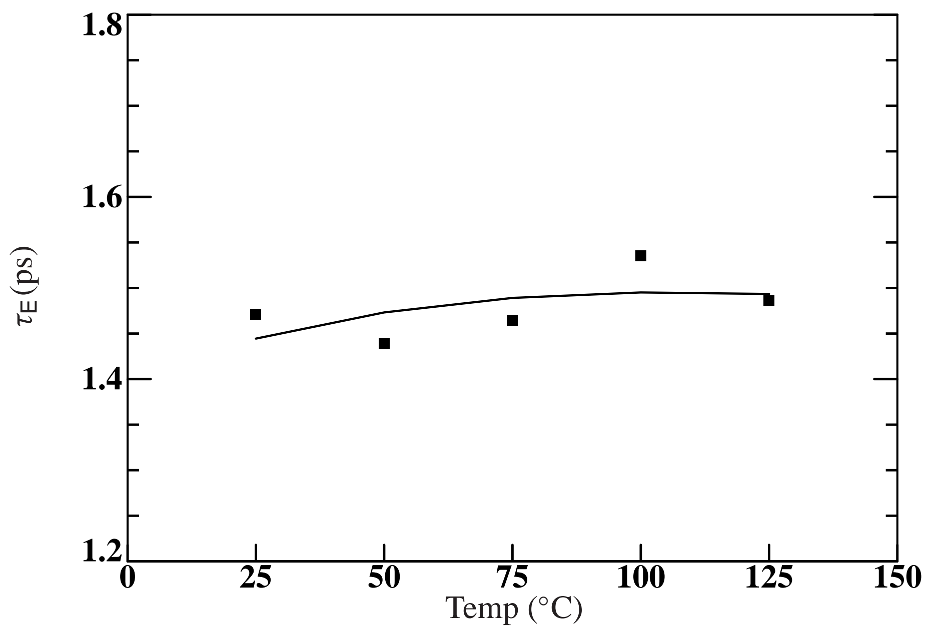

Figure 39: *Extracted (markers) and simulated (line) values of the emitter transit time.*

4 Geometric scaling

In IC design it is important to have a geometrically scalable transistor model. The Mextram model has a sound physical base and describes the various physical parts of the transistor. Therefore the parameters of Mextram scale excellently with geometry. Using this physically based geometry scaling it is possible to introduce statistical modelling [6].

A very simple MULT-scaling is present in the model. This scaling is accurate when transistors are put in parallel. All current and capacitance parameters are multiplied with MULT and the resistances are divided by MULT.

For IC transistors with different emitter dimensions the MULT-scaling is not very accurate especially for narrow devices. Therefore we will provide geometric scaling rules for the main electrical parameters for use in an IC process. Note that these geometric scaling rules are not part of the Mextram model. What we will show is a simple way to describe the geometry scaling of Mextram. It can act as the basis of a scaling model. A complete scaling model is only possible if the actual process is know, since number of base and collector contacts and precise design (the number of emitter fingers for instance) determine the eventual model. It is for this reason that Mextram itself does not contain a scaling model.

Many of the Mextram parameters scale with an area component and one or two sidewall components. The scaling parameters are then the specific value per unit area or per unit sidewall length. To be able to extract reliable scaling parameters it is important to have transistors available with a large aspect ratio between the emitter area and perimeter.

In general the parameters describing the high collector current regime and degradation of the cut-off frequency f_T are correlated in some extend and therefore it is difficult to discriminate these parameters unambiguously for a single transistor. Especially the geometric scaling rules of the collector epilayer parameters gives additional information to discriminate these parameters.

This chapter of the report is organised as follows. In the following section we discuss the general procedure for geometric scaling. We discuss the effect of the difference Δ between the mask dimensions and the dimension in silicon. A method to determine Δ of the emitter is given. Next the selection of transistor geometries to be used is treated in more detail. Then the geometric scaling of most of the Mextram parameters is presented. Finally, we briefly discuss statistical modelling.

4.1 General procedure

Many of the Mextram parameters scale with an area component and one or two sidewall components (corner components can be included if necessary)

$$P = P^b \, H \, L + 2 \, P^s \, (H + L) \, . \tag{4.1}$$

Here P is the actual parameter, P^b is the bottom component, P^s is the sidewall component, and H and L are the effective width and length (these might be the emitter dimen-

 ©Koninklijke Philips Electronics N.V. 2001

sions, or the base dimensions, etc., depending on the parameter). Note that the so-called unity parameters [6] P, P^b and P^s all have different units. The expression (4.1) holds for non-walled emitters. In the case of walled emitters a difference must be made between oxide sidewalls and silicon sidewalls. We will not discuss this case here.

To determine the bottom and sidewall components we we plot from our extraction results $P/(H\,L)$ versus the aspect ratio $2\,(H+L)/(H\,L)$. This should give a straight line. The bottom component P^b is the intersection with the vertical axis. The slope of the line gives the sidewall component P^s.

Some other parameter do not scale with an area. The formula we use then is Eq. (4.1) divided by the area:

$$P = P^b + P^s \left(\frac{2}{H} + \frac{2}{L}\right). \tag{4.2}$$

The bottom and sidewall components are now determined by plotting P itself versus the aspect ratio $2/H + 2/L$.

In many cases the complete layout of the transistor (i.e., the dimensions of all the masks), is determined by the emitter width H_{em} and length L_{em}. The dimensions of the base (H_{base} and L_{base}), the collector, the isolation etc. are then given as function of the emitter dimensions. In such a case there are only two dimensions that can be changed independently.

The possibility to determine more unity parameters for a single electrical parameter depends on the number of independent geometric dimensions. The base-collector depletion capacitance, for instance, depends on base dimensions, but also on the emitter dimensions. It is, therefore, useful to be able to vary the base dimensions independently of the emitter dimensions. One possibility is to make use of different layout styles, like having either one or two base contacts, one or two collector contacts, or multiple emitter fingers. (Again, since the possible variations are endless, geometric scaling is not an integral part of Mextram, but must be done outside the model.)

4.1.1 Mismatch between mask and electrical dimensions

In some cases we do not only need the value of the parameter (like $\mathsf{C_{jE}}$) but also the ratio of the sidewall component and the area component (needed for instance for $\mathsf{XC_{jE}}$). It is then important to know what the actual sidewall component is. The extracted value depends however very much on the dimensions we take in Eq. (4.1), as we will show below.

In general we can write for the effective lengths

$$H = H^m - \Delta H, \tag{4.3a}$$
$$L = L^m - \Delta L, \tag{4.3b}$$

with H^m and L^m the mask dimensions and ΔH and ΔL the difference between the mask dimensions and the real (or electrical) dimension. These differences might be due to out-

diffusions, oxide spacer etc. Normally we know only the mask dimension H^m and L^m, while ΔH and ΔL are unknown.

Note that in most cases it is not useful to have both a ΔH and a ΔL. From a process point of view there should often be no difference. Furthermore, the Δ is most important for the smaller dimension (H) and has already less influence on the other dimension.

When we plot from our extraction results $P/(H^m\, L^m)$ versus the aspect ratio $2\,(H^m + L^m)/(H^m\, L^m)$ we get a straight line in which P^b is the intersection with the vertical axis and $P^s_{\rm eff}$ the slope of the line. The extracted area component of the parameter is independent of the assigned difference between mask and effective dimension. However, the sidewall component is strongly affected. Substitution of Eq. (4.3) into Eq. (4.1) with $\Delta H = \Delta L = \Delta$ gives

$$\begin{aligned} P &= P^b \left(H^m\, L^m - \Delta\, \left(H^m + L^m\right) + \Delta^2\right) + 2\, P^s\, \left(H^m + L^m - 2\,\Delta\right) \\ &\simeq P^b\, H^m\, L^m + 2\, \left(H^m + L^m\right)\, \left(P^s - \tfrac{1}{2} P^b\, \Delta\right). \end{aligned} \tag{4.4}$$

We see that the effective sidewall component is given by $P^s_{\rm eff} = P^s - \frac{1}{2} P^b\, \Delta$. So the actual sidewall component P^s one finds depends directly on the Δ one uses. Note that the effective sidewall component can take any value (positive or negative). For most parameters it is not very important which Δ one chooses. For a parameter like $\mathsf{XC_{jE}}$ we need the actual sidewall component P^s and not the effective one. To extract P^s accurately in this case one needs to know the value of Δ.

4.1.2 Determination of the effective junction lengths

There is no direct and obvious way to determine the length offset Δ from electrical measurements. The easiest way to give at least a reasonable value is by looking at the process and determining a physical value for Δ. This value (or the one found below) should then be used for all parameters that scale with emitter geometry. The same can be done for other dimensions.

As an alternative for finding Δ using electrical measurements one can consider the collector current in the forward-Gummel measurement. This can be done at a given base-emitter bias of, say, $V_{BE} = 0.7$ V. The main contribution to Δ is due to the oxide L-spacers and/or out-diffusions. To determine Δ the collector current is defined as

$$I_C = I_C^b\, \left(H^m_{\rm em} - \Delta_{\rm em}\right)\, \left(L^m_{\rm em} - \Delta_{\rm em}\right), \tag{4.5}$$

where we did not include the sidewall contribution. The parameters I_C^b and $\Delta_{\rm em}$ are obtained from a least square fit to the data measured for various geometries.

For the collector-base junction the mask dimension of the base region may be used and for the collector-substrate junction the mask dimension of the buried layer (BN). These junction areas are usually much larger than the emitter area and therefore a correction with $\Delta_{\rm base}$ or $\Delta_{\rm coll}$ is less important. For simplicity we will neglect those in the following (i.e.

 ©Koninklijke Philips Electronics N.V. 2001

we take $\Delta_{\text{base}} = \Delta_{\text{coll}} = 0$). Note that taking another value for these offset values will result in other values of the scaling parameter for the sidewall components, as discussed before. But again one should use the same Δ_{base} or Δ_{coll} for all parameters.

Once we have effective widths and lengths H_{em}, L_{em}, H_{base}, L_{base} etc. we use these for all Mextram parameters related to the emitter-base, base-collector or collector-substrate area.

4.1.3 Choice of scaling parameters

From the previous discussion we see that there are actually two different ways of including sidewall components. One can either use Eq. (4.1), once the dimensions H and L are given, or one can use

$$P = P^b\,(H - \Delta)\,(L - \Delta). \tag{4.6}$$

(This second method can not be used in the case we need the actual ratio of sidewall and bottom components, as discussed before.) In the first case the two fitting parameters are P^b and P^s. In the second case they are P^b and Δ. Using however all three parameters P^b, P^s and Δ as fitting parameters is not very sensible, since P^s and Δ have almost the same effect. Hence we recommend to fix Δ and use Eq. (4.1) with the correct dimensions. If one needs a third fitting parameter one can include a corner contribution P^c in Eq. (4.1).

4.2 Selection of transistors

To be able to extract reliable unity parameters it is important to select transistors with a large aspect ratio. The aspect ratio is defined as the ratio between perimeter and area

$$\text{aspect ratio} = \frac{2\,(H + L)}{H\,L} = \left(\frac{2}{H} + \frac{2}{L}\right). \tag{4.7}$$

The aspect ratio of the largest (square) transistor should be sufficiently small ($H = L = 10 \ldots 20\,\mu$m) to extract accurate floor components. This is especially important for the depletion capacitances, avalanche currents, Early effect and the saturation currents of collector, base and substrate. These large structures can not be used for the high current related parameters due to self-heating and current crowding in the active base region.

It is recommended to have at least one row of say five transistors with constant lateral emitter width and various emitter stripe lengths and one row of transistors with constant emitter stripe length with various lateral widths, all having the same transistor layout. This means that we need at least nine transistors.

Next devices with different layout styles (one or two base contacts, one or two collector contacts etc.) may be added. For comparison purposes it is convenient that the emitter dimensions of these devices also exist in the two standard rows.

©Koninklijke Philips Electronics N.V. 2001

For a good extraction the selected devices should also be available with a short between the emitter and substrate terminals. These structures are needed for the high frequency S-parameter measurements.

4.3 Geometric scaling of Mextram parameters

In the following sections the geometric scaling of the various Mextram parameters will be treated. The extraction of the geometric parameters should be done parallel with the extraction of the electrical parameters. This means for instance that after the extraction of the capacitances one should first do the geometric scaling of the capacitances before going on with the extraction of the other electrical parameters. In the subsequent extraction steps one must then not use the originally extracted values of the capacitance parameters, but rather the scaled values. In this way extraction noise and correlation between the parameters can be reduced. (For instance, if the value of $\mathsf{p_E}$ shows some optimiser noise, this will affect the value of $\mathsf{V_{er}}$, since these are correlated. By taking the value of $\mathsf{p_E}$ after geometric scaling, this correlation will have no effect when one does the geometric scaling of $\mathsf{V_{er}}$).

4.3.1 Base-Emitter depletion capacitance

The base-emitter depletion capacitance C_{BE} has three parameters: the zero volt capacitance $\mathsf{C_{jE}}$, the diffusion voltage $\mathsf{V_{d_E}}$ and the grading coefficient $\mathsf{p_E}$. (We will discuss the overlap capacitance in the next section.) It is assumed that $\mathsf{C_{jE}}$ is made up by a bottom component $C^f_{j_E}$ and a sidewall component $C^p_{j_E}$. For simplicity we neglect a corner contribution. It may be important for the minimum size transistor. However, the capacitance of this transistor is difficult to measure accurately due to the small size (relatively large spread). Therefore we have as a simple geometric scaling rule

$$C^f_{j_E} = C^b_{j_E} H_{\mathrm{em}} L_{\mathrm{em}}, \tag{4.8a}$$
$$C^p_{j_E} = 2\, C^s_{j_E} \left(H_{\mathrm{em}} + L_{\mathrm{em}}\right), \tag{4.8b}$$
$$\mathsf{C_{jE}} = C^f_{j_E} + C^p_{j_E}, \tag{4.8c}$$
$$\mathsf{XC_{jE}} = \frac{C^p_{j_E}}{\mathsf{C_{jE}}}. \tag{4.8d}$$

The Mextram parameter $\mathsf{XC_{jE}}$ is the fraction of $\mathsf{C_{jE}}$ that belongs to the sidewall.

The bias dependency of the capacitance is given by the diffusion voltage and the grading coefficient. We assume that the bottom and sidewall part have their own bias dependency. Then the bias dependency of the compound capacitance is approximated with the weighted sum of bottom and sidewall component of the capacitance

$$\mathsf{V_{d_E}} = \left(1 - \mathsf{XC_{jE}}\right) V^b_{d_E} + \mathsf{XC_{jE}}\, V^s_{d_E}, \tag{4.9a}$$
$$\mathsf{p_E} = \left(1 - \mathsf{XC_{jE}}\right) p^b_E + \mathsf{XC_{jE}}\, p^s_E. \tag{4.9b}$$

 ©Koninklijke Philips Electronics N.V. 2001

Because $\mathsf{V_{d_E}}$ and $\mathsf{p_E}$ depend on $C^f_{j_E}$ and $C^p_{j_E}$ we have to optimise them after $\mathsf{C_{j_E}}$. The advantage of the above formulation is that for any geometry the diffusion voltage and the grading coefficient always lie between the value specified for the bottom and sidewall component. This can not be guaranteed when a first order approximation is used e.g. for the grading coefficient

$$\mathsf{p_E} = p^b_E + p^p_E \frac{2\,(H_{\mathrm{em}} + L_{\mathrm{em}})}{H_{\mathrm{em}}\,L_{\mathrm{em}}}. \tag{4.10}$$

For a negative value of p^p_E (as is usual the case) the grading coefficient decreases with aspect ratio and may become negative for large aspect ratio's.

The diffusion voltage $\mathsf{V_{d_E}}$ of the base-emitter junction is relatively high and difficult to extract from measurements. It is also strongly correlated with the grading coefficient. Therefore we often make the diffusion voltage geometry independent ($V^b_{d_E} = V^s_{d_E}$).

4.3.2 Base-Emitter overlap capacitance

The extraction of the overlap capacitance is not an easy one. This is due to fact that there is some ambiguity between the overlap capacitance and the grading coefficient: both can be used to describe the same measurement. Our first remark is, therefore, that in many cases it is very well possible to do without it (i.e., setting $\mathsf{C_{BEO}} = 0$). It is almost impossible to see the difference between having part of the base-emitter capacitance in the overlap capacitance or having all of it in the depletion capacitance.

The next best thing one can do is try to calculate its value from process knowledge and use that value. (As mentioned in the introduction we do not discuss any extraction methods related to special structures.)

If one really wants to do the extraction of the overlap capacitance from measurements on normal transistors one must start with some approximations to reduce the ambiguity. As mentioned before it is best to start with a geometry-independent diffusion voltage. But also the grading coefficient should be made geometry independent. Its value should be chosen as the grading coefficient of the bottom (as extracted above): $\mathsf{p_E} = p^b_E$. For the total capacitance we use the relations

$$\mathsf{C_{BEO}} = 2\,C^s_{BEO}(H_{\mathrm{em}} + L_{\mathrm{em}}), \tag{4.11a}$$

$$C_{BE}(\mathcal{V}_{\mathrm{BE}}) = C_{t_E}(\mathcal{V}_{\mathrm{BE}}) + \mathsf{C_{BEO}}. \tag{4.11b}$$

The latter relation is basically the same as Eq. (2.16). Now one must determine the bottom part and the side-wall part, in the way discussed before, if possible for every bias point. The relation for the bottom part is

$$C^f_{BE} = \frac{C^b_{j_E}\,H_{\mathrm{em}}\,L_{\mathrm{em}}}{(1 - \mathcal{V}_{\mathrm{BE}}/\mathsf{V_{d_E}})^{\mathsf{p_E}}}. \tag{4.12}$$

©Koninklijke Philips Electronics N.V. 2001

Once the bottom part is known, the grading coefficient can be extracted. Given the grading coefficient one can make a distinction between the overlap capacitance and the side-wall part of the depletion capacitance using the side-wall component of the total capacitance:

$$C^p_{BE} = \left(\frac{C^s_{j_E}}{(1 - \mathcal{V}_{\mathrm{BE}}/\mathrm{V_{d_E}})^{\mathrm{p_E}}} + C^s_{BEO} \right) 2\,(H_{\mathrm{em}} + L_{\mathrm{em}}). \tag{4.13}$$

The bias dependence of the first part is fixed. Hence the bias dependence of the total sidewall component can be fitted by optimising $C^s_{j_E}$ and C^s_{BEO}.

4.3.3 Base-Collector depletion capacitance

The base-collector depletion capacitance can be treated in the same way as the base-emitter depletion capacitance. However for an advanced bipolar transistor with a selective implanted collector (SIC) the bottom capacitance is not homogeneous over the floor area. Therefore the base-collector capacitance may be treated in a somewhat different way than the base-emitter capacitance.

We start with the simplest implementation, in which it is assumed that $\mathrm{C_{jC}}$ scales with the area of the SIC (which is the mask dimension of the emitter) and with the length of the peripheral of the base-collector junction. Also the bottom area besides the emitter is treated as sidewall.

The diffusion voltage $\mathrm{V_{dC}}$ and the grading coefficient $\mathrm{p_C}$ are treated in the same way as for the base-emitter junction.

$$C^f_{j_C} = C^b_{j_C}\, H^m_{\mathrm{em}}\, L^m_{\mathrm{em}}, \tag{4.14a}$$

$$C^p_{j_C} = 2\, C^s_{j_C}\, (H_{\mathrm{base}} + L_{\mathrm{base}}) \tag{4.14b}$$

$$\mathrm{C_{jC}} = C^f_{j_C} + C^p_{j_C}, \tag{4.14c}$$

$$\mathrm{XC_{jC}} = \frac{C^f_{j_C}}{\mathrm{C_{jC}}}, \tag{4.14d}$$

$$\mathrm{V_{dC}} = \mathrm{XC_{jC}}\, V^b_{dC} + \left(1 - \mathrm{XC_{jC}}\right)\, V^s_{dC}, \tag{4.14e}$$

$$\mathrm{p_C} = \mathrm{XC_{jC}}\, p^b_C + \left(1 - \mathrm{XC_{jC}}\right)\, p^s_C, \tag{4.14f}$$

$$\mathrm{X_p} = \text{geometry independent},$$

$$\mathrm{m_C} = \text{geometry independent}.$$

In the Mextram model the diffusion voltage $\mathrm{V_{dC}}$ has a strong impact on the output conductance in quasi-saturation. It has a minor impact on collector capacitance. Furthermore $\mathrm{V_{dC}}$ is also correlated with the grading coefficient $\mathrm{p_C}$. From experiences in modelling quasi-saturation we found that a geometry independent $\mathrm{V_{dC}}$ gives satisfactory results in most cases. Due to current spreading for small devices (i.e. large aspect ratio) $\mathrm{V_{dC}}$ might decrease slightly with increasing aspect ratio. The main effect of current spreading for

 ©Koninklijke Philips Electronics N.V. 2001

small devices has to taken into account by the collector resistance parameters being $\mathsf{R_{Cv}}$, $\mathsf{SCR_{Cv}}$ and $\mathsf{I_{hc}}$.

The last two parameters $\mathsf{X_p}$ and $\mathsf{m_C}$ of the collector capacitance may vary with geometry. However, these parameters are not always easy to extract and a geometry independent value normally meets the needs. The minimum of the unity capacitance of the collector beneath the emitter is approximately $\varepsilon / W_{\rm epi}$. The parameter $\mathsf{X_p}$ accounts for this minimum [$\mathsf{X_p} = \varepsilon/(C^b_{jC}\, W_{\rm epi})$]. The effect of $\mathsf{m_C}$ is mainly seen in the variation of the increase of f_T for different V_{CB}, for currents up to the top of the f_T. A small value of $\mathsf{m_C}$ gives a larger variation of f_T with V_{CB} than a large value of $\mathsf{m_C}$. It should not be larger than, say, 0.5.

More components of the zero bias capacitance can be added if needed. Note that these extra components can only be determined if there enough independent geometric dimensions (as discussed in Sec. 4.1). In such a case one can for instance use an equation like

$$\begin{aligned} \mathsf{C_{jC}} &= C^{Eb}_{jC}\, H^m_{\rm em}\, L^m_{\rm em} + 2\, C^{Es}_{jC}\, (H^m_{\rm em} + L^m_{\rm em}) \\ &+ C^{Bb}_{jC}\, H_{\rm base}\, L_{\rm base} + 2\, C^{Bs}_{jC}\, (H_{\rm base} + L_{\rm base}) \end{aligned} \tag{4.15}$$

4.3.4 Base-collector overlap capacitance

The same arguments that we have given for the base-emitter overlap capacitance also hold for the base-collector overlap capacitance. However, the situation for the base-collector capacitance is more complex, because there is more variation in geometry possible. At the same time this added complexity helps to discriminate between the various components (again only if there are enough independent geometrical dimensions available).

The basis of the extraction must again be a general formula for the total base-collector capacitance. Equation (4.15) can act as a starting point. Given the layouts that are available one change or add terms to Eq. (4.15), based on a physical idea of the various contributing elements. The overlap capacitance is one of them. We can give no general expression for the geometry dependence of the various contributions. Once this formulation is ready one can optimise the unity parameters from the available measurements.

4.3.5 Substrate-collector depletion capacitance

The scaling of the collector-substrate capacitance is treated in the same way as the base-emitter capacitance. The capacitance is assumed to scale with the dimension of the buried layer (BN) area:

$$C^f_{jS} = C^b_{jS}\, H_{\rm coll}\, L_{\rm coll}, \tag{4.16a}$$

$$C^p_{jS} = 2\, C^s_{jS}\, (H_{\rm coll} + L_{\rm coll})\,, \tag{4.16b}$$

$$\mathsf{C_{jS}} = C^f_{jS} + C^p_{jS} \tag{4.16c}$$

$$XC_{jS} = \frac{C^p_{jS}}{\mathsf{C_{jS}}}, \tag{4.16d}$$

$$\mathsf{V_{dS}} = \left(1 - XC_{jS}\right) V^b_{dS} + XC_{jS}\, Vd^s_S, \tag{4.16e}$$

$$\mathsf{p_S} = \left(1 - XC_{jS}\right) p^b_S + XC_{jS}\, p^s_S. \tag{4.16f}$$

In many cases the sidewall component is much larger than the floor component and therefore the floor component is difficult to extract directly from C-S capacitance measurements. Because the contribution to the total capacitance is then small an estimated value based on the substrate doping level is sufficient. For the same reason taking $\mathsf{V_{dS}}$ and $\mathsf{p_S}$ independent of geometry is sufficient in most cases. Note that XC_{jS} is not a parameter of Mextram itself.

4.3.6 Avalanche parameters

The avalanche parameters $\mathsf{W_{avl}}$ and $\mathsf{V_{avl}}$ are more or less constant in a certain process. The weak geometry dependence can simply be described with a first order term

$$\mathsf{W_{avl}} = W^b_{\mathrm{avl}} + W^s_{\mathrm{avl}} \left(\frac{2}{H_{\mathrm{em}}} + \frac{2}{L_{\mathrm{em}}}\right), \tag{4.17a}$$

$$\mathsf{V_{avl}} = \text{geometry independent},$$

$$\mathsf{S_{fH}} = S^s_{fH} \left(\frac{2}{H_{\mathrm{em}}} + \frac{2}{L_{\mathrm{em}}}\right). \tag{4.17b}$$

The avalanche current is mainly determined by the effective thickness of the epilayer parameter $\mathsf{W_{avl}}$ and the applied collector voltage. The punch through voltage $\mathsf{V_{avl}}$ determines the curvature of I_B with V_{CB}. Because of the weak dependence of both parameter with geometry the avalanche parameter $\mathsf{V_{avl}}$ can be treated as a constant. The current spreading factor $\mathsf{S_{fH}}$ modulates the electric field distribution at high current densities ($I_C > \mathsf{I_{hc}}$). This feature is activated with an on/off switch EXAVL. The value of S^s_{fH} is about $\mathsf{W_{avl}}/3$ assuming that the spreading angle is 45 degrees.

4.3.7 Reverse and forward Early effect

The reverse Early voltage $\mathsf{V_{er}}$ and the forward Early voltage $\mathsf{V_{ef}}$ are slightly geometry dependent and in most cases a first order scaling is sufficient:

$$\mathsf{V_{er}} = V^b_{er} + V^s_{er} \left(\frac{2}{H_{\mathrm{em}}} + \frac{2}{L_{\mathrm{em}}}\right), \tag{4.18a}$$

$$\mathsf{V_{ef}} = V^b_{ef} + V^s_{ef} \left(\frac{2}{H_{\mathrm{em}}} + \frac{2}{L_{\mathrm{em}}}\right). \tag{4.18b}$$

The Early voltages V^b_{er} and V^b_{ef} are for an infinitely large area.

From the unity depletion capacitances ($C^b_{j_E}$, $C^b_{j_C}$) and the Early voltages (V^b_{er}, V^b_{ef}) we can find the approximate doping level and pinched sheet resistance of the base. For pure silicon transistors (no SiGe base) the products $C^b_{j_E}\, V^b_{er}$ and $C^b_{j_C}\, V^b_{ef}$ have to be more or less

 ©Koninklijke Philips Electronics N.V. 2001

equal to each other. This relation can be used to check the extraction results. The value thus found is the (area component) of the neutral base charge Q^b_{B0}. Assuming asymmetric junctions we can roughly estimate the doping level of the base from the base-emitter capacitance and the doping level of the collector epilayer from the collector capacitance:

$$N_A = \frac{2\,(C^b_{j_E})^2\,V_{d_E}}{\varepsilon\,q}, \tag{4.19a}$$

$$N_{\rm epi} = \frac{2\,(C^b_{j_C})^2\,V_{d_C}}{\varepsilon\,q}. \tag{4.19b}$$

Again these values can act as a check on the extraction results.

From the base doping level N_A and the neutral base charge Q^b_{B0} we can estimate the pinched base sheet resistance $\rho^b_\square$. A simple mobility model for the p-doped base can be used

$$\rho^b_\square = \frac{1}{C^b_{j_E}\,V^b_{er}\,\mu_p}, \tag{4.20}$$

where μ_p is the mobility in the base, which can be calculated from Eqs. (2.10)–(2.12) of Section 2.3.3. The actual pinch sheet resistance may be considerable lower due to the emitter plug effect. This makes the scaling of $\mathsf{V_{er}}$, $\mathsf{V_{ef}}$ and $\mathsf{R_{Bv}}$ very difficult.

4.3.8 Collector currents

The collector saturation current $\mathsf{I_s}$ and the knee current $\mathsf{I_k}$ scale with the emitter area

$$\mathsf{I_s} = I^b_{s_C}\,H_{\rm em}\,L_{\rm em} + 2\,I^s_{s_C}\,(H_{\rm em} + L_{\rm em}), \tag{4.21a}$$

$$\mathsf{I_k} = I^b_k\,H_{\rm em}\,L_{\rm em} + 2\,I^s_k\,(H_{\rm em} + L_{\rm em}). \tag{4.21b}$$

The extracted value for the sidewall component $I^s_{s_C}$ will be small and may be either positive or negative. As mentioned in Section 4.1.1 the value of the sidewall component strongly depends on the difference Δ between the mask and electrical dimension of the emitter. The value of Δ can be extracted from the collector current, see Eq. (4.5), where the sidewall component of the collector current is assumed to be zero. This does not imply that also the sidewall component of collector saturation current $\mathsf{I_s}$ is zero. Due to the forward and reverse Early effects we still can find a small positive or negative sidewall component for $I^s_{s_C}$.

The physical interpretation of I^b_k and I^s_k should not be misunderstood. The extracted value I^b_k for the bottom part may be small due to DC current crowding. Then the main part of the emitter floor area does not contribute to the total collector current at high bias. Often $\mathsf{I_k}$ only scales with the perimeter of the emitter. This means that I^s_k is not the physical knee current of the sidewall collector current, but rather the dependence of the total knee current on the perimeter.

©Koninklijke Philips Electronics N.V. 2001

4.3.9 Base currents

The total base current consists of an ideal and a non-ideal component. The parameter of the ideal base current component is β_{f}. We will not scale β_{f} directly but use the base saturation current $I_{s_B} = \mathrm{I_s}/\beta_{\mathrm{f}}$. It is assumed that also the non-ideal base current scales with the emitter area

$$I_{s_B} = I_{s_B}^b\, H_{\mathrm{em}}\, L_{\mathrm{em}} + 2\, I_{s_B}^s\ (H_{\mathrm{em}} + L_{\mathrm{em}})\,, \tag{4.22a}$$

$$\mathrm{I_{Bf}} = I_{Bf}^b\, H_{\mathrm{em}}\, L_{\mathrm{em}} + 2\, I_{Bf}^s\ (H_{\mathrm{em}} + L_{\mathrm{em}})\,, \tag{4.22b}$$

$$\beta_{\mathrm{f}} = \frac{\mathrm{I_s}}{I_{s_B}}, \tag{4.22c}$$

$$\mathrm{XI_{B_1}} = \frac{2\, I_{s_B}^s\ (H_{\mathrm{em}} + L_{\mathrm{em}})}{I_{s_B}}, \tag{4.22d}$$

$$\mathrm{m_{Lf}} = \text{geometry independent.}$$

From the scaling of the ideal base current we can compute the Mextram parameter $\mathrm{XI_{B_1}}$, which is the fraction of the ideal base current that belongs to the sidewall of the base-emitter junction. At high current levels the base-emitter bias at the sidewall is somewhat higher then the internal base-emitter junction bias due to the voltage drop in the base resistance. This result in an additional decrease of the forward current gain. We need the correct forward gain for the extraction of some high current parameters. For this reason we must make sure that we use the scaled value of $\mathrm{XI_{B_1}}$ when we do further parameter extraction.

The slope of the non-ideal base current $\mathrm{m_{Lf}}$ should be taken as geometry independent otherwise the scaling of $\mathrm{I_{Bf}}$ becomes cumbersome.

The internal reverse base current of the NPN transistor is the difference between the total reverse base current and the substrate current. As with the forward base current also the (internal) reverse base current consists of an ideal and a non-ideal component. The parameter of the ideal part is β_{ri} and the parameters of the non-ideal part are $\mathrm{I_{Br}}$ and $\mathrm{V_{Lr}}$. The transition voltage $\mathrm{V_{Lr}}$ sets a minimum for the gain $I_E/(I_B - I_{\mathrm{sub}})$ at small current levels. Instead of scaling β_{ri} directly we use again the saturation current $I_{s_{Br}} = \mathrm{I_s}/\beta_{\mathrm{ri}}$. Both the saturation current of the ideal and of the non-ideal reverse base currents are assumed to scale with the base area

$$I_{s_{Br}} = I_{s_{Br}}^b\, H_{\mathrm{base}}\, L_{\mathrm{base}} + 2\, I_{s_{Br}}^s\ (H_{\mathrm{base}} + L_{\mathrm{base}})\,, \tag{4.23a}$$

$$\mathrm{I_{Br}} = I_{Br}^b\, H_{\mathrm{base}}\, L_{\mathrm{base}} + 2\, I_{Br}^s\ (H_{\mathrm{base}} + L_{\mathrm{base}})\,, \tag{4.23b}$$

$$\beta_{\mathrm{ri}} = \frac{\mathrm{I_s}}{I_{s_{Br}}}, \tag{4.23c}$$

$$\mathrm{V_{Lr}} = \text{geometry independent,}$$

$$\mathrm{X_{ext}} = \frac{X_{\mathrm{ext}}^s\ (H_{\mathrm{base}} + L_{\mathrm{base}})}{H_{\mathrm{base}}\, L_{\mathrm{base}} + X_{\mathrm{ext}}^s\ (H_{\mathrm{base}} + L_{\mathrm{base}})}. \tag{4.23d}$$

The cross-over voltage $\mathrm{V_{Lr}}$ should be taken geometry independent otherwise the scaling

 ©Koninklijke Philips Electronics N.V. 2001

of $I_{s_{Br}}$ will be disturbed. The partitioning factor $\mathsf{X_{ext}}$ is the ratio between the sidewall area and the total area of the base-collector junction.

4.3.10 Substrate current

The substrate current has two parameters, being the saturation current $\mathsf{I_{Ss}}$ and the high injection current $\mathsf{I_{ks}}$. High injection effects are seen already at relative small currents due to the low doping level of the epitaxial layer which is part of the base of the PNP transistor. The substrate current parameters scale with the dimension of the base-collector area. However the contributions from the different sidewalls need not be the same (depending on the process). There might be four different components: an area component $I^b_{Ss}\, H_{\rm base}\, L_{\rm base}$, a component from the sidewall where the collector plug resides $I^{L_1}_{Ss}\, L_{\rm base}$, one from the opposite sidewall without collector plug $I^{L_2}_{Ss}\, L_{\rm base}$, and a component from the two other sidewalls $2\, I^H_{Ss}\, H_{\rm base}$. Since the knee currents corresponds to high-injection effects, these effects will be largest where the doping is smallest. Hence the $I^{L_2}_{Ss}\, L_{\rm base}$ is the most important term. The scaling rule of the substrate saturation current $\mathsf{I_{Ss}}$ and its knee current $\mathsf{I_{ks}}$ may then read

$$\begin{aligned} \mathsf{I_{Ss}} &= I^b_{Ss} H_{\rm base} L_{\rm base} + N_{\rm coll} I^{L_1}_{Ss} L_{\rm base} + (2-N_{\rm coll})\, I^{L_2}_{Ss} L_{\rm base} + 2 I^H_{Ss} H_{\rm base}, &(4.24a)\\ \mathsf{I_{ks}} &= (N_{\rm coll}-1)\left(I^b_{ks}\, H_{\rm base}\, L_{\rm base} + 2\, I^{L_1}_{ks}\, L_{\rm base}\right) + \\ &\quad (2-N_{\rm coll})\; I^{L_2}_{ks}\, L_{\rm base} + 2\, I^H_{ks}\, H_{\rm base}, &(4.24b) \end{aligned}$$

where $N_{\rm coll}$ is the number of collector contacts ($N_{\rm coll} = 1$ or 2). The saturation current contains the four terms described above. The contribution of bottom component (I^b_{Ss}) and the sidewall where the collector plug is ($I^{L_1}_{Ss}$) are small and might be taken the same $I^{L_1}_{Ss} = I^b_{Ss}\, H_{\rm base}$.

The physical interpretation of the coefficients of the knee current $\mathsf{I_{ks}}$ of the substrate is rather difficult, just as in the case of the intrinsic transistor. For a transistor with only one collector plug high current effects are dominated by the low-doped regions (and the knee current of the BN is very high and must be neglected). The main contribution is then $I^{L_2}_{ks}\, L_{\rm base}$. In the case of two collector contacts the knee current is much higher. It therefore has a different functional dependence. Note that in processes with deep trench isolation there will in general not be a low doped n-region between base and substrate. The formulas for 2 collector contacts must then be used, independent of the actual number of contacts.

4.3.11 Series resistances

The extraction of the base and emitter resistance from high frequency Y-parameter measurements is described in detail in [21]. In this section we will first outline the separation of the base resistance R_b in a constant part $\mathsf{R_{Bc}}$ and a bias dependent part $\mathsf{R_{Bv}}$. Then the geometric scaling of both parameters is treated.

©Koninklijke Philips Electronics N.V. 2001

We can not simply add the Mextram base resistance parameters $\mathsf{R_{Bc}}$ and $\mathsf{R_{Bv}}$ to get the total base resistance as extracted from the measurements. The variable part[2] decreases due to base width modulation and DC current crowding. To separate the total measured base resistance R_B in a constant and variable part it is assumed that R_{Bv} varies in the same way as the DC current gain

$$R_B = \mathsf{R_{Bc}} + \frac{I_C}{I_B}\frac{\mathsf{R_{Bv}}}{\boldsymbol{\beta}_\mathsf{f}}, \tag{4.25}$$

in which $\boldsymbol{\beta}_\mathsf{f}$ is the Mextram parameter of the ideal forward current gain. For each transistor we take the measured total base resistance R_B, the collector current I_C and the base current I_B at the maximum of the cut-off frequency for $V_{CB} = 0\,\mathrm{V}$. For one transistor we can not separate $\mathsf{R_{Bc}}$ and R_{Bv}. However, when we apply a geometric scaling rule for $\mathsf{R_{Bc}}$ and $\mathsf{R_{Bv}}$ we can discriminate between both parameters.

The constant part $\mathsf{R_{Bc}}$ takes into account the resistance between the base terminal and the sidewall of the emitter

$$\mathsf{R_{Bc}} = \frac{\rho_{BE}\, H_{BE}}{N_\mathrm{base}\, L_\mathrm{base}} + \frac{R_\mathrm{link}}{2\,(H_\mathrm{em} + L_\mathrm{em})}. \tag{4.26}$$

The first contribution is from the p$^+$ poly layer with length L_base, a width H_{BE}, and a sheet resistance ρ_{BE}. N_base is the number of base stripes (N_base = 1 or 2). The second contribution is from the base link region and this resistance decreases proportional with the perimeter of the emitter. The parameters to be extracted are ρ_{BE} and R_link.

For non-walled devices the (zero-bias) resistance of the variable part $\mathsf{R_{Bv}}$ is reduced due to the end regions of the emitter. For a four sided contacted square emitter the resistance is approximately $\rho_\square^\mathrm{act}/28$, independent of the emitter dimension, where $\rho_\square^\mathrm{act}$ is the actual pinched base resistance. For non-square emitters it is assumed that we can apply the well know 1D relation to the middle region. Then both resistances are placed in parallel. The scaling rule of $\mathsf{R_{Bv}}$ for non-walled devices then becomes

$$R_1 = \frac{\rho_\square^\mathrm{act}}{28}, \tag{4.27a}$$

$$R_2 = \frac{\rho_\square^\mathrm{act}\, H_\mathrm{em}}{3\, N_\mathrm{base}^2\, (L_\mathrm{em} - H_\mathrm{em})}, \tag{4.27b}$$

$$\mathsf{R_{Bv}} = \frac{R_1\, R_2}{R_1 + R_2}. \tag{4.27c}$$

The resistance of the middle part R_2 depends on the number of base contacts. However, we have found that for a non-walled device with a silicided base poly the resistance around the emitter might be small enough to make the potential at the two sides of the emitter

[2] As in the model documentation [2] the variable part of the base resistance is loosely denoted by R_{Bv}, although it is described in the model by a current source $I_{B_1B_2}$. The corresponding parameter is $\mathsf{R_{Bv}}$.

 ©Koninklijke Philips Electronics N.V. 2001

almost equal, even if there is only one base contact. This means that for the calculation of R_2 the number of base contacts is then effectively 2, instead of 1.

This simple approach gives reasonable results compared with numerical simulations of $\mathsf{R_{Bv}}$ for emitters with different aspect ratios. In reality we have to account for the difference in pinch resistance between small and large devices due to emitter plug effects. A useful way to measure this is to use the reverse Early voltage. It is assumed that the variation in the reverse Early voltage is mainly caused by the variation in base charge. The pinch resistance is directly related to the base charge. The actual pinch resistance of a device then becomes

$$\rho_{\square}^{\mathrm{act}} = \rho_{\square} \frac{V_{er}^{b}}{\mathsf{V_{er}}}, \tag{4.28}$$

where $\mathsf{V_{er}}$ is the scaled reverse Early voltage as derived in Section 4.3.7 and V_{er}^{b} the reverse Early voltage of an infinity large device. The parameter to be extracted for $\mathsf{R_{Bv}}$ is the $\rho_{\square}$, the pinched base sheet resistance of an infinitely large device.

The total base resistance then becomes:

$$R_B = R_0 + \mathsf{R_{Bc}} + \mathsf{R_{Bv}}. \tag{4.29}$$

A constant resistance R_0 is added to account for probes, wiring etc., but in general it should be very small if de-embedding is done properly [4]. In total we have 4 parameters (ρ_{BE}, R_{link}, $\rho_{\square}$ and R_0) to be extracted. Often $\rho_{\square}$ and ρ_{BE} are known from the process and therefore only the resistance of the base link region R_{link} (and possibly R_0) has to be extracted. This procedure may also be used to verify the total measured base resistance when all process parameters are known in advance. Since it is difficult to extract accurate base resistance parameters from only one transistor a cross-check with known process parameters is important.

There are at least three methods to obtain the emitter resistance. Straight forward is the flyback method (open collector, and measure the collector voltage versus the emitter current). Because we know already the base resistance we can also use the forward Gummel plot to extract $\mathsf{R_E}$. The emitter resistance can also be extracted from small signal Y-parameters [21]. It is assumed that $\mathsf{R_E}$ scales with the emitter area, but we add a constant resistance to account for wiring etc.

$$\mathsf{R_E} = R_E^{c} + \frac{\rho_{R_E}}{H_{\mathrm{em}}\, L_{\mathrm{em}}}. \tag{4.30}$$

In the particular case of emitter resistance taking a different Δ might improve the fit, since the emitter area in the active device is not always the same as that within the emitter plug.

The collector resistance $\mathsf{R_{Cc}}$ depends on the the sheet resistance and the dimension of the buried layer. The distance between the collector plug and the last emitter stripe is denoted as H_{C_1}. Underneath the emitter(s) the lateral collector current decreases. A linear decrease of the collector current over a distance H_{C_2} is assumed. For one emitter

©Koninklijke Philips Electronics N.V. 2001

stripe $H_{C_2} = H_{\rm em}$ and for multi emitters H_{C_2} is the distance between the first and last emitter stripe plus 2 $H_{\rm em}$. Taking also into account the resistance of the collector plug and a constant series resistance the scaling rule for $\mathsf{R_{Cc}}$ reads

$$\mathsf{R_{Cc}} = R^c_{Cc} + \frac{R^{\rm plug}_{Cc}}{N_{\rm coll}\,L_{\rm base}} + \rho_{\rm BN}\,\frac{H_{C_1} + H_{C_2}/(3\,N_{\rm coll})}{N_{\rm coll}\,L_{\rm base}}, \tag{4.31}$$

whereas $N_{\rm coll}$ is the number of collector stripes. The contribution of H_{C_2} for single emitter stripes is small. The contributions of the buried layer and the collector plug both scale with $N_{\rm coll}\,L_{\rm base}$ and therefore the parameters $\rho_{\rm BN}$ and $R^{\rm plug}_{Cc}$ are strongly correlated. It helps when at least one of them is known from the process.

4.3.12 High current parameters

The epilayer parameters $\mathsf{R_{Cv}}$, $\mathsf{SCR_{Cv}}$ and $\mathsf{I_{hc}}$ may be calculated using an effective dope $N_{\rm epi}$, thickness $W_{\rm epi}$ and spreading factors at low and high current levels [10]

$$\mathsf{R_{Cv}} = C_{\mathsf{R_{Cv}}}\,\frac{W_{\rm epi}}{q\,N_{\rm epi}\,\mu_0\,H_{\rm em}\,L_{\rm em}}\,\frac{1}{\left(1+S_{fL}\right)^2}, \tag{4.32a}$$

$$\mathsf{SCR_{Cv}} = C_{\mathsf{SCR_{Cv}}}\,\frac{W^2_{\rm epi}}{2\,\varepsilon\,v_{\rm sat}\,H_{\rm em}\,L_{\rm em}}\,\frac{1}{\left(1+S_{fH}\right)^2}, \tag{4.32b}$$

$$\mathsf{I_{hc}} = C_{\mathsf{I_{hc}}}\,q\,N_{\rm epi}\,H_{\rm em}\,L_{\rm em}\,v_{\rm sat}\,\left(1+S_{fL}\right)^2, \tag{4.32c}$$

where

$$S_{fL} = \frac{W_{\rm epi}}{4}\left(\frac{2}{H_{\rm em}} + \frac{2}{L_{\rm em}}\right), \tag{4.32d}$$

$$S_{fH} = \frac{W_{\rm epi}}{3}\left(\frac{2}{H_{\rm em}} + \frac{2}{L_{\rm em}}\right). \tag{4.32e}$$

The mobility μ_0 and some other constants can be found in Section 2.3.3. Multipliers $C_{\mathsf{I_{hc}}}$, $C_{\mathsf{R_{Cv}}}$ and $C_{\mathsf{SCR_{Cv}}}$ are put in front of the hot carrier current $\mathsf{I_{hc}}$, the ohmic resistance $\mathsf{R_{Cv}}$ and the space charge resistance $\mathsf{SCR_{Cv}}$ respectively. They should be close to one. In this way you can easily see how ”physical” the extracted epilayer parameters are.

4.3.13 Transit time parameters

The next parameters to scale over geometry are the transit times. The scaling rules for the transit time parameters may read

$$\tau_{\mathsf{E}} = \tau^b_E + \tau^s_E\left(\frac{2}{H_{\rm em}} + \frac{2}{L_{\rm em}}\right), \tag{4.33a}$$

 ©Koninklijke Philips Electronics N.V. 2001

$$\tau_B = C_{\tau_B} \frac{V_{er}\,(1 - XC_{jE})\,C_{jE}}{I_k}, \tag{4.33b}$$

$$\tau_{epi} = \tau^b_{epi} + \tau^s_{epi}\left(\frac{2}{H_{em}} + \frac{2}{L_{em}}\right), \tag{4.33c}$$

$$\tau_R = (\tau_B + \tau_{epi})\left(1 - \frac{H_{em}\,L_{em}}{H_{base}\,L_{base}}\right), \tag{4.33d}$$

$$m_\tau = \text{geometry independent},$$

$$a_{x_i} = \text{geometry independent}.$$

The total transit time is the sum of the emitter, base and collector transit times. At the maximum of f_T the contribution of the collector transit time is well known, because it is mainly determined by series resistances and depletion capacitances. Then the remaining minimum transit time is given by the sum of τ_B and τ_E. The shape of the f_T curve in quasi-saturation is affected by many other parameters like τ_{epi}. Therefore an unambiguous determination of τ_B and τ_E is cumbersome. The solution is to calculate τ_B from the reverse Early voltage V_{er} and the base-emitter depletion capacitance parameters C_{jE} and XC_{jE}. A pre-factor may be used (the same for all geometries) to adjust the obtained parameter value of τ_B. In this way a proper scaling of τ_B over geometry is achieved. One can then extract the other parameters needed to describe f_T.

It is recommended to take m_τ and a_{x_i} as geometry independent parameters. Parameter m_τ has a strong impact on the scaling of τ_E and a_{x_i} on the scaling of τ_{epi}. So to make scaling more easy one should keep them constant over geometry.

To get good scaling equations it is probably best to fix one of the scaling equations together with its parameters after the first optimisation run, and then re-optimise the other parameters. Then the next parameter gets fixed over geometry, etc.

To achieve an accurate description of the (maximum of the) cut-off frequency f_T over geometry it is desired to repeat as a final step the extraction of just τ_E while all other Mextram parameters have there geometric scaled value (including the other transit times). After this has been done for every transistor, one can rescale τ_E itself over geometry.

Usually the reverse f_T is not measured and therefore the reverse transit time τ_R can not be extracted. A first order value and scaling may be obtained using τ_B, τ_{epi} and and the surface ration $XC_{jC} = H_{base}\,L_{base}/H_{em}\,L_{em}$. If for some reason XC_{jC} has a slightly different scaling rule, one should still use the ratio of the active base and emitter areas for the scaling of τ_R.

4.3.14 Noise parameters

In general it is difficult to extract the flicker noise parameters, since specialised measurements have to be done, and since it is difficult to get from the measurements to the parameters. Furthermore, flicker noise can vary from one device to the other. Nevertheless, scaling should not be a problem. We use the fact that having MULT devices in parallel implies that the total noise density is MULT times the noise density of a single device. This is also used in MULT-scaling [2]. Flicker noise therefore scales with a surface,

which we call A_f. Which surface one should use depends where the noise is generated in the specific process (e.g. the interfacial oxide between the poly and mono silicon of the emitter, or some other surface area with lots of traps). The parameters then scale as

$$\mathsf{K_f} = K_{f,\mathrm{ref}} \left(\frac{A_f}{A_{f,\mathrm{ref}}}\right)^{1-\mathsf{A_f}}, \tag{4.34a}$$

$$\mathsf{K_{fN}} = K_{fN,\mathrm{ref}} \left(\frac{A_f}{A_{f,\mathrm{ref}}}\right)^{1-[2(\mathsf{m_{Lf}}-1)+\mathsf{A_f}(2-\mathsf{m_{Lf}}]}, \tag{4.34b}$$

where $K_{f,\mathrm{ref}}$ and $K_{fN,\mathrm{ref}}$ are the parameters belonging to the arbitrary reference surface $A_{f,\mathrm{ref}}$.

4.3.15 Scaling of thermal parameters

The scaling of the thermal parameters $\mathsf{R_{th}}$ and $\mathsf{C_{th}}$ depends very much on the kind of process and the way in which the dissipated heat is removed from the transistor. The most simple scaling is

$$\mathsf{R_{th}} = R^s_{th}/(H_{\mathrm{em}}\, L_{\mathrm{em}}), \tag{4.35a}$$

$$\mathsf{C_{th}} = C^s_{th}\, H_{\mathrm{em}}\, L_{\mathrm{em}}. \tag{4.35b}$$

We refer to Ref. [19] for more details. In practice $\mathsf{R_{th}}$ might not decrease as fast as shown (i.e. proportional to the emitter area). A modified scaling formula then has to be used. From dimensional considerations [11] scaling $\mathsf{R_{th}}$ with the (inverse of the) square root of the emitter area might be a good idea.

4.4 Making use of special structures

Sometimes one has special devices available for the extraction of geometric scaling parameters. As this is in general not the case we do not want to say very much about this. However, we will make one general comment.

Let us look at the base-emitter capacitance as an example. Suppose that we have two large structures available to measure specifically this capacitance. One of them has a large surface area and a relatively small perimeter, while the other has a large perimeter and a relatively small area. Using these structures we would like to do the geometric scaling. We can do this in the same way as before. However, a more logical way to do geometric scaling is using the measurements of both structures and calculate the area and sidewall components of the capacitance as weighted averages, using the actual area and sidewall length of the structures. Having done this for every bias point, one can then extract the parameters corresponding to the area and to the perimeter separately. So instead of first extracting parameters, and then scaling these, using the special structures one can actually scale the measurements and then extract the parameters.

 ©Koninklijke Philips Electronics N.V. 2001

In principle one can do the same thing with the many transistor results as used before. This means that one has to do a scaling on the measurements for every bias point. Only after the scaling one extracts the scaling parameters for area and sidewall components. The disadvantage is that one cannot simply calculate the two values of the area and sidewall components, using all the measurements, since one has many geometries and only two scaling parameters. One must do an optimisation for every bias point. This is not only very time consuming, it is also very prone to noise. We therefore do not recommend this method.

4.5 Statistical modelling

The unity parameters mentioned in Sec. 4.1 and used throughout this chapter depend on the process steps and are strongly related to certain process quantities, characterised my measured (or simulated) PCM data. Once the statistical variation of a selected number of the PCM parameters is known, one can calculate the statistical variation of the electrical parameters. More detailed information about statistical modelling can be found in Ref. [6]. It is important to realise that statistical modelling, even more so than geometric scaling, depends on the process or the applications and their sensitivity to statistical variations. A good statistical model can, therefore, only be made by those doing process characterisation. The implementation of statistical modelling into a circuit simulator depends very much on the simulator and will not be discussed here.

To establish the relations between the PCM data and the unity parameters we must rely on device physics. The basis for this is both a physical model, like Mextram, as well as physical geometric scaling rules, described in this chapter.

For statistical modelling the aim is to select a minimum number of process quantities that are preferably statistically uncorrelated. This minimum number, however, must be large enough to determine all the involved unity parameters one wants to model statistically. We then vary these quantities over a certain range that covers all expected variations. In this way we create a matrix batch, consisting of a set of process variations where each set contains a number of geometries. Such a matrix batch can be made in real silicon or it can be composed by computer simulations. The relations between the unity parameters u and the process quantities $p_1, p_2, \ldots$ can usually be written in the form of

$$u = a \; p_1^{b_1} \; p_2^{b_2}, \tag{4.36}$$

where a is a pre-factor and $b_1, b_2, \ldots$ are powers. Dependence on more than two process quantities is very rare in practice.

To be able to find the correct relations one must correlate the PCM data to extracted electrical parameters. To do this one must be sure that the electrical parameter can be extracted fairly easy. This includes most low-current parameters. For the high current parameters, however, parameter extraction is to complicated to determine good correlations. For these it is better to use directly the geometric scaling relations to determine the influence of the variation of a PCM quantity on the variation of the parameter.

©Koninklijke Philips Electronics N.V. 2001

Sometimes it is easier to determine the statistical variation of an electrical model parameter directly, without using a related PCM quantity. This is especially so when there is no PCM quantity available that correlates directly to the electrical parameter one wants to model statistically.

Table 8: *An example of a list of process parameters for which statistical knowledge is available and the parameters they (might) influence.* $G_{\rm em}$ *stands for the emitter Gummel number. For the electrical parameters given in brackets it is a good idea to verify the correlation with the process parameter before using it in the statistical modelling.*

process parameter	Electrical model parameter
$\rho_{\square}^{\rm base}$	$\mathsf{I_s}$, $\mathsf{C_{jE}}$, $\boldsymbol{\beta}_{\mathsf{f}}$, ($\mathsf{V_{er}}$, $\mathsf{V_{ef}}$)
$G_{\rm em}$	$\boldsymbol{\beta}_{\mathsf{f}}$
$N_{\rm epi}$	$\mathsf{I_{hc}}$, $\mathsf{R_{Cv}}$
$W_{\rm epi}$	$\mathsf{I_{hc}}$, $\mathsf{R_{Cv}}$, $\mathsf{SCR_{Cv}}$, $\mathsf{S_{fH}}$, ($\mathsf{W_{avl}}$)
N_{re}	$\mathsf{R_E}$
N_{cjc}	$\mathsf{C_{jC}}$
N_{cjs}	$\mathsf{C_{jS}}$

In Table 8 we have given an example of a number of ‘process’ parameters and the electrical model parameters these influence. We do not give the precise relations between the two. These can be determined either from the physical relation between the process parameter and the electrical parameter, or from correlation measurements. The last three quantities in the list give an example using the statistical variation of an electrical parameter directly. In the process-parameter column we have given a multiplier. One can then write, for instance, $\mathsf{R_E} = N_{re} \times \mathsf{R_{E0}}$, to include the statistical variation.

 ©Koninklijke Philips Electronics N.V. 2001

5 Implementation in IC-CAP

In this chapter we give a short description of the use of IC-CAP of Agilent for parameter extraction of Mextram. For more documentation and example files we refer directly to Agilent.

5.1 Usage of the built-in C-functions

In this section we describe the use of the IC-CAP built-in C-functions that can be used for extraction. Note that this document is not the official documentation, since we do not have control over the precise implementation. Furthermore, not all details of the code are understood by us. However we think it is a good idea to include some of the information in this document.

The functions are based on Chapter 2 of this report.

We will try to give for any function the inputs and outputs. Most of the inputs are used for the calculation of the output (obviously). The rest is only used for checking the validity of the approximation made in the formulas (checking for instance whether the substrate current is not too large for the approximation to work). Especially the difference between these two kinds of inputs is badly documented at the moment, and therefore only scarcely known.

For all transforms and functions the parameters used are those of the ambient temperature, unless otherwise stated.

5.1.1 The function `MXT_show_parms`

This function prints all the Mextram parameters at the actual ambient temperature, as they are used in the functions. This includes the initialisation features described in Section 2.6.3.

Some extra information is also given. For some SiGe transistors (when $\mathsf{dE_g} \neq 0$) the effective Early parameters $V_{\rm ef,I}$ and $V_{\rm er,I}$ are not equal to the actual Early parameters $\mathsf{V_{ef}}$ and $\mathsf{V_{er}}$. The Early effect (of the collector current, hence the subindex I) can be modelled by a factor q_1. For small biases this factor is

$$q_1 \simeq \left[1 + \frac{\mathcal{V}_{\rm BE}}{V_{\rm er,I}} + \frac{\mathcal{V}_{\rm BC}}{V_{\rm ef,I}}\right]^{-1}, \tag{5.1}$$

which uses the effective Early parameters, rather than the standard expression $q_1 \simeq 1/\left[1 + \mathcal{V}_{\rm BE}/\mathsf{V_{er}} + \mathcal{V}_{\rm BC}/\mathsf{V_{ef}}\right]$. The same correction is used in `MXT_VER` and `MXT_VEF`. When $\mathsf{dE_g} = 0$ there is no difference.

For the high current parameters we show not only $\mathsf{R_{Cv}}$, $\mathsf{SCR_{cv}}$ and $\mathsf{I_{hc}}$ but also (within parenthesis) the critical voltage for velocity saturation $V_{\rm lim} = \mathsf{I_{hc}}\ \mathsf{R_{cv}}$ and the punch-through voltage $V_{PT} = \mathsf{I_{hc}}\ \mathsf{SCR_{cv}}$.

©Koninklijke Philips Electronics N.V. 2001

Also for the transit time more than just the parameters are given. The transit time parameters as calculated from Eq. (2.67) are also given (within parenthesis). In this way one can see whether the actual parameter values still have a physical relation w.r.t. each other.

5.1.2 The function `MXT_cbe`

Used in section: 2.5.1
Input: $\mathcal{V}_{\rm BE}$
Output: C_{BE}
This function calculates the total base-emitter depletion capacitance C_{BE} using Eqs. (2.16)–(2.18).

5.1.3 The function `MXT_cbc`

Used in section: 2.5.2
Input: $\mathcal{V}_{\rm BC}$
Output: C_{BC}
This function calculates the total base-collector depletion capacitance C_{BC} using Eq. (2.21).

5.1.4 The function `MXT_csc`

Used in section: 2.5.3
Input: $\mathcal{V}_{\rm SC}$
Output: C_{SC}
This function calculates the total substrate-collector depletion capacitance C_{SC} using Eq. (2.22).

5.1.5 The function `MXT_cj0`

Used in sections: 2.5.1–2.5.3
Inputs: V_J, C_J
Choice of outputs: E/C/S
Sets the value of: C_{jE} / C_{jC} / C_{jS}
This function calculates the value of the capacitance at zero bias. This initial value is then used to set the corresponding parameter (C_{jE}, C_{jC}, C_{jS}). The total bias range needs to include $V = 0$, but it is not necessary that one of the V_J values is indeed zero.

The capacitance values C_J are smoothed, according to Section 5.2.2.

5.1.6 The function `MXT_jun_cap`

Used in sections: 2.5.1–2.5.3
Input: $\mathcal{V}_{\rm jun}$
Choice of outputs: E/C/S
Output: C_{BE}/C_{BC}/C_{SC}
This function combines the functionality of the three functions `MXT_cbe`, `MXT_cbc`,

 ©Koninklijke Philips Electronics N.V. 2001

and MXT_csc . By choosing one of the outputs one gets the corresponding capacitance formula. (Note that the formulas for the three different capacitances are somewhat different, since for instant $\mathsf{X_p}$ has to be taken into account for the base-collector capacitance.) The value of $\mathcal{V}_{\rm jun}$ is one of $\mathcal{V}_{\rm BE}$, $\mathcal{V}_{\rm BC}$ or $\mathcal{V}_{\rm SC}$.

When AUTO_SELECT has a positive value than the variables start and stop are set to the values of the first and the last point of $\mathcal{V}_{\rm jun}$.

5.1.7 The function MXT_I0

Used in sections: 2.5.4–2.5.6 and 2.8.2
Input: $I_{\rm data}$
Choice of outputs: E/C/B
Sets the value of: IE0 / IC0 / IB0.
This very simple function uses the array of current data $I_{\rm data}$ and takes the first one of these. It then sets the value of the variable IE0, IC0, or IB0. This function can be used in the forward-Early and reverse-Early measurements to get a first estimate of the offset of the current.

5.1.8 The function MXT_VER

Used in section: 2.5.5
Inputs: $\mathcal{V}_{\rm EB}$, I_E
Sets the value of: $\mathsf{V_{er}}$
This function gives an estimate of the reverse Early voltage and sets the parameter $\mathsf{V_{er}}$. It does so by using the equation

$$\mathsf{V_{er}} = I_E(\mathcal{V}_{\rm BE}{=}0) \times \frac{\partial \mathcal{V}_{\rm BE}}{\partial I_E}. \tag{5.2}$$

The derivative is approximated by taking the first and the *third* point in the curve.

When the parameter $\mathsf{dE_g} \neq 0$, we need to make a correction. We then use

$$\mathsf{V_{er}} = I_E(\mathcal{V}_{\rm BE}{=}0) \times \frac{\partial \mathcal{V}_{\rm BE}}{\partial I_E} \times \frac{\mathsf{dE_g}/V_T}{1-\exp(-\mathsf{dE_g}/V_T)}. \tag{5.3}$$

We see that the parameter $\mathsf{V_{er}}$ is larger than the actual reverse Early voltage.

No correction is made when the actual temperature is different from the reference temperature $\mathsf{T_{ref}}$.

5.1.9 The function MXT_VEF

Used in section: 2.5.6
Inputs: $\mathcal{V}_{\rm CB}$, I_C
Sets the value of: $\mathsf{V_{ef}}$

©Koninklijke Philips Electronics N.V. 2001

This function gives an estimate of the forward Early voltage and sets the parameter $\mathsf{V_{ef}}$. It does so by using the equation

$$\mathsf{V_{ef}} = I_C(\mathcal{V}_{\mathrm{BC}}=0) \times \frac{\partial \mathcal{V}_{\mathrm{BC}}}{\partial I_C}. \tag{5.4}$$

The derivative is approximated by taking the first and the *third* point in the curve.

When the parameter $\mathsf{dE_g} \neq 0$, we need to make a correction. We then use

$$\mathsf{V_{ef}} = I_C(\mathcal{V}_{\mathrm{BC}}=0) \times \frac{\partial \mathcal{V}_{\mathrm{BC}}}{\partial I_C} \times \frac{\mathsf{dE_g}/V_T}{\exp(\mathsf{dE_g}/V_T) - 1}. \tag{5.5}$$

We see that the parameter $\mathsf{V_{ef}}$ is smaller than the actual forward Early voltage.

No correction is made when the actual temperature is different from the reference temperature $\mathsf{T_{ref}}$.

5.1.10 The function `MXT_veaf_ib`

Used in sections: 2.5.4 and 2.8.2
Inputs: $\mathcal{V}_{\mathrm{CB}}$, I_C
Output: I_B
This function calculates

$$I_B = \mathtt{IB0} - I_C\ G_{EM}(\mathcal{V}_{\mathrm{CB}}), \tag{5.6}$$

where G_{EM} is the generation rate as defined in Eq. (2.24).

When the parameter $\mathsf{X_{rec}} \neq 0$ the formula is extended, according to Eq. (2.78).

5.1.11 The function `MXT_veaf_ic`

Used in section: 2.5.6
Inputs: $\mathcal{V}_{\mathrm{CB}}$, $\mathcal{V}_{\mathrm{EB}}$, I_B
Output: I_C
This function calculates the (forward) current given by

$$I_C = I_{C0}\,\frac{1 + \dfrac{V_{t_E}}{\mathsf{V_{er}}}}{1 + \dfrac{V_{t_E}}{\mathsf{V_{er}}} + \dfrac{V_{t_C}}{\mathsf{V_{ef}}}}, \tag{5.7}$$

where V_{t_E} and V_{t_C} are given in Eq. (2.26).

The value of $\mathcal{V}_{\mathrm{EB}}$ is assumed to be constant.

The input I_B is only used for auto-ranging (see Sec. 5.2.1). The function starts at low V_{CB} and keeps account of the (running) average of I_B. When a certain value of I_B is below

 ©Koninklijke Philips Electronics N.V. 2001

0.99 times this running average avalanche is assumed to be important, and the equation above should be corrected for avalanche. This can be done as in Eq. (2.28). Auto-ranging is then not necessary. Furthermore, when $\mathsf{X}_{\mathsf{rec}} \neq 0$ this auto-ranging does not work.

5.1.12 The function `MXT_vear_ie`

Used in section: 2.5.5
Inputs: $\mathcal{V}_{\mathrm{EB}}$, $\mathcal{V}_{\mathrm{CB}}$
Output: I_E
This function calculates the (reverse) current given by Eqs. (2.25) and (2.26).

The value of $\mathcal{V}_{\mathrm{CB}}$ is assumed to be constant.

5.1.13 The function `MXT_forward_ic`

Used in section: 2.5.7
Inputs: $\mathcal{V}_{\mathrm{EB}}$, $\mathcal{V}_{\mathrm{CB}}$, I_C
Output: I_C
This function calculates the almost ideal forward collector current from Eq. (2.30).

Auto ranging is done on I_C (see Sec. 5.2.1): When, due to series resistances or saturation effects, the logarithm $\ln I_C$ becomes less that 0.98 its running average the function assumes that Eq. (2.30) is no longer valid. Optionally this $\ln I_C$ is smoothed before hand (see Sec. 5.2.2).

Noise filtering (see Sec. 5.2.3) is done by removing (i.e. setting the final results to zero) those points where $|\partial^2 \ln I_C / \partial \mathcal{V}_{\mathrm{BE}}^2| > 10.0$.

5.1.14 The function `MXT_forward_hfe`

Used in section: 2.5.8
Input: $\mathcal{V}_{\mathrm{EB}}$, $\mathcal{V}_{\mathrm{CB}}$, I_C
Output: h_{fe}
This function calculates h_{fe}, according to Eqs. (2.31)–(2.33).

Auto ranging and noise filtering is done on the collector current ($\ln I_C$) in the same way as is done in `MXT_forward_ic`.

5.1.15 The function `MXT_forward_vbe`

Used in section: 2.5.9
Inputs: I_C, I_B, $\mathcal{V}_{\mathrm{EB}}$
Output: $\mathcal{V}_{\mathrm{BE}}$
This function calculates the total voltage drop between the external nodes E and B, according to Eq. (2.37).

In various functions we must calculate the internal junction from a given base current. We will describe this here. The base current can be written as a function of $\mathcal{V}_{\mathrm{B_2E_1}}$:

$$I_B = g(\mathcal{V}_{\mathrm{B_2E_1}}) = I_{B_1}(\mathcal{V}_{\mathrm{B_2E_1}}) + I_{B_2}(\mathcal{V}_{\mathrm{B_2E_1}}). \tag{5.8}$$

Knowing I_B we must solve for $\mathcal{V}_{\mathrm{B_2E_1}}$. This is done by a Newton-Rhapson method on $\ln g(\mathcal{V}_{\mathrm{B_2E_1}}) - \ln I_B$. This means that we start by an initial value, which is either 0.5 V or the result from the previous point. Then we calculate a new value of the voltage using

$$\mathcal{V}'_{\mathrm{B_2E_1}} = \mathcal{V}_{\mathrm{B_2E_1}} - (\ln g - \ln I_B)\,\frac{g}{g'}, \tag{5.9}$$

and repeating this until the step $\mathcal{V}_{\mathrm{B_2E_1}}$ is smaller than 1 μV. Here g' is the derivative of g.

Auto ranging is again done on $\ln I_C$, as in `MXT_forward_ic` (and here the input V_{EB} is used).

5.1.16 The function `MXT_hard_sat_isub`

Used in section: 2.5.10
Inputs: $\mathcal{V}_{\mathrm{BC}}$, I_C, I_B
Output: I_{sub}
This function calculates the substrate current in hard saturation from Eqs. (2.42) and (2.43). When the input I_B is set to zero, the influence of the base current is not taken into account.

5.1.17 The function `MXT_reverse_isub`

Used in section: —
Input: $\mathcal{V}_{\mathrm{BC}}$
Output: I_{sub}
This function calculates the substrate current for low reverse conditions:

$$I_{\mathrm{sub}} = \mathsf{I_{Ss}}\,\left(e^{\mathcal{V}_{\mathrm{BC}}/V_T} - 1\right). \tag{5.10}$$

Auto ranging and noise-filtering is done in the same way as in `MXT_forward_ic`. Now however not $\ln I_C$ is used, but $\ln I_{\mathrm{sub}}$.

This function could be used for the extraction of $\mathsf{I_{Ss}}$, but we recommend another method (see Sec. 2.5.11).

5.1.18 The function `MXT_reverse_hfc_sub`

Used in section: 2.5.11
Inputs: $\mathcal{V}_{\mathrm{EB}}$, $\mathcal{V}_{\mathrm{CB}}$, I_E, I_S
Output: $h_{\mathrm{fc,sub}}$
This function calculates the substrate to emitter current gain $h_{\mathrm{fc,sub}}$ from Eq. (2.47) (using only $\mathcal{V}_{\mathrm{EB}}$ and $\mathcal{V}_{\mathrm{CB}}$).

Auto ranging and noise-filtering is done in the same way as in `MXT_forward_ic`. Now however not $\ln I_C$ is used, but both $\ln I_E$ and $\ln I_S$ are monitored.

 ©Koninklijke Philips Electronics N.V. 2001

5.1.19 The function `MXT_reverse_hfc`

Used in section: 2.5.12
Inputs: $\mathcal{V}_{\rm CB}$, $\mathcal{V}_{\rm EB}$, I_E
Output: $h_{\rm fc}$
Choice of outputs: Substrate y/n ('n' is the default)
This function calculates the reverse current gain $h_{\rm fc}$, given by Eq. (2.51):

$$h_{\rm fc} = \frac{I_E}{I_{\rm ex} + I_{B_3}}, \tag{5.11}$$

where $I_{\rm ex}$ and I_{B_3} are given by Eqs. (2.49) and (2.50). When the substrate current should be included we use instead

$$h_{\rm fc} = \frac{I_E}{I_{\rm ex} + I_{B_3} + I_{\rm sub}}, \tag{5.12}$$

where $I_{\rm sub}$ is given in Eq. (2.42).

When neutral base recombination is present ($\mathsf{X_{rec}} \neq 0$) we must also take the forward base current into account, which can be simplified to

$$I_{B_1} = \frac{\mathsf{I_s}}{\beta_{\mathsf{f}}} \,(1 - \mathsf{XI_{B_1}})\, \mathsf{X_{rec}} \left(1 + \frac{V_{t_C}}{\mathsf{V_{ef}}}\right) \left(e^{\mathcal{V}_{\rm B_1C_1}/V_T} - 1\right). \tag{5.13}$$

It will add to the base current, but it makes the emitter current smaller. Hence this is taken it into account when calculating $\mathcal{V}_{\rm B_1C_1}$ from the measured emitter current.

Auto ranging and noise-filtering is done in the same way as in `MXT_forward_ic`. Now however not $\ln I_C$ is used, but $\ln I_E$. Auto-ranging is useful only when the substrate current is not included.

5.1.20 The function `MXT_reverse_currents`

Used in section: 2.6.7
Input: $\mathcal{V}_{\rm BC}$, $\mathcal{V}_{\rm BE}$, I_E
Outputs: $I_E/I_B/I_{\rm sub}$
Choice of outputs: E/B/S
Given the voltages $\mathcal{V}_{\rm BC}$ and $\mathcal{V}_{\rm BE}$ this function calculates in an iterative way the (reverse) currents I_E, I_B or $I_{\rm sub}$, including the high-current behaviour, as described in Eqs. (2.69)–(2.73).

The base current that is due to neutral base recombination can be added in the same way as in `MXT_reverse_hfc` (using $\mathcal{V}_{\rm B_2C_2}$ instead of $\mathcal{V}_{\rm B_1C_1}$), but we will still neglect the voltage drop over $\mathsf{R_{Bv}}$.

Auto ranging is done in the same way as in `MXT_forward_ic`. Now however not $\ln I_C$ is used, but $\ln I_E$.

©Koninklijke Philips Electronics N.V. 2001

5.1.21 The function `MXT_ic_vce`

Used in section: 2.6
Inputs: $\mathcal{V}_{\rm CE}$, I_B, I_C, $\mathcal{V}_{\rm BE}$, $I_{\rm sub}$
Output: $I_C/\mathcal{V}_{\rm BE}$
Choice of outputs: I/V and avalanche (n/y)

This function calculates the collector current I_C as function of the voltage difference $\mathcal{V}_{\rm CE}$ and the base current I_B. It uses I_C only to correct for resistances. $\mathcal{V}_{\rm BE}$ and I_S are used for initial values, checking the results, and auto-ranging only.

The collector current is calculated as described in Sec. 2.6.2. We will not give all the equations used, since many equations are needed. They can be found in Ref. [2]. This includes the temperature rules since we take self-heating into account, using Eq. (2.52). Two internal quantities, $\mathcal{V}_{\rm B_2E_1}$ and $I_{C_1C_2}$ need to be solved. The internal bias $\mathcal{V}_{\rm B_2C_1}$ is calculated from Eq. (2.56) using $\mathcal{V}_{\rm B_2E_1}$, $\mathcal{V}_{\rm CE}$ and the measured currents. Then $\mathcal{V}^*_{\rm B_2C_2}$ and other internal quantities can be calculated. This means that in principle all quantities can be written as function of $\mathcal{V}_{\rm B_2E_1}$ and $I_{C_1C_2}$. The following two equations need to be solved iteratively

$$I_{B,\rm m} = I_{B,\rm f}(\mathcal{V}_{\rm B_2E_1}, I_{C_1C_2}) - G_{\rm em}(\mathcal{V}_{\rm B_2E_1}, I_{C_1C_2})\, I_{C_1C_2}, \qquad (5.14a)$$

$$I_N(\mathcal{V}_{\rm B_2E_1}, I_{C_1C_2}) = I_{C_1C_2}\,[1 - G_{\rm em}(\mathcal{V}_{\rm B_2E_1}, I_{C_1C_2})]. \qquad (5.14b)$$

Here $I_{B,\rm m}$ is the measured base current, $I_{B,\rm f}$ is the sum of all forward base currents (I_{B_1} including neutral base recombination, $I^S_{B_1}$ and I_{B_2}) and $G_{\rm em}$ is the generation rate of the avalanche current (we assume $G_{\rm max} \to \infty$). The equations are solved using the Newton-Rhapson method for two variables.

The routine by default does not take avalanche into account (i.e. $G_{\rm em} = 0$). It is an optional feature. This has been done to prevent possible convergency problems that might arise close to $BV_{\rm ceo}$.

When the internal voltages are known it is possible to calculate $\mathcal{V}_{\rm BE}$ according to

$$\mathcal{V}_{\rm BE} = \mathcal{V}_{\rm B_2E_1} + \mathcal{V}_{\rm B_1B_2} + I_B\, \mathsf{R_{BcT}} + (I_C + I_B)\, \mathsf{R_{ET}}. \qquad (5.15)$$

This is needed when not the current but the base-emitter bias needs to be calculated by the routine. The voltage drop $\mathcal{V}_{\rm B_1B_2}$ can be estimated as

$$\mathcal{V}_{\rm B_1B_2} = V_T \log\left(1 + \frac{\mathsf{R_{BvT}}\, I_B\, (1 - \mathsf{XI_{B_1}})}{V_T\, q^Q_B}\right), \qquad (5.16)$$

using the known internal voltages to calculate the normalised base charge q^Q_B.

The input $\mathcal{V}_{\rm BE}$ is used only for initial guesses and to do a check afterwards to make sure that $\mathcal{V}_{\rm B_2E_1} < \mathcal{V}_{\rm BE}$. This is needed especially when the measurements of the low currents are noisy.

 ©Koninklijke Philips Electronics N.V. 2001

Auto ranging is done in two ways. In both cases the function tries to determine whether the transistor is in hard-saturation (where the assumptions made no longer hold) or not. The first way of auto-ranging monitors the base-collector bias $\mathcal{V}_{\mathrm{B_2C_1}}$, given by Eq. (2.56). The transistor is assumed to be in hard-saturation when $\mathcal{V}_{\mathrm{B_2C_1}}$ exceeds $0.8\,\mathsf{V}_{\mathsf{dC}}$. The precise value can be changed by using the variable `HARD_SAT_MAX` (which is by default 0.8). The second way of auto-ranging monitors the substrate current for the curve which has the highest substrate current (at highest $\mathcal{V}_{\mathrm{CE}}$). Then a running average of I_{sub} for this curve is calculated, assuming the the first points are at the highest $\mathcal{V}_{\mathrm{CE}}$. When the substrate current grows more than a factor `NORM_LIMIT` (which is 1.2 by default) than the running average, the transistor is assumed to be in hard saturation. This second way of testing for hard-saturation is probably not necessary. Furthermore, it is rather sensitive to noise in the substrate current. This might lead to auto-ranging effects (making the output zero) in bias-regions where this is certainly not the case. Using an arbitrary but constant value for I_{sub} in the input resolves this problem.

Note that for $\mathcal{V}_{\mathrm{BE}}$ the auto-ranging routine does not make the result zero when the function is no longer valid. Instead the minimum of the measured base-emitter voltage is used (see Fig. 17). In this way the vertical axis remains small enough to see details.

Auto-ranging is always done in this routine, independent of the value of the variable `MXT_AUTO_RANGE`.

5.1.22 The function `MXT_ft`

Used in section: 2.6
Inputs: I_C, $\mathcal{V}_{\mathrm{BE}}$, $\mathcal{V}_{\mathrm{CE}}$
Output: f_T

This function calculates the cut-off frequency f_T as function of I_C, $\mathcal{V}_{\mathrm{BE}}$ and $\mathcal{V}_{\mathrm{CE}}$.

The first step is solving in an iterative way $\mathcal{V}_{\mathrm{B_2E_1}}$. When in an iteration $\mathcal{V}_{\mathrm{B_2E_1}}$ is known, the other internal biases can be calculated by calculating the voltage drops over the resistances, using the given collector current and the base current as calculated from $\mathcal{V}_{\mathrm{B_2E_1}}$. The voltage drop $\mathcal{V}_{\mathrm{B_1B_2}}$ is calculated just as in `MXT_forward_vbe`. (The influence of voltage drops over the base resistances is small. So the fact that I_B is not completely correct is negligible. For that reason we assume $\mathsf{dE_g} = 0$ and we neglect neutral base recombination.) When $\mathcal{V}_{\mathrm{B_2C_1}}$ has been calculated (using $\mathcal{V}_{\mathrm{BC}}$), the bias $V^*_{B_2C_2}$ can be found. All the internal voltage differences are then known and the main current I_N can be calculated. The bias $\mathcal{V}_{\mathrm{B_2E_1}}$ is now found in an iterative loop by demanding that $I_N = I_C$.

In the calculation above, we keep track of all the derivatives. Using the two equations

$$\mathrm{d}\mathcal{V}_{\mathrm{CE}} = \frac{\partial \mathcal{V}_{\mathrm{CE}}}{\partial \mathcal{V}_{\mathrm{B_2E_1}}}\,\mathrm{d}\mathcal{V}_{\mathrm{B_2E_1}} + \frac{\partial \mathcal{V}_{\mathrm{CE}}}{\partial \mathcal{V}_{\mathrm{B_2C_1}}}\,\mathrm{d}\mathcal{V}_{\mathrm{B_2C_1}} + \frac{\partial \mathcal{V}_{\mathrm{CE}}}{\partial I_{C_1C_2}}\,\mathrm{d}I_{C_1C_2} = 0, \qquad (5.17a)$$

$$\mathrm{d}I_N = \frac{\partial I_N}{\partial \mathcal{V}_{\mathrm{B_2E_1}}}\,\mathrm{d}\mathcal{V}_{\mathrm{B_2E_1}} + \frac{\partial I_N}{\partial \mathcal{V}_{\mathrm{B_2C_1}}}\,\mathrm{d}\mathcal{V}_{\mathrm{B_2C_1}} + \frac{\partial I_N}{\partial I_{C_1C_2}}\,\mathrm{d}I_{C_1C_2} = \mathrm{d}I_{C_1C_2}, \qquad (5.17b)$$

we can then find $\mathrm{d}\mathcal{V}_{\mathrm{B_2E_1}}/\mathrm{d}I_{C_1C_2}$ and $\mathrm{d}\mathcal{V}_{\mathrm{B_2C_1}}/\mathrm{d}I_{C_1C_2}$, both under the condition that $\mathcal{V}_{\mathrm{CE}}$ is constant.

Next we need to calculate all the (derivatives) of the charges. Again these derivatives are taken w.r.t. $\mathcal{V}_{\mathrm{B_2E_1}}$, $\mathcal{V}_{\mathrm{B_2C_1}}$ and $I_{C_1C_2}$. This leads to the variation of the charge

$$\mathrm{d}Q = \frac{\partial Q}{\partial \mathcal{V}_{\mathrm{B_2E_1}}}\,\mathrm{d}\mathcal{V}_{\mathrm{B_2E_1}} + \frac{\partial Q}{\partial \mathcal{V}_{\mathrm{B_2C_1}}}\,\mathrm{d}\mathcal{V}_{\mathrm{B_2C_1}} + \frac{\partial Q}{\partial I_{C_1C_2}}\,\mathrm{d}I_{C_1C_2}. \tag{5.18}$$

The transit time can now be given as

$$\tau_T = \frac{\partial Q}{\partial \mathcal{V}_{\mathrm{B_2E_1}}}\frac{\mathrm{d}\mathcal{V}_{\mathrm{B_2E_1}}}{\mathrm{d}I_{C_1C_2}} + \frac{\partial Q}{\partial \mathcal{V}_{\mathrm{B_2C_1}}}\frac{\mathrm{d}\mathcal{V}_{\mathrm{B_2C_1}}}{\mathrm{d}I_{C_1C_2}} + \frac{\partial Q}{\partial I_{C_1C_2}}, \tag{5.19}$$

and finally the cut-off frequency is given as $f_T = 1/(2\pi\tau_T)$.

Note that just as in the case of the extraction of the parameters of the depletion capacitances the overlap capacitances $\mathsf{C_{BEO}}$ and $\mathsf{C_{BCO}}$ are included.

Auto-ranging is done in almost the same way as in the function `MXT_ic_vce`. When the transistor is in hard saturation (when $\mathcal{V}_{\mathrm{B_2C_1}}$ exceeds $0.8\,\mathsf{V_{dC}}$) the assumptions are no longer valid and result will become zero. (The variable `HARD_SAT_MAX` can be used here also.) No noise filtering is used.

5.1.23 Changes w.r.t. Mextram 503

For some of the functions mentioned above the name or the input/output variables have been changed. When IC-CAP can not find a function or a variable name this can lead to a crash. When rewriting a Mextram 503 modelfile to a Mextram 504 modelfile one needs to take care of the following changes.

`MXT_ic_vce`: The input V_B has been changed into V_{BE}, which is the correct expression when $\mathcal{V}_{\mathrm{E}} \neq 0$. Note that IC-CAP *will* crash when no input for V_{BE} is given. Furthermore, a choice whether to include avalanche or not has been added.

`MXT_is_reverse` has been renamed to `MXT_reverse_isub` for clarity and conformity. Note that this function is not used in the way we presented the parameter extraction.

`MXT_veaf_ib`: The input $\mathcal{V}_{\mathrm{EB}}$ has been removed since it is not used.

`MXT_fwd_hfe`: It is no longer possible to get the output I_B. To calculate I_B one must use $I_B = I_C/h_{\mathrm{hfe}}$, with I_C the same I_C that goes as input into the function.

`MXT_fwd_vbe`: The input V_{CB} has been removed, since it is not needed.

5.2 Parameters that influence C-functions

5.2.1 Autoranging

Some of the functions have the possibility of auto-ranging. This means that the function uses some extra input to determine the validity of the approximations made. (For instance,

©Koninklijke Philips Electronics N.V. 2001

the substrate current may not increase too much, or the transistor may not be in hard saturation.) The auto-ranging feature is only used when MXT_AUTO_RANGE = 1 (except for the functions MXT_ic_vce and MXT_ft that always do auto-ranging). When the function decides that it is out of the range of its validity, the value of the result will be set to zero.

The general way this auto ranging works is as follows. An extra quantity is monitored while stepping through the various points of the inputs. The average of this extra quantity is calculated using all previous (bias) points (but not those to come). This is called a running average. When the new point of the extra quantity differs from this running average by some given amount (given by the quantity NORM_LIMIT, the function is assumed to be out of its range. Note that not for all of the functions the actual variable NORM_LIMIT is used. Sometimes a fixed internal value is used.

5.2.2 Smoothing

Smoothing is sometimes used to avoid that the result of the function flips more than once between some real value and zero (due to auto-ranging). Smoothing is done per curve. Each curve consists of a number of values x_i, where $i = 0, \ldots, N-1$. The smoothed version of this curve is defined by

$$x_0^{(sm)} = x_0, \tag{5.20a}$$

$$x_{N-1}^{(sm)} = x_{N-1}, \tag{5.20b}$$

$$x_i^{(sm)} = \tfrac{1}{3}(x_{i-1} + x_i + x_{i+1}) \qquad \text{for } 0 < i < N-1. \tag{5.20c}$$

This smoothing is done only when the variable MXT_AUTO_SMOOTH is set and has the value 1 (so the default is no smoothing). The function that does this smoothing is the internal function smooth_data.

5.2.3 Noise filtering

For some functions the noisiness of the data is checked. This is controlled by the variable MXT_NOISE_FILTER. When the data is too noisy, the result is put to zero, just as for auto ranging.

5.2.4 Type of transistor

All functions must of course work both for NPN and for PNP transistors. To this end a system variable can be used named POLARITY which can either be ‘NPN’ or ’PNP’ (or without capitals ‘npn’ or ‘pnp’). The default is NPN.

5.3 Optimisation using some simulator

The parameter extraction we have sketched in this document makes use of built-in functions of e.g. IC-CAP. As an alternative one can make use of an external simulator to calculate the response of the Mextram model. However, making use of built-in functions has a few advantages we will now discuss.

Every parameter extraction strategy has a certain order in which the parameters have to be extracted. This order is such that one does not need to know parameters that will be extracted later. This also means that one can not always use all the points of a measurements for the extraction of a certain parameter: for low-current parameters one can not use data-points in the high-current regimes. For extracting the current gain parameter for instance, one must not use the points where the gain is dropping due to high-injection effects. The functions reflect these approximations. From Fig. 10 it is clear that one should not use points beyond $\mathcal{V}_{\rm BE} = 0.8$ V. So the built-in functions help judging which range to take for the parameter extraction.

Some of the parameters, like the Early voltages and the avalanche parameters can be extracted without correct modelling of the absolute value of the current. For these extractions dummy parameters are optimised together with the Mextram parameters. For instance the extraction of the avalanche parameters needs the correct base current at zero $\mathcal{V}_{\rm CB}$. This is more difficult when using a simulator. As dummy parameter one must then use for instance $\mathbf{I_s}$ or $\boldsymbol{\beta}_{\mathbf{f}}$ to get the zero bias current correct (unless of course the model is perfect). After the optimisation one must then reset the dummy parameter to its value extracted from other measurements. (Note that this is only necessary when one of these optimisations is re-done, not when it is done for the first time. Unfortunately in practice it is hardly impossible to get away with only one run through all the parameters.)

One of the other reasons for not using a simulator is that it is much easier to correct for resistances. Look for instance at the calculation of the forward current gain. This gain is calculated for a given collector current. This current determines the internal base-emitter bias, which is then used for further calculations. This is more accurate than taking the external base-emitter bias, especially in the region where resistances start to influence the results. The collector current is a much better indicator of the internal state of the transistor than the bias. For the calculation of f_T this is even more important since the currents are much higher. The effect of the external resistances is then also much higher. When these resistances are not completely correct at the given bias, the f_T plotted versus $\mathcal{V}_{\rm BE}$ will be off. When plotted versus I_C it will still be correct.

Another reason for not wanting to optimise f_T using an external simulator is the fact that (at least at the moment) it takes a very long time, because using the simulator is much slower than using the built-in functions.

We discussed before that self-heating must be taken into account for the extraction of the high-current parameters. At the moment self-heating is not available in (all) simulators. When the simulator cannot handle self-heating, a good parameter extraction using only a simulator is very difficult or even impossible. The built-in functions take self-heating into account (where needed).

 ©Koninklijke Philips Electronics N.V. 2001

References

[1] For the most recent model descriptions, source code, and documentation, see the web-site http://www.semiconductors.philips.com/Philips_Models.

[2] J. C. J. Paasschens and W. J. Kloosterman, “The Mextram bipolar transistor model, level 504,” Unclassified Report NL-UR 2000/811, Philips Nat.Lab., 2000. See Ref. [1].

[3] W. J. Kloosterman, J. A. M. Geelen, and D. B. M. Klaassen, “Efficient parameter extraction for the Mextram model,” in *Proc. of the Bipolar Circuits and Technology Meeting*, pp. 70–73, 1995.

[4] M. C. A. M. Koolen, J. A. M. Geelen, and M. P. J. G. Versleijen, “An improved de-embedding technique for on-wafer high-frequency characterization,” in *Proc. of the Bipolar Circuits and Technology Meeting*, 1991. Paper 8.2.

[5] S. M. Sze, *Physics of Semiconductor Devices*. Wiley, New York, 2nd ed., 1981.

[6] H. C. de Graaff and F. M. Klaassen, *Compact transistor modelling for circuit design*. Springer-Verlag, Wien, 1990.

[7] N. D. Arora, J. R. Hauser, and D. J. Roulston, “Electron and hole mobilities in silicon as function of concentration and temperature,” *IEEE Trans. Elec. Dev.*, vol. ED-29, pp. 292–295, 1982.

[8] D. B. M. Klaassen, “A unified mobility model for device simulation—II. temperature dependence of carrier mobility and lifetime,” *Solid-State Elec.*, vol. 35, no. 7, pp. 961–967, 1992.

[9] D. B. M. Klaassen, “A unified mobility model for device simulation—I. model equations and concentration dependence,” *Solid-State Elec.*, vol. 35, no. 7, pp. 953–959, 1992.

[10] H. C. de Graaff and W. J. Kloosterman, “Modeling of the collector epilayer of a bipolar transistor in the Mextram model,” *IEEE Trans. Elec. Dev.*, vol. ED-42, pp. 274–282, Feb. 1995.

[11] J. C. J. Paasschens, W. J. Kloosterman, and R. van der Toorn, “Physical background of the bipolar transistor model Mextram, level 504,” Unclassified Report , Philips Nat.Lab., 2001. In preparation.

[12] B. Kulke and S. L. Miller, “Accurate measurement of emitter and collector series resistances in transistors,” *Proc. IRE*, vol. 45, p. 90, Jan. 1957.

[13] L. J. Giacoletto, “Measurement of emitter and collector series resistances,” *IEEE Trans. Elec. Dev.*, vol. ED-19, pp. 692–693, 1972.

©Koninklijke Philips Electronics N.V. 2001

[14] T. H. Ning and D. D. Tang, “Method for determining the emitter and base series resistances of bipolar transistors,” *IEEE Trans. Elec. Dev.*, pp. 409–412, 1984.

[15] K. Morizuka, O. Hidaka, and H. Mochizuki, “Precise extraction of emitter resistance from an improved floating collector measurement,” *IEEE Trans. Elec. Dev.*, vol. ED-42, pp. 266–273, 1995.

[16] R. Gabl and M. Reisch, “Emitter series resistance from open-collector measurements — influence of the collector region and the parasitic pnp transistor,” *IEEE Trans. Elec. Dev.*, vol. ED-45, pp. 2457–2465, 1998.

[17] V. Van, M. J. Deen, J. Kendall, D. S. Malhi, S. Voinigescu, and M. Schroter, “DC extraction of the base and emitter resistances in polysilicon-emitter npn BJTs,” *Can. J. Phys (Suppl.)*, vol. 74, pp. S172–S176, 1996.

[18] H. Tran, M. Schröter, D. J. Walkey, D. Marchesan, and T. J. Smy, “Simultaneous extraction of thermal and emitter series resistances in bipolar transistors,” in *Proc. of the Bipolar Circuits and Technology Meeting*, pp. 170–173, 1997. Paper 10.7.

[19] D. T. Zweidinger, R. M. Fox, J. S. Brodsky, T. Jung, and S.-G. Lee, “Thermal impedance extraction for bipolar transistors,” *IEEE Trans. Elec. Dev.*, vol. ED-43, pp. 342–346, 1996.

[20] D. J. Walkey, T. J. Smy, D. Marchesan, H. Tran, C. Reimer, T. C. Kleckner, M. K. Jackson, M. Schröter, and J. R. Long, “Extraction and modelling of thermal behavior in trench isolated bipolar structures,” in *Proc. of the Bipolar Circuits and Technology Meeting*, pp. 97–100, 1999. Paper 6.2.

[21] W. J. Kloosterman, J. C. J. Paasschens, and D. B. M. Klaassen, “Improved extraction of base and emitter resistance from small signal high frequency admittance measurements,” in *Proc. of the Bipolar Circuits and Technology Meeting*, pp. 93–96, 1999. Paper 6.1.

[22] M. J. Deen, “High-frequency noise modelling and the scaling of noise parameters of polysilicon emitter bipolar junction transistors,” *Can. J. Phys. (Suppl.)*, vol. 74, pp. S195–S199, 1996.

[23] P. Llinares, G. Ghibaudo, N. Gambetta, Y. Mourier, A. Monroy, G. Lecoy, and J. A. Chroboczek, “A novel method for base and emitter resistance extraction in bipolar junction transistors from static and low frequency noise measurements,” in *Proc. of the Int. Conf. Microelectronic Test Structures*, pp. 67–71, 1998.

[24] A. J. Scholten, H. J. Tromp, L. F. Tiemeijer, R. van Langevelde, R. J. Havens, P. W. H. de Vreede, R. F. M. Roes, P. H. Woerlee, A. H. Montreen, and D. B. M. Klaassen, “Accurate thermal noise model for deep-submicron CMOS,” in *IEDM Tech. Digest*, pp. 155–158, 1999.

 ©Koninklijke Philips Electronics N.V. 2001

[25] Y. T. Tang and J. S. Hamel, “An electrical method for measuring the difference in bandgap across the neutral base in SiGe HBT’s,” *IEEE Trans. Elec. Dev.*, vol. 47, pp. 797–804, 2000.

[26] J. S. Hamel, “Separating the influences of neutral base recombination and avalanche breakdown on base current reduction in SiGe HBT’s,” *IEEE Trans. Elec. Dev.*, vol. 44, pp. 901–903, 1997.

[27] W. Redman-White, M. S. K. Kee, B. M. Tenbroek, M. J. Uren, and R. J. T. Bunyan, “Direct extraction of MOSFET dynamical thermal characteristics from standard transistor structures using small signal measurements,” *Electron. Lett.*, vol. 29, pp. 1180–1181, 1993.

[28] B. M. Tenbroek, M. S. L. Lee, W. Redman-White, J. T. Bunyan, and M. J. Uren, “Self-heating effects in SOI MOSFET’s and their measurement by small signal conductance techniques,” *IEEE Trans. Elec. Dev.*, vol. 43, pp. 2240–2248, 1996.